Development and Evaluation of the Tree-Level Equations and Their Combined Stand-Level Behavior in the Red Alder Plantation Version of ORGANON

By

David W. Hann
Professor
Department of Forest Engineering, Resources, and Management

Andrew A. Bluhm
Faculty Research Associate
Department of Forest Ecosystems and Society

David E. Hibbs
Professor
Department of Forest Ecosystems and Society

Forest Biometrics Research Paper 1

January 2011

Table of Contents

Development and Evaluation of the Tree-Level Equations and Their Combined Stand-Level Behavior in the Red Alder Plantation Version of ORGANON

1.0 Overview

1.1 Justification for Work

The justification for developing a new variant of ORGANON for red alder plantations (RAP-ORGANON) is best summarized by the following statement from a regional strategy meeting concerning red alder modeling (drafted by Barri Herman and dated 6/22/2004):

> "There has been growing interest in a public Red Alder Growth and Yield Model as there has been expanded acceptance of Red Alder as both a tree crop as well as an important biodiversity component of stands. The introduction of new environmental constraints on harvesting riparian areas and the perceived increase in value of alder versus Douglas fir or hybrid-popular have been strong drivers of this interest. There is relatively good information available relating to silvicultural practices for stand establishment and tending. The most notable technological gap is the lack of a good growth and yield simulator for forecasting future yields of managed Red Alder stands (both intensively managed Red Alder plantations and mixed species stands). Having this capacity is critical to assessing the potential value of silvicultural investments and making decisions to manage forest-land for Red Alder. Hence, there is considerable regional interest in developing a robust growth and yield model."

1.2 Previous Work

Before RAP-ORGANON was developed, there were five sources of growth and yield information for red alder in western Washington and/or Oregon that were publicly available and that had received independent peer review through the publication process:

1. The normal yield tables of Worthington et al. (1960).

2. The empirical yield tables of Chambers (1973).

3. The SPS model of Arney (1985), a whole-stand/diameter-class growth and yield model.

4. The Westside Cascades (Donnelly and Johnson 1997) and the Pacific Northwest Coast (Donnelly 1997) variants of FVS, a single-tree/distance-independent growth and yield model. FVS uses a 10-year time step and does not model stands with significant non-tree competing vegetation (approximately under 10 years old).

5. The ORGANON model of Hann (2003), a single-tree/distance-independent growth and

yield model. ORGANON uses a 5 year time step.

All five sources of red alder growth and yield information were developed using data from just natural, unmanaged stands, and much of the data used in FVS and ORGANON came from mixed species stands.

Normal yield tables, such as that of Worthington et al. (1960), and empirical yield tables, such as that of Chambers (1973), provided only stand level estimates of development and, therefore, their use was limited to projecting even-aged, pure species stands, and they had limited usefulness for evaluating wood quality issues. Whole-stand/diameter-class growth and yield models, such as SPS, provided both stand level and diameter class estimates of development, which increased their utility for projecting different stand structures and evaluating wood quality issues (though SPS's architecture limited its use to even-aged stands). Finally, single-tree/distance-independent growth and yield models, such as FVS and ORGANON, produce both stand level and tree level estimates of development (including crown size), which provides the greatest utility in predicting the development of different stand structures and for evaluating wood quality issues.

Puettmann (1994) reported the results of comparing predictions from the first three sources of growth and yield information to actual growth records from 46 permanent plots in natural, unmanaged stands in the Pacific Northwest. He concluded that (page 234):

1. "The Normal Yield Table is not sufficiently accurate for yield estimates of pure and mixed red alder stands, especially in stands below 30 and over 50 years of age."

2. "Measuring basal area allows usage of the Empirical Yield Table and is recommended as giving the most accurate yield estimates."

3. "SPS cannot be recommended for growth projection of red alder stands, because, both in pure and mixed stands, the mortality estimates were too high and in mixed stands the diameter growth rate was overestimated."

The data base for this alder modeling effort combined research plantation data from the OSU Hardwood Silviculture Cooperative and Weyerhaeuser Company. This data base comprised 53 research sites, each planted in blocks across a broad range of initial densities with later thinning treatments imposed on plots within blocks. Permanent, buffered plots had individually tagged trees that were remeasured from year 3 to the present at 3 to 5 year intervals. Stand age of the measurements extended up to total ages of 18 years for some of the installations. The geographic distribution of the study sites was from the south central Oregon coast to Vancouver Island, BC, and included a wide range of site qualities.

The resulting red alder data set was the most comprehensive ever gathered in the region. A strength of the data was that most if not all of the plantation data were collected starting at or near establishment using more recent measurement protocols that included a substantial subsample of tree heights, heights to crown base and often largest crown widths.

The dominant height growth of the new plantations appeared to follow a different path than found in previous studies of natural red alder. It was also believed that the height growth rate of red alder was affected by both high and low density. Given that the plantation data started at very young ages and at a variety of densities, it was thought that the development of new dominant height growth equations from the plantation data that included density effects could be

successfully accomplished. This new equation could then be applied to the plantation data to estimate the site index of red alder in the plantations.

Preliminary examination of some of the OSU data indicated that red alder DBH growth rate peaked at around 6 years of age and height growth rate peaked at around 3 to 7 years in plantations. An examination of data summaries for the data set indicated that the plantation data was probably adequate for developing a new plantation model that extrapolated well to the 25 to 30 year rotation ages expected.

Another advantage of developing a fourth version of ORGANON for just plantation data was that it would be possible to use an annual growth period rather than the 5-year period used in the other versions of ORGANON. Given that the rotation age of red alder will probably be in the range of 25 to 30 years of age, it was felt that an annual growth period might be very useful in designing prescriptions for red alder plantations.

1.3 Project Objectives

The objectives of the project were:

1. Construct modeling data sets from the basic data collected for such work.
2. Use the resulting modeling data sets for plantations to develop the height-diameter; top-height/site-index; maximum crown width; largest crown width; crown profile; branch diameter; height-to-crown-base; annual diameter increment; annual height increment; annual crown recession; annual mortality rate; maximum size-density trajectory; upper, middle, and lower residuals for the diameter increment and height increment equations; and thinning modifier equations needed to parameterize a new version of ORGANON for red alder plantations (RAP-ORGANON).
3. Modify the ORGANON software to incorporate the new version of ORGANON (RAP-ORGANON).

The results of this work are reported in the remaining part of this document.

2.0 Red Alder Height-Diameter Equations

The height-diameter equation in RAP-ORGANON is used to impute missing tree heights (Larsen and Hann 1987, Wang and Hann 1988, Hanus et al. 1999a, Hanus et al. 1999b). Two equation forms were used to characterize the relationship: The exponential equation form of Larsen and Hann (1987) predicts total tree height (H) from diameter at breast height (D). The equation form of Krumland and Wensel (1988) predicts H from D, the top height of the stand (H40), and the average D associated with the top height trees (D40). The exponential model form can be applied to any stand structure, while the Krumland and Wensel (1988) equation form is applicable to only even-aged stands/plantations. In general, the Krumland and Wensel (1988) will have better precision than the exponential model form in even-aged stands/plantations.

2.1 Data

Subsampling was used to measure heights on trees in the modeling data set. The data for fitting the equations came from all of the undamaged and damaged subsampled trees on the control plots and those measurements taken before treatment on the thinned plots. Table 2.1 presents a summary of the data.

Table 2.1 Descriptive statistics for the modeling data set used in the height-diameter equations for plantation grown red alder (N=157,232).

Attribute	Mean	Minimum	Maximum	Std. Deviation
H (ft.)	24.79	4.6	84.3	13.11
D (in.)	2.71	0.2	14.2	1.92

2.2. Data Analysis and Results

The exponential equation form is:

$$H = 4.5 + \exp(b_0 + b_1 D^{b_2})$$

The equation was fit to the data using weighted nonlinear regression and a weight of 1.0/D. The resulting parameter estimates and their standard errors are shown in Table 2.2. The weighted MSE for the fit was 6.5327.

Table 2.2 Parameter estimates and their standard errors for the exponential height-diameter equation.

Parameter	Estimate	Standard Error
b_0	6.76804202	0.03413025
b_1	-4.6370303	0.03399883
b_2	-0.23108894	0.00205978

The Krumland and Wensel (1988) equation form is:

$$H = 4.5 + (H40 - 4.5)\frac{\exp[b_0 D^{b_1 + b_2 (H40 - 4.5)}]}{\exp[b_0 D40^{b_1 + b_2 (H40 - 4.5)}]}$$

The equation was fit to the data using weighted nonlinear regression and a weight of 1.0/D. The resulting parameter estimates and their standard errors are shown in Table 2.3. The weighted MSE for the fit was 2.3774.

Table 2.3 Parameter estimates and their standard errors for the Krumland and Wensel (1988) height-diameter equation.

Parameter	Estimate	Standard Error
b_0	-1.7477875	0.00426099
b_1	-0.40004105	0.00154583
b_2	-0.00497111	0.00011901

2.3 Literature Cited

Krumland, B.E. and L.C. Wensel. 1988. A generalized height-diameter equation for coastal California species. Western Journal of Applied Forestry 3: 113-115.

Hanus, M.L., D.D. Marshall, and D.W. Hann. 1999a. Height-diameter equations for six species in the coastal regions of the Pacific Northwest. Forest Research Lab., Oregon State University, Corvallis, Oregon. Research Contribution 25. 11p.

Hanus, M.L., D.W. Hann, and D.D. Marshall. 1999b. Predicting height for undamaged and damaged trees in southwest Oregon. Forest Research Lab., Oregon State University, Corvallis, Oregon. Research Contribution 27. 22p.

Larsen, D.R. and D.W. Hann. 1987. Height-diameter equations for seventeen tree species in southwest Oregon. Oregon State University, Forest Research Laboratory, Corvallis, OR. Research Paper 49. 16p.

Wang,C.-H. and D.W. Hann. 1988. Height-diameter equations for sixteen tree species in the central western Willamette Valley of Oregon. Oregon State University, Forest Research Laboratory, Corvallis, Oregon. Research Paper 51. 7p.

3.0 Top-Height/Site-Index Equation for Red Alder

The procedures and results from developing a top-height/site-index prediction equation for red alder plantations are described in detail in Weiskittel et al., (2009). The equation is used in RAP-ORGANON to predict the potential height increment of trees. The equation is also employed by RAP-ORGANON users to calculate the appropriate site index for their input tree lists.

Application of the equation to the red alder plantation modeling data found that site index was under predicted for plots with low planting densities. Therefore, a site index correction equation was also developed. The following is a summary of the equation and how it can be used to predict site index.

Site index uncorrected for planting density is calculated by:

$$SI = H40_M \cdot e^{b_1(20.0^{b_2} - A_M{}^{b_2})}$$

Where,

$H40_M$ = Measured H40 (i.e., top height) in feet
A_M = Measured total stand age from seed
SI = Predicted site index (H40 at a total stand age from seed of 20 years) in feet

Table 3.1 Regression parameters for the red alder plantation site index equation:

Parameter	Estimate	Standard Error
b_1	-4.481266	0.09841014
b_2	-0.658884	0.03442515

The above site index value must be corrected for planting densities (PDEN) under 500 trees per acre. To do this, one must calculate a relative site index (*RSI*) using the following equation:

$$RSI = 1.0 - b_3 e^{(b_4 \times PDEN^{1.5})}$$

The equation's parameters and their standard errors are found in Table 3.2 and a graph of the relationship is found in Figure 3.1.

Table 3.2 Regression parameters for the red alder plantation site index planting density correction equation (RSI):

Parameter	Estimate	Standard Error
b_3	0.36979789	0.03984259
b_4	-0.00042264	0.00004880

The corrected site index (SI_C) is then calculated by:

$SI_C = SI/RSI$

Figure 3.1 Graph of relative site index (RSI) plotted over planting density.

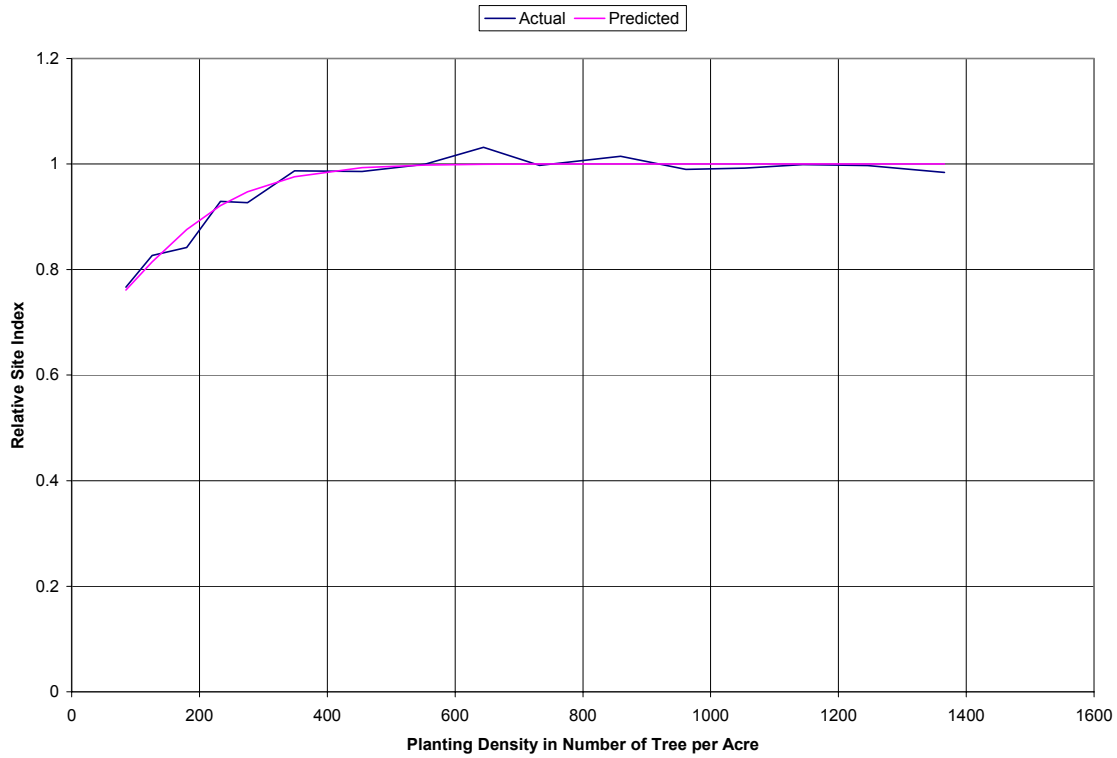

RAP-ORGANON requests the SI_C of the plantation and the PDEN value of the plantation when creating the .INP file in ORGEDIT.EXE or when using ORGEDIT.DLL and ORGRUN.DLL.

Literature Cited

Weiskittel, A.R., D.W. Hann, D.E. Hibbs, T.Y. Lam, and A.A. Bluhm. 2009. Modeling top height growth of red alder plantations. Forest Ecology and Management 258: 323-331.

4.0 Maximum Crown Width Equation for Red Alder

The maximum crown width (MCW) equation is used in RAP-ORGANON to calculate the largest crown width of stand grown trees (LCW) and crown competition factor in larger diameter trees (CCFL). CCFL is used in the RAP-ORGANON height to crown base equation.

4.1 Data

MCW modeling data set was created using selected LCW measurements from the red alder modeling data set and crown width measurements from the Champion Tree data for red alder. The Champion Tree data came from the National Champion (located in California), the Idaho State Champion, and one of the British Columbia Big trees. The red alder modeling LCW data were screened using the following criteria to choose appropriate trees for the MCW data set:

1. Crown Ratio = 1.0
2. $(H - 4.5)/D \leq 5.0$
3. $1.0 \leq LCW/H \leq 0.7$

Where,

H = Total height of the tree
D = Diameter at breast height of the tree

This data plus the three Champion Tree data resulted in 65 observations available for modeling MCW (Table 4.1).

Table 4.1 Descriptive statistics for the modeling data set used in the maximum crown width equation for plantation grown red alder (N=65).

Attribute	Mean	Minimum	Maximum	Std. Deviation
MCW (ft.)	19.42	3.54	100.0	13.03
D (in.)	6.06	0.12	91.7	11.80

4.2. Data Analysis and Results

After screening a number of alternatives including those in Paine and Hann (1982), the following equation form was fit to the MCW data set using linear regression:

$$MCW = b_0 + b_1 \times D^{0.6}$$

The resulting parameter estimates and their standard errors are found in Table 4.2 and a graph of the modeling data and predicted relationship is found in Figure 4.1.

Table 4.2 Regression parameters and their standard errors for the red alder plantation maximum crown width equation.

Parameter	Estimate	Standard Error
b_0	2.320746348	0.346911257
b_1	6.661401926	0.108114095

Figure 4.1 Actual maximum crown widths (MCW) and predicted crown widths for red alder plotted over diameter at breast height.

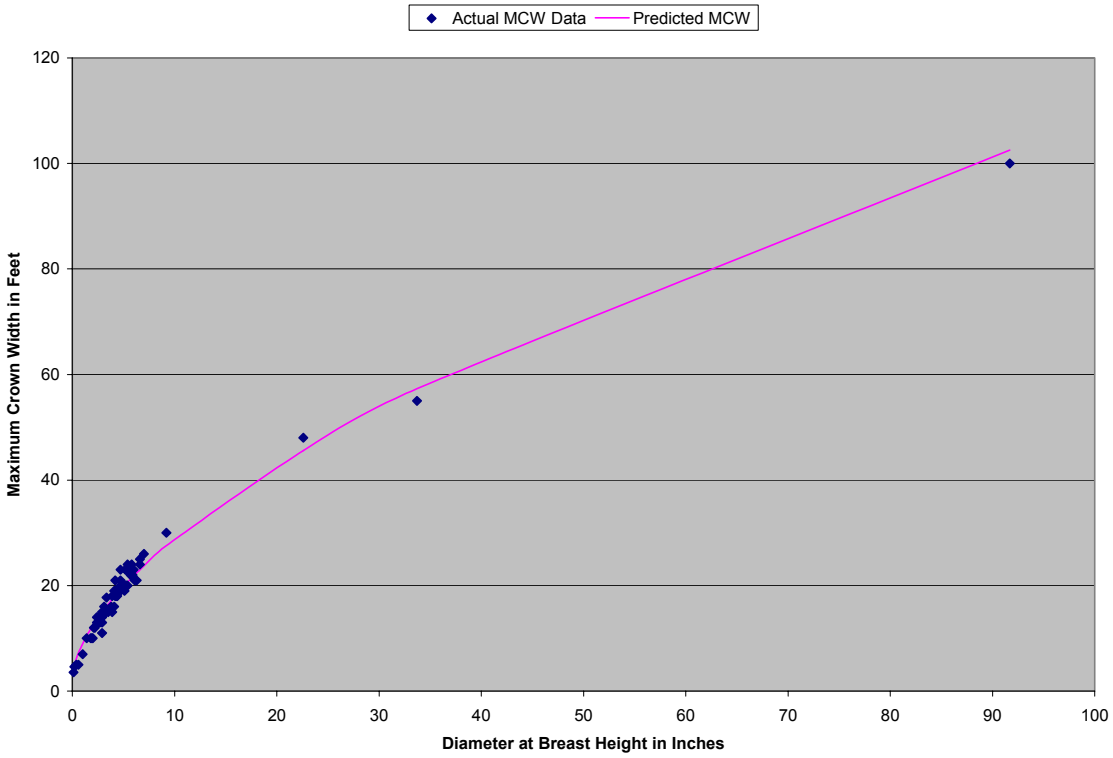

4.3 Literature Cited

Paine, D.P. and D.W. Hann. 1982. Maximum crown-width equations for southwestern Oregon tree species. Oregon State University, Forest Research Laboratory, Corvallis, OR. Research Paper 46. 20p.

5.0 Largest Crown Width Equation for Red Alder

The largest crown width of a stand grown tree (*LCW*) is used in RAP-ORGANON to predict the crown profile of a tree and the sum of largest crown areas of the stand, which can be converted to an estimate of crown closure using the conversion equation of Crookston and Stage (1999). All versions of ORGANON found in Edition 9.0 now report estimated crown closure using this conversion equation.

5.1 Data

LCW measurements were subsampled on a subset of the installations in the modeling data set. The LCW equation uses maximum crown width (MCW) predicted from diameter at breast height (D) and the crown ratio of the tree (CR). The resulting LCW modeling data set is described in Table 5.1.

Table 5.1 Descriptive statistics for the modeling data set used in the largest crown width equation for plantation grown red alder (N=33,980).

Attribute	Mean	Minimum	Maximum	Std. Deviation
LCW (ft.)	10.29	1.0	30.0	3.93
D (in.)	2.90	0.2	10.3	1.54
CR	0.82	0.09	1.00	0.20

5.2. Data Analysis and Results

Examination of the basic model form of Hann (1997) resulted in the following simplified model form being used to fit the data:

$$LCW / \hat{MCW} = b_0 \times CR^{b_1}$$

Where,

$$\hat{MCW} = \text{Predicted } MCW$$

The parameters were estimated using nonlinear regression. The resulting parameter estimates and their standard errors are found in Table 5.2.

Table 5.2 Regression parameters and their standard errors for the red alder plantation largest crown width equation.

Parameter	Estimate	Standard Error
b_0	0.78160725	0.00128068
b_1	0.44092737	0.00547738

The parameter a_0 is a modification on the *MCW* equation to adjust the equation through the average *LCW* for stand grown trees with a crown ratio of 1.0. The red alder data set has a large number of trees with crown ratio of 1.0 and the range in *LCW* values for a given DBH is quite wide in this subset of the data. The average *LCW/MCW* for this subset of the data was 0.7947147 with a standard deviation of 0.1977667. Not adjusting for this situation produced residuals with a strong trend.

The model form for predicting *LCW* is:

$$LCW = b_0 \times \hat{MCW} \times CR^{b_1}$$

5.3 Literature Cited

Crookston, N.L. and A.R. Stage. 1999. Percent canopy cover and stand structure statistics from the Forest Vegetation Simulator. USDA, Forest Service, Rocky Mountain Research Station, Fort Collins, CO. General Technical Report RMRS-GTR-24. 11p.

Hann, D.W. 1997. Equations for predicting the largest crown width of stand-grown trees in western Oregon. Oregon State University, Forest Research Laboratory, Corvallis, OR. Research Contribution 17. 14p.

6.0 Crown Profile Equations for Red Alder

The crown profile equation is used in RAP-ORGANON to calculate crown closure at the tip of the tree (CCH) (Hann 1999, Hann and Hanus 2001, Marshall et al. 2003). CCH is the density variable used in the RAP-ORGANON height increment equation.

6.1 Data

The crown profile data set consisted of measurements taken by the HSC on 46 trees from four sites and by the TASS group on 29 trees from three sites. A description of the modeling data is found in Table 6.1.

Table 6.1 Descriptive statistics for the modeling data set used in the crown profile equations for plantation grown red alder.

Attribute	Mean	Minimum	Maximum	Std. Deviation
Branch-Level Attributes Above LCW (N=362)				
CWA (ft.)	15.95	0.84	61.36	10.43
RPA	0.4930	0.0027	1.0000	0.3443
Branch-Level Attributes Below LCW (N=60)				
CWB (ft.)	23.85	8.74	61.36	11.82
RPB	0.7766	0.0000	1.0000	0.2880
Tree-Level Attributes (N=75)				
LCW (ft.)	24.77	6.06	61.36	11.44
HLCW (ft.)	37.59	7.32	116.4	25.53
DACB (ft.)	12.61	0.16	38.89	8.81
D (in.)	6.87	0.7	18.1	3.41
H (ft.)	51.02	13.1	124.0	23.83
CL (ft.)	26.04	5.76	49.65	10.20

6.2. Data Analysis and Results

Crown profile is predicted by the following equations developed by Hann (1999):

$$CWA_h = LCW \times RPA_h^{[b_0 + b_1 RPA_h^{1/2} + b_2 (H/D)]}$$

$$RPA_h = \frac{H - h}{H - HLCW}$$

$$DACB = b_3 CL \times e^{[b_4 (1.0 - \frac{H}{140})^3]}$$

$$CWB_h = LCW \times [RPB_h + b_5 (1.0 - RPB_h)]$$

$$RPB_h = \frac{h - HCB}{DACB}$$

Where,

CWA_h = Crown width, in feet, above *HLCW* at a height of h feet from the ground

HLCW = Height from ground where *LCW* occurs in feet

LCW = Largest crown width of the tree in feet

RPA_h = Relative position above *HLCW* where CWA_h is to be predicted

CWB_h = Crown width, in feet, below *HLCW* at a height of h feet from the ground

RPB_h = Relative position below *HLCW* where CWB_h is to be predicted

DACB = Distance above *HCB* to *HLCW* in feet

H = Total tree height in feet

D = Diameter at breast height in inches

HCB = Height to crown base in feet

CL = Crown length in feet (*H* – *HCB*)

h = Distance from the ground to the point where crown width is to be predicted in feet

The equations are linked by:

$$CW_h = I \bullet CWA_h + (1.0 - I) \bullet CWB_h$$

Where,

$I = 1.0$ of $h \geq HLCW$

$= 0.0$ if $h < HLCW$

The equations were fit using weighted nonlinear regression for the CWA and DACB equations and weighted linear regression for the CWB equation. The weights were $1.0/LCW^2$ for the CWA and CWB equations and $1.0/CL^2$ for the DACB equation. The resulting parameter estimates and their standard errors are found in Table 6.2. A graph of relative crown width (CWA/LCW) plotted over relative height above LCW (RPA) for various values of H/D is found in Figure 6.1.

Table 6.2 Parameter estimates and associated standard errors for the crown profile equations.

Parameter	Estimate	Standard Error
b_0	0.63420194	0.06560089
b_1	0.17649614	0.08446688
b_2	-0.02315018	0.00588773
b_3	0.63619616	0.04977539
b_4	-1.2180562	0.27600720
b_5	0.61409315	0.05053406

Figure 6.1 Relative crown width (CWA/LCW) plotted over relative height above LCW (RPA) for various values of total height divided by diameter at breast height (H/D).

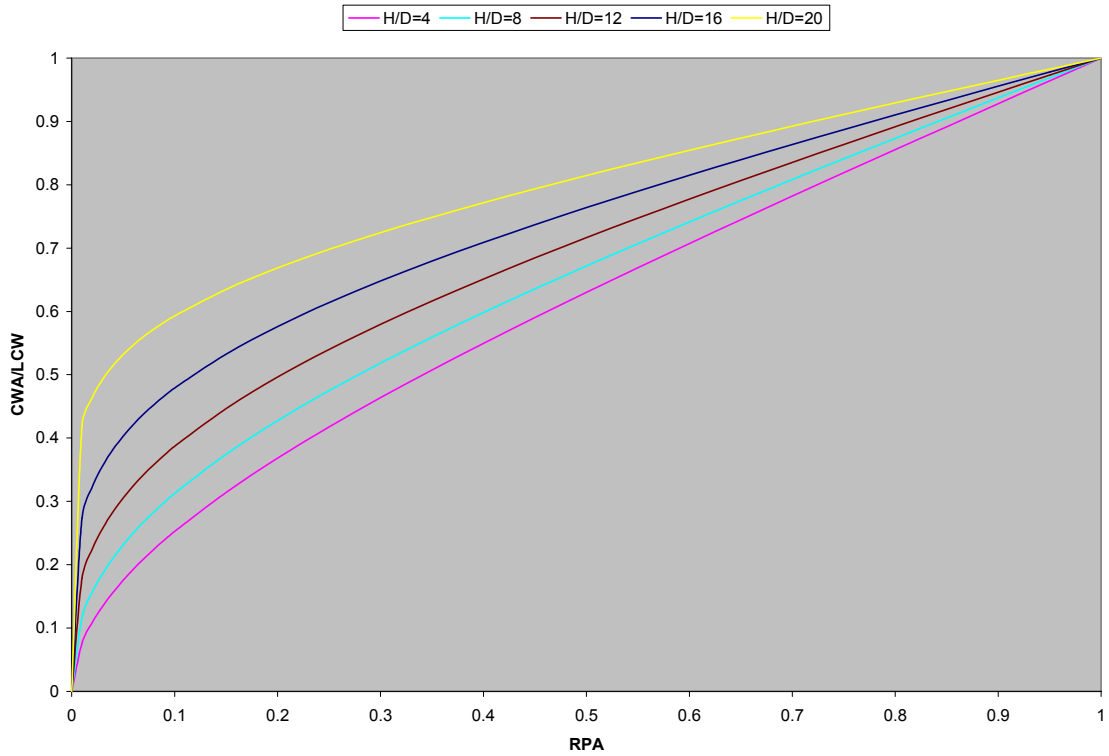

6.3 Literature Cited

Hann, D.W. 1999. An adjustable predictor of crown profile for stand-grown Douglas-fir trees. Forest Science 45:217-225.

Hann, D.W. and M.L. Hanus. 2001. Enhanced mortality equations for trees in the mixed conifer zone of southwest Oregon. Forest Research Lab., Oregon State University, Corvallis, Oregon. Research Contribution 34. 34p.

Marshall, D.D., G.P. Johnson and D.W. Hann. 2003. Crown profile equations for stand grown western hemlock in northwestern Oregon. Canadian Journal of Forest Research33: 2059-2066.

7.0 Branch Diameter Equation for Red Alder

The branch diameter (BD) equation is used in RAP-ORGANON to calculate wood quality attributes of the main stem of selected species. CCH is the density variable used in the RAP-ORGANON height increment equation.

7.1 Data

The branch diameter data set consisted of measurements taken by the HSC on 46 trees from four sites and by the TASS group on 29 trees from three sites. The attributes used to predict branch diameter is the depth into the crown (DINC) for the base of the branch, tree diameter at breast height (D), and tree crown length (CL). A description of the modeling data is found in Table 7.1.

Table 7.1 Descriptive statistics for the modeling data set used in the branch diameter equation for plantation grown red alder.

Attribute	Mean	Minimum	Maximum	Std. Deviation
Branch-Level Attributes (N=422)				
BD (in.)	1.13	0.2	3.31	0.54
DINC (ft.)	16.07	1.22	59.2	10.32
Tree-Level Attributes (N=75)				
D (in.)	6.87	0.7	18.1	3.41
CL (ft.)	26.04	5.76	49.65	10.20

7.2. Data Analysis and Results

The equation form used to predict the branch diameter of red alder in plantations is:

$$DB = b_0 DINC^{b_1 + b_2 DINC/CL} e^{b_3 D}$$

The parameters of the equation were estimated by weighted nonlinear regression with a weight of 1.0/DINC. The resulting parameter estimates and their standard errors are found in Table 7.2.

Table 7.2 Parameter estimates and associated standard errors for the branch diameter equation.

Parameter	Estimate	Standard Error
b_0	0.160884735	0.00992272
b_1	0.747251187	0.03550088
b_2	-0.132263075	0.0221245
b_3	0.024891787	0.003567198

8.0 Height-to-Crown-Base Equation for Red Alder

Two equations were developed for predicting height to crown base (HCB) in feet (Ritchie and Hann 1987, Zumrawi and Hann 1989, Hanus et al. 2000, Hann et al. 2003). The first equation was developed with a data set that included both damaged and undamaged trees and it is used in RAP-ORGANON to impute missing measurements of HCB. The second equation was developed with a data set that includes only undamaged trees and it is used in RAP-ORGANON to predict crown recession via the indirect method.

8.1 Data

Subsampling was used to measure HCB on the research plots. A detailed evaluation of the data sets found that the definition of HCB varied between two of the major contributors of data. One of the data sets defined HCB as the lowest contiguous live whorl in which ½ of the branches were alive, while the other defined HCB as the lowest contiguous live whorl in which 3/4 of the branches were alive. Both used point of branch insertion rather that bottom of foliage in their definitions. After contemplation of these findings, it was decided that the ¾ rule was the more commonly used definition of HCB equations and, therefore, that data set was used to model HCB. The data set was then divided into two subsets for modeling HCB:

1. The control plots
2. The measurements taken on the treatment plots before the treatments were applied to the plots. These data sets were first used for validation purposes and they are, therefore, called the validation plots.

Tree and stand attributes used in the HCB equation include total tree height (H), tree diameter at breast height (D), crown competition factor in larger D trees (CCFL), stand basal area (BA), and stand site index (Weiskittel et al., 2009). Tables 8.1 and 8.2 present the means, minimums, maximums, and standard deviations for the tree and stand attributes used to form the response and predictor variables. Table 8.1 describes the control plot data set and Table 8.2 describes the combined control plot and validation plot data sets.

Table 8.1 Descriptive statistics for the control plot only modeling data set used in the height-to-crown-base equation for plantation grown red alder.

Attribute	Mean	Minimum	Maximum	Standard Deviation
Tree Level attributes (N=32,675)				
HCB (ft.)	7.74	0.1	62.7	10.13
H (ft.)	23.32	4.6	84.3	15.64
CCFL (%)	105.04	0.0	672.8	123.79
D/H (in./ft.)	0.0987	0.0204	0.5886	0.0410
Plot/Measurement Level Attribute (N=456)				
BA ($ft.^2$/ac.)	41.13	0.1	153.0	37.85
Plot Level Attribute (N=102)				
SI (ft.)	62.55	32.2	85.4	11.84

Table 8.2 Descriptive statistics for the combined control plot and validation plot data set used in the height-to-crown-base equation for plantation grown red alder.

Attribute	Mean	Minimum	Maximum	Standard Deviation
Tree Level attributes (N=64,136)				
HCB (ft.)	6.10	0.0	62.7	8.62
H (ft.)	20.17	4.6	84.3	14.05
CCFL (%)	96.61	0.0	672.8	104.59
D/H (in./ft.)	0.0914	0.0105	0.5886	0.0358
Plot/Measurement Level Attribute (N=648)				
BA ($ft.^2$/ac.)	33.64	0.1	153.0	34.94
Plot Level Attribute (N=194)				
SI (ft.)	59.76	22.7	85.4	11.87

8.2 Data Analysis and Results

The basic model form of Ritchie and Hann (1987) was fit to the reduced data set and graphs of resulting residuals indicated that the constraint of predicting a zero value of either bole ratio (BR; BR = HCB/H) or HCB when BA approached zero was not reasonable. Instead, BR or HCB will approach a positive value as BA approaches zero. Mean HCB values were calculated for control plots with BA values less than 2 square feet per acre. The average HCB was 2.0 feet for the reduced data set. The following adjusted model form was therefore developed to incorporate the fact that BR (HCB) do not go to zero as BA approaches zero:

$$ABR = \{1 + EXP[b_0 + b_1 \cdot H/100 + b_2 \cdot CCFL/100 + b_3 \cdot \ln(BA) + b_4 \cdot \ln(D/H) + b_4(SI-4.5)/100]\}^{-1}$$

Where,

ABR = Adjusted Bole Ratio, (HCB-K)/(H-K)

K = Average HCB when BA $\rightarrow$0.0

The resulting equation for predicting HCB is:

$$HCB = \{H-K\}\{1 + EXP[b_0 + b_1 \cdot H/100 + b_2 \cdot CCFL/100 + b_3 \cdot \ln(BA) + b_4 \cdot \ln(D/H) + b_4(RASI-4.5)/100]\}^{-1} + K$$

The adjusted model form was fit to all measured trees on the control plots using nonlinear regression. Table 8.3 presents the resulting parameter estimates, the standard errors of the parameter estimates, the mean squared error (MSE), the adjusted coefficient of determination (R^2_{Adj}), and the bias (defined as the mean of predicted value minus the actual value) for the resulting equation.

Table 8.3 Parameter estimates and associated standard errors for the adjusted height-to-crown-base equation fit to all measured trees on the control plots.

Parameter/Statistic	Estimate	Standard Error
b_0	4.58824941	0.07879883
b_1	-1.4102602	0.09368034
b_2	-0.17053365	0.00701801
b_3	-1.3763543	0.02206727
b_4	6.56773786	0.29299522
b_5	2.91350012	0.07243143
K	2.0	NA
MSE	0.020908339	NA
R^2_{Adj}	0.6884	NA
Bias	0.0098	NA
No. Observations	32,675	NA

The adjusted BR equation was used to predict HCB for all measured trees in the modeling data set. The resulting MSE was 11.1765575, the resulting R^2_{Adj} was 0.8912, and the resulting bias was 0.0007.

The adjusted model form was also fit to all undamaged trees on the control plots using nonlinear regression. Table 8.4 presents the resulting parameter estimates, the standard errors of the parameter estimates, the mean squared error (MSE), the adjusted coefficient of determination (R^2_{Adj}), and the bias (defined as the mean of predicted value minus the actual value) for the resulting equation.

Table 8.4 Parameter estimates and associated standard errors for the adjusted height-to-crown-base equation fit to just undamaged trees on the control plots.

Parameter/Statistic	Estimate	Standard Error
b_0	2.94284934	0.06535780
b_1	-2.5574342	0.09200493
b_2	-0.18472801	0.00678202
b_3	-0.93098553	0.01808788
b_4	7.72176946	0.27813182
b_5	3.09658564	0.07244121
K	2.0	NA
MSE	0.018826917	NA
R^2_{Adj}	0.7002	NA
Bias	0.0237	NA
No. Observations	23,866	NA

The resulting adjusted BR equation was used to predict HCB for the undamaged trees in the control plot data set. The resulting MSE was 11.4139462, the resulting R^2_{Adj} was 0.8928 and the resulting bias was 0.2789.

8.3 Validation of Results

The measurement data for all measured trees on the treatment plots that were taken before thinning were used as a validation data set. The equation for the combined undamaged and damaged trees was applied to the validation data set and the MSE, R^2_{Adj}, and bias for both BR and HCB were calculated for the residuals and presented in Table 8.5. In addition, the measurement data for undamaged trees only on the treatment plots that were taken before thinning were also used as a validation data set. The equation for undamaged trees only was applied to the validation data set and the MSE, R^2_{Adj}, and bias for both BR and HCB were calculated for the residuals from the equation and also presented in Table 8.5.

Table 8.5 Validation statistics for predictions of BR and HCB from the equation fit to all measured trees data set and for predictions of BR and HCB from the equation fit to just the measured undamaged trees.

Data Set & Variable	MSE	R^2_{Adj}	Bias
Undamaged and Damaged Trees Combined (N = 31,461)			
BR	0.020287283	0.4963	0.0328
HCB	5.62709904	0.8560	0.4811
Undamaged Trees Alone (N = 23,289)			
BR	0.019604649	0.5167	0.0473
HCB	6.13569832	0.8609	0.6818

The all measured trees model and the undamaged only measured tree model validated well. Therefore, the control and validation data sets were combined to produce strengthen data sets for estimating the "final" equations.

8.4 Parameter estimates for the Combined Data

Table 8.6 contains the parameter estimates and associated standard errors for the fit of the revised model to all measured trees on the combined control and validation plots. As before, the mean HCB values were calculated for combined control and validation plots with BA values less than 2 square feet per acre. The average HCB was 1.6 feet for the HSC data set which was, therefore, used as K. The adjusted BR equations were also used to predict HCB for the data sets. The resulting MSE was 8.40309143, the resulting R^2_{Adj} was 0.8868, and the resulting bias was -0.0920.

Table 8.6 Parameter estimates and associated standard errors for the adjusted height-to-crown-base equation fit to all trees on the combined control and validation plots.

Parameter/Statistic	Estimate	Standard Error
b_0	3.98915507	0.04803913
b_1	-1.9280895	0.07071294
b_2	-0.17632543	0.00542250
b_3	-1.1178816	0.01453670
b_4	7.12804469	0.22986339
b_5	2.40273988	0.05382220
K	1.6	NA
MSE	0.018188503	NA
R^2_{Adj}	0.6164	NA
Bias	-0.0097	NA
No. Observations	64,136	NA

Table 8.7 contains the parameter estimates and associated standard errors for the fit of the revised model to undamaged measured trees on the combined control and validation plots. The adjusted BR equations were also used to predict HCB for the data sets. The resulting MSE was 8.43862534, the resulting R^2_{Adj} was 0.8922, and the resulting bias was -0.0746.

Table 8.7 Parameter estimates and associated standard errors for the adjusted height-to-crown-base equation fit to all just undamaged trees on the combined control and validation plots.

Parameter/Statistic	Estimate	Standard Error
b_0	3.73113020	0.05215223
b_1	-2.1546486	0.07716051
b_2	-0.16572840	0.00568966
b_3	-1.0649544	0.01530245
b_4	7.47699601	0.24497601
b_5	2.52953320	0.05916438
K	1.6	NA
MSE	0.016105393	NA
R^2_{Adj}	0.6469	NA
Bias	-0.0081	NA
No. Observations	47,155	NA

8.5 Literature Cited

Hann, D.W. D.D. Marshall and M.L. Hanus. 2003. Equations for predicting height-to-crown-base, 5-year diameter growth rate, 5-year height growth rate, 5-year mortality rate and maximum size-density trajectory for Douglas-fir and western hemlock in the coastal region of the Pacific Northwest. Forest Research Lab., Oregon State University, Corvallis, Oregon. Research Contribution 40. 83p.

Hanus, M.L., D.W. Hann, and D.D. Marshall. 2000. Predicting height to crown base for undamaged and damaged trees in southwest Oregon. Forest Research Lab., Oregon State University, Corvallis, Oregon. Research Contribution 29. 35p.

Ritchie, M.W. and D.W. Hann. 1987. Equations for predicting height to crown base for fourteen tree species in southwest Oregon. Oregon State University, Forest Research Laboratory, Corvallis, OR. Research Paper 50. 14p.

Weiskittel, A.R., D.W. Hann, D.E. Hibbs, T.Y. Lam, and A.A. Bluhm. 2009. Modeling top height growth of red alder plantations. Forest Ecology and Management 258: 323-331.

Zumrawi, A.A. and D.W. Hann. 1989. Height to crown base equations for six tree species in the central western Willamette Valley of Oregon. Oregon State University, Forest Research Laboratory, Research Paper 52. 9p.

9.0 Annual Diameter Increment Equation for Red Alder

The diameter growth rate (ΔD) used in RAP-ORGANON is a function of tree and plot attributes (Hann and Larsen 1991, Zumrawi and Hann 1993, Hann and Hanus 2002, Johnson 2002, Hann et al. 2003, Hann et al. 2006, Hann et al. 2008, and Gould et al. 2008). The tree attributes include diameter at breast height (D), crown ratio (CR), and basal area per acre in larger trees (BAL). The plot attributes include site index [Weiskittel et al. (2009) red alder site index (SI) in this case] and basal area per acre (BA). The definition of these variables depended upon the specific approach used to estimate the parameters. Three different approaches were used to fit the ΔD equation to the control plot data:

1. A weighted nonlinear regression fit to periodic annual increment (PAI) data, where the periodic annual variables were determined for the central year of the growth period using linear interpolation. The predictor variables used in this analysis were D, CR, BAL, BA at the start of the central, annual growth period and RASI of the plot. As with the development of previous ORGANON diameter growth rate equations, the weight used in this approach was predicted ΔD. Weighting was accomplished by dividing both sides of the equation by the square root of predicted ΔD.

2. An unweighted nonlinear regression fit to the periodic data by applying the summation of annual growth predictions procedure used by Cao (2000). The predictor variables needed in this analysis were D_S, D_E, CR_S, CR_E, BAL_S, BAL_E, BA_S, BA_E, and SI, where a subscript of S indicates the variable at the start of the variable length measurement period and a subscript of E indicates the variable at the end of the variable length measurement period. Linear interpolation was used to calculate the value of each predictor variable (except RASI, which is constant across growth periods) at the start of every annual growth period in the measurement period. The initial parameter estimates for the annual ΔD equation were then used to predict each year's ΔD and the values summed to provide an estimate of the periodic growth rate. The objective of the nonlinear regression analysis was to find the parameters of the annual ΔD equation that minimized the squared difference between the predicted and actual periodic growth rate.

3. A weighted nonlinear regression fit to the periodic data by applying a modification of the summation of annual growth predictions procedure used by Cao (2000). The approach is the same as #2 except each observation was weighted by dividing both sides of the equation by the sum of the square root of all predicted annual ΔD in the measurement period.

9.1 Data

A description of the control plots employed to form the modeling data set used in approach #1 is found in Table 9.1, and a description of the modeling data set used in approaches #2 and #3 is found in Table 9.2. A validation data set was created by including all measurements on the treatment plots that had not yet received their treatments. Therefore, the validation data set averaged smaller trees than the modeling data set. A description of the validation data set used in approach #1 is found in Table 9.3, and a description of the validation data set used in approaches #2 and #3 is found in Table 9.4.

Table 9.1 Descriptive statistics for the modeling data set used in the central PAI procedure to fit the annual ΔD equations for plantation grown red alder.

Attribute	Mean	Minimum	Maximum	Std. Deviation
Tree Level Attributes: N = 31,977				
ΔD (in.)	0.47	-0.43	2.13	0.26
D (in.)	3.51	0.2	12.8	1.91
CR	0.7539	0.0523	1.0000	0.1856
BAL ($ft.^2$/ac.)	21.54	0.00	130.31	21.20
Plot/Measurement Level Attribute: N = 600				
BA ($ft.^2$/ac.)	43.89	0.46	131.83	31.89
Plot Level Attribute: N = 196				
SI (ft.)	64.1	32.2	89.9	10.25

Table 9.2 Descriptive statistics for the modeling data set used in the summation procedures to fit the annual ΔD equations for plantation grown red alder.

Attribute	Mean	Minimum	Maximum	Std. Deviation
Tree Level Attributes: N = 31,977				
D_S (in.)	3.00	0.2	12.1	1.92
D_E (in.)	4.50	0.3	14.1	1.96
CR_S	0.8112	0.0234	1.0000	0.1986
CR_E	0.6463	0.0209	1.0000	0.2168
BAL_S ($ft.^2$/ac.)	16.18	0.00	116.91	19.41
BAL_E ($ft.^2$/ac.)	31.69	0.00	152.80	26.00
Plot/Measurement Level Attribute: N = 600				
BA_S ($ft.^2$/ac.)	35.97	0.05	118.80	31.32
BA_E ($ft.^2$/ac.)	58.72	1.12	153.02	33.68
LEN (yrs.)	3.33	1.00	7.00	0.82
Plot Level Attribute: N = 196				
SI (ft.)	64.1	32.2	89.9	10.25

Table 9.3 Descriptive statistics for the validation data set used to evaluate the central PAI procedure's annual ΔD equations for plantation grown red alder.

Attribute	Mean	Minimum	Maximum	Std. Deviation
Tree Level Attributes: N = 39,355				
ΔD (in.)	0.47	-0.75	1.65	0.22
D (in.)	2.72	0.2	9.9	1.29
CR	0.78	0.1517	1.0000	0.1507
BAL ($ft.^2$/ac.)	19.14	0.00	105.53	15.98
Plot/Measurement Level Attribute: N = 401				
BA ($ft.^2$/ac.)	40.49	2.18	105.79	23.65
Plot Level Attribute: N = 217				
SI (ft.)	60.8	33.6	86.9	9.13

Table 9.4 Descriptive statistics for the validation data set used to evaluate the summation procedures' annual ΔD equations for plantation grown red alder.

Attribute	Mean	Minimum	Maximum	Std. Deviation
Tree Level Attributes: N = 39,355				
D_S (in.)	3.00	0.2	9.6	1.28
D_E (in.)	4.50	0.2	10.8	1.44
CR_S	0.8659	0.0814	1.0000	0.1637
CR_E	0.6206	0.0484	1.0000	0.1957
BAL_S ($ft.^2$/ac.)	12.40	0.00	91.37	13.59
BAL_E ($ft.^2$/ac.)	31.63	0.00	129.14	22.11
Plot/Measurement Level Attribute: N = 401				
BA_S ($ft.^2$/ac.)	28.23	0.67	91.69	23.59
BA_E ($ft.^2$/ac.)	61.65	5.45	129.28	26.04
LEN (yrs.)	3.80	1.00	14.00	1.58
Plot Level Attribute: N = 217				
SI (ft.)	60.8	33.6	86.9	9.13

9.2 Data Analysis and Results

The following general model form of Hann et al. (2006) was used to characterize the ΔD of red alder growing in plantations:

$$\Delta D = e^{\sum_{i=0}^{6} b_i X_i} + \varepsilon_{\Delta D}$$

Where,

$X_0 = 1.0$
$X_1 = \ln(D + 1.0)$
$X_2 = D$
$X_3 = \ln[(CR + 0.2)/1.2]$
$X_4 = \ln(SI - 4.5)$
$X_5 = BAL/\ln(D + 1.0)$
$X_6 = BA^{1/2}$

The resulting parameters and their standard errors are found in Table 9.5. Each set of parameters was evaluated for how well they characterized the modeling data using both the central PAI method modeling data set and the summation method modeling data set. Each set of parameters was then validated by determining how well they characterized their respective validation data sets.

Table 9.5 Parameter estimates and their standard errors (in parentheses) for the red alder plantation ΔD equation by parameter estimation procedure.

Parameter	Weighted Central PAI Procedure	Unweighted Summation Procedure	Weighted Summation Procedure
b_0	-4.73013017 (0.04451872)	-4.6053410 (0.04324810)	-4.622849554 (0.0453393239)
b_1	0.617078735 (0.01871113)	0.46225651 (0.01703508)	0.5112200516 (0.0182059258)
b_2	-0.131579226 (0.003813577)	-0.10017843 (0.00340619)	-0.1040194568 (0.0038011080)
b_3	0.986723686 (0.0136133)	0.93919897 (0.01434444)	0.9536538143 (0.0138717802)
b_4	1.07659521 (0.01057909)	1.06721707 (0.01007074)	1.0659344724 (0.0110452327)
b_5	-0.0192994773 (0.0002247258)	-0.01968837 (0.00025341)	-0.0193047405 (0.0002369541)
b_6	-0.0718362682 (0.001593528)	-0.07194478 (0.00150313)	-0.0773539455 (0.0016475382)

9.3 Model Evaluations

For the central PAI evaluation, the periodic annual diameter growth rate was predicted for each observation in the modeling data set and the residual of predicted ΔD minus actual ΔD was then calculated. The mean residual (a measure of bias), the root mean square error (RMSE, a measure of accuracy), and the adjusted coefficient of determination (R_a^2) were then calculated from the residuals. The results are found in Table 9.6. Not surprisingly, the parameters fit using the weighted central PAI procedure had the best fit statistics. However, the two sets of parameters that were fit using the summation procedures were very close to the results from the weighted central PAI procedure. The weighted summation parameters provided somewhat better fit statistics than the unweighted summation parameters.

Table 9.6 Evaluation fit statistics for unweighted residuals (predicted minus actual) from estimating the central PAI data set using the annual ΔD model form and parameters estimated using the three alternative parameter estimation procedures.

Estimation Procedure	Bias	RMSE	R_a^2
Weighted Central PAI	+0.0000	0.1362	0.7308
Unweighted Summation	-0.0098	0.1371	0.7271
Weighted Summation	-0.0066	0.1368	0.7283

For the summation method data set evaluation, the annual diameter growth rate equations were used to predict the periodic increment for the various growth periods found in the modeling data set. This was done using the same linear interpolation procedures as was used in the parameter estimation process. Length of the growth periods varied from one to seven years. For each growth period, the mean residual, the standard deviation of the residuals (a measure of precision), and the R_a^2 were then calculated from the periodic residuals. The results were summarized by growth period and are presented in Table 9.7. In general, the three procedures produced similar fit statistics. The central PAI procedure had the best fit statistics for short growth periods and the unweighted summation procedure had the best fit statistics for longer growth periods. The fit statistics for the weighted summation procedure fell between the central PAI procedure and the unweighted summation procedure.

Table 9.7 Evaluation fit statistics for unweighted residuals (predicted minus actual) from estimating the summation procedure data set using the ΔD model form and parameters estimated using the three alternative parameter estimation procedures.

Length of Growth Period (yrs.)	Number of Observation	Weighted Central PAI Procedure	Unweighted Summation Procedure	Weighted Summation Procedure
Bias (in.)				
1	330	-0.1044	-0.1213	-0.1124
2	579	+0.0013	-0.0279	-0.0149
3	24127	+0.0108	-0.0163	-0.0069
4	4171	+0.0952	+0.0515	+0.0621
5	2391	+0.0177	+0.0102	+0.0212
6	313	+0.2745	+0.1965	+0.2426
7	66	+0.1673	+0.1649	+0.1649
Standard Deviation of Residuals (in.)				
1	330	0.2133	0.2206	0.2177
2	579	0.3120	0.3134	0.3127
3	24127	0.4332	0.4331	0.4332
4	4171	0.4255	0.4235	0.4235
5	2391	0.5001	0.4951	0.4966
6	313	0.7641	0.7495	0.7566
7	66	0.3556	0.3525	0.3524
R_a^2				
1	330	0.3690	0.2885	0.3264
2	579	0.7310	0.7259	0.7287
3	24127	0.7001	0.7000	0.7002
4	4171	0.7098	0.7221	0.7202
5	2391	0.6495	0.6567	0.6541
6	313	0.3375	0.3946	0.3635
7	66	0.4990	0.5003	0.5004

9.4 Model Validations

For the central PAI validation, the periodic annual diameter growth rate was predicted for each observation in the validation data set and the residual of predicted ΔD minus actual ΔD was then calculated. The mean residual (a measure of bias), the root mean square error (RMSE, a measure of accuracy), and the adjusted coefficient of determination (R_a^2) were then calculated from the residuals. The results are found in Table 9.8. Again, the parameters fit using the weighted central PAI procedure had the best fit statistics. However, the two sets of parameters that were fit using the summation procedures were very close to the results from the weighted central PAI procedure. The weighted summation parameters provided somewhat better fit statistics than the unweighted summation parameters.

Table 9.8 Validation fit statistics for unweighted residuals (predicted minus actual) from estimating the central PAI data set using the annual ΔD model form and parameters estimated using the three alternative parameter estimation procedures.

Estimation Procedure	Bias	RMSE	R_a^2
Weighted Central PAI	-0.0276	0.1360	0.6100
Unweighted Summation	-0.0368	0.1373	0.6025
Weighted Summation	-0.0357	0.1371	0.6034

For the summation method data set validation, the annual diameter growth rate equations were used to predict the periodic increment for the various growth periods found in the validation data set. This was done using the same linear interpolation procedures as is used in the parameter estimation process. Length of the growth periods varied from one to fourteen years. For each growth period, the mean residual, the standard deviation of the residuals (a measure of precision), and the R_a^2 were then calculated from the periodic residuals. The results were summarized by growth period and are presented in Table 9.9. Unlike the evaluation using the modeling data set, the weighted central PAI procedure had the worst bias and R_a^2 statistics for short growth periods and the best values of the statistics for long growth periods, while it produced the worst standard deviation statistics across almost all growth periods. The unweighted summation procedure produced the best standard deviation statistics across almost all growth periods. It should be emphasized that the differences between the three equations were often small in size.

Table 9.9 Validation fit statistics for unweighted residuals (predicted minus actual) from estimating the summation procedure data set using the ΔD model form and parameters estimated using the three alternative parameter estimation procedures.

Length of Growth Period (yrs.)	Number of Observation	Weighted Central PAI Procedure	Unweighted Summation Procedure	Weighted Summation Procedure
Bias (in.)				
1	155	-0.2827	-0.2802	-0.2795
2	3091	-0.3246	-0.3163	-0.3191
3	24367	-0.0042	-0.0342	-0.0301
4	7069	+0.0476	+0.0107	+0.0175
5	2812	-0.0916	-0.1178	-0.1163
6	1057	-0.7232	-0.7577	-0.7555
9	385	-1.2323	-1.2520	-1.2563
11	220	-0.9350	-0.9939	-0.9931
12	72	-0.6959	-0.7698	-0.7755
14	127	-0.7357	-0.7875	-0.7881
Standard Deviation of Residuals (in.)				
1	155	0.2078	0.2065	0.2068
2	3091	0.3324	0.3341	0.3331
3	24367	0.3889	0.3878	0.3877
4	7069	0.3851	0.3838	0.3840
5	2812	0.5463	0.5421	0.5451
6	1057	0.7538	0.7434	0.7504
7	385	0.7103	0.7058	0.7081
11	220	0.9186	0.8811	0.8873
12	72	0.5121	0.5009	0.5062
14	127	0.8923	0.8622	0.8744
R_a^2				
1	155	-1.6213	-1.5801	-1.5006
2	3091	0.1189	0.1359	0.1315
3	24367	0.6136	0.6127	0.6137
4	7069	0.7229	0.7287	0.7280
5	2812	0.6909	0.6899	0.6870
6	1057	0.1258	0.0972	0.0915
7	385	-0.1275	-0.1512	-0.1590
11	220	-1.6436	-1.7153	-1.7296
12	72	0.3176	0.2283	0.2154
14	127	-0.3332	-0.3598	-0.3818

9.5 Discussion

The results of this study indicate that the weighted central PAI procedure provided predictions that are very close to those from the two summation procedures. This finding contradicts the results reported in McDill and Amateis (1993) and Cao (2000). McDill and Amateis (1993) examined alternative methods of interpolating multiple year growth intervals to obtain estimates of annual growth rate. These methods included an "averaging" method and a "midpoint" method.

Both methods used average growth rate over the measurement interval as an estimate of the annual response variable. The averaging method used predictor variables at the start of the measurement period and the midpoint method used predictor variables at the center of the measurement period (similar to the central PAI procedure used in this study). McDill and Amateis (1993) found that both procedures produced bias estimates of annual growth rate, and Cao (2000) found that the averaging method was biased in comparison to his unweighted summation method.

One possible explanation for the difference in findings is whether or not age is used as a predictor variable in the equation. Both McDill and Amateis (1993) and Cao (2000) used age as predictor variables in their equations, while this study did not. The implication of these results is that the change in growth rate may be more linear over change in tree and/or stand size than it is over change in tree and/or stand age.

The analysis indicated that the weighted summation procedure often produced results that were a compromise between the other two procedures. As a result, this option was incorporated into RAP-ORGANON for evaluation of its behavior when combined with all of the other equations. Graphs of predictions from this equation are found in Figures 9.1 to 9.4. Figure 9.1 shows the maximum predicted ΔD for an open grown tree plotted across D for SI values of 40, 60, and 80-feet. For each SI value, an open grown tree was simulated by setting CR to 0.0, BAL to 0.0, and BA to the tree's basal area per acre (i.e., $BA = 0.005454154 \times D^2$). Figure 9.2 shows the multiplicative modifier for adjusting the predicted maximum ΔD to the tree's CR. Figure 9.3 shows the multiplicative modifier for adjusting the predicted maximum ΔD to the tree's BAL and D. Figure 9.4 shows the multiplicative modifier for adjusting the predicted maximum ΔD to the plot's measured BA.

Figure 9.1 Maximum predicted ΔD for an open grown tree with a measured D and SI. An open grown tree was simulated by setting CR to 0.0, BAL to 0.0, and BA to the tree's basal area per acre (i.e., $BA = 0.005454154 \times D^2$). Parameters of the model were determined using the weighted summation method.

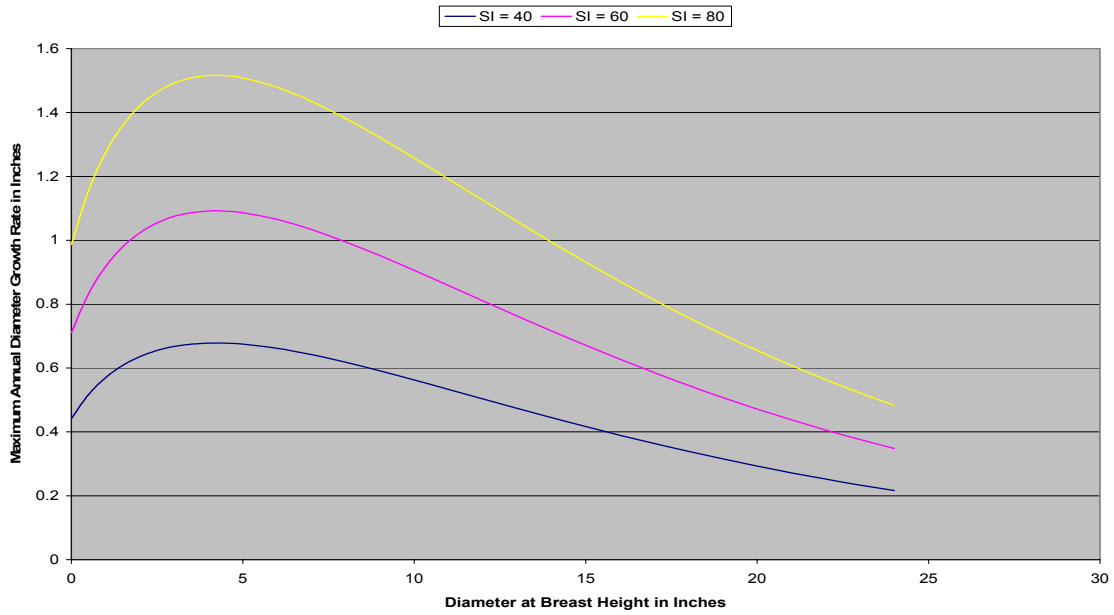

Figure 9.2 Multiplicative modifier for adjusting the predicted maximum ΔD to the tree's measured crown ratio. Parameters of the model were determined using the weighted summation method.

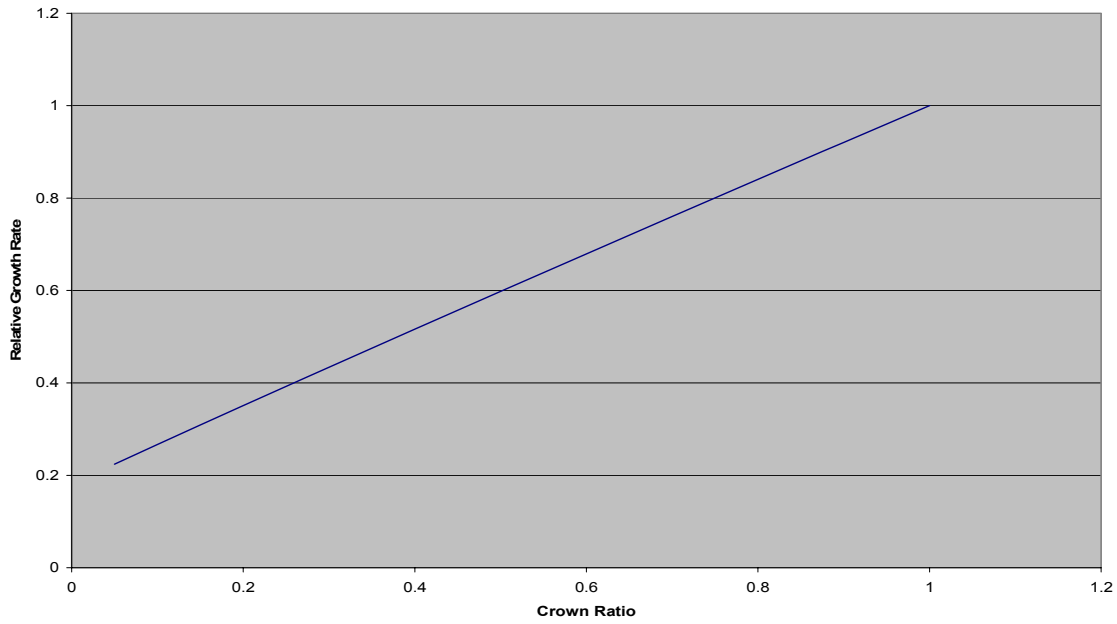

Figure 9.3 Multiplicative modifier for adjusting the predicted maximum ΔD to the tree's measured basal area in larger diameter trees and diameter at breast height (D). Parameters of the model were determined using the weighted summation method.

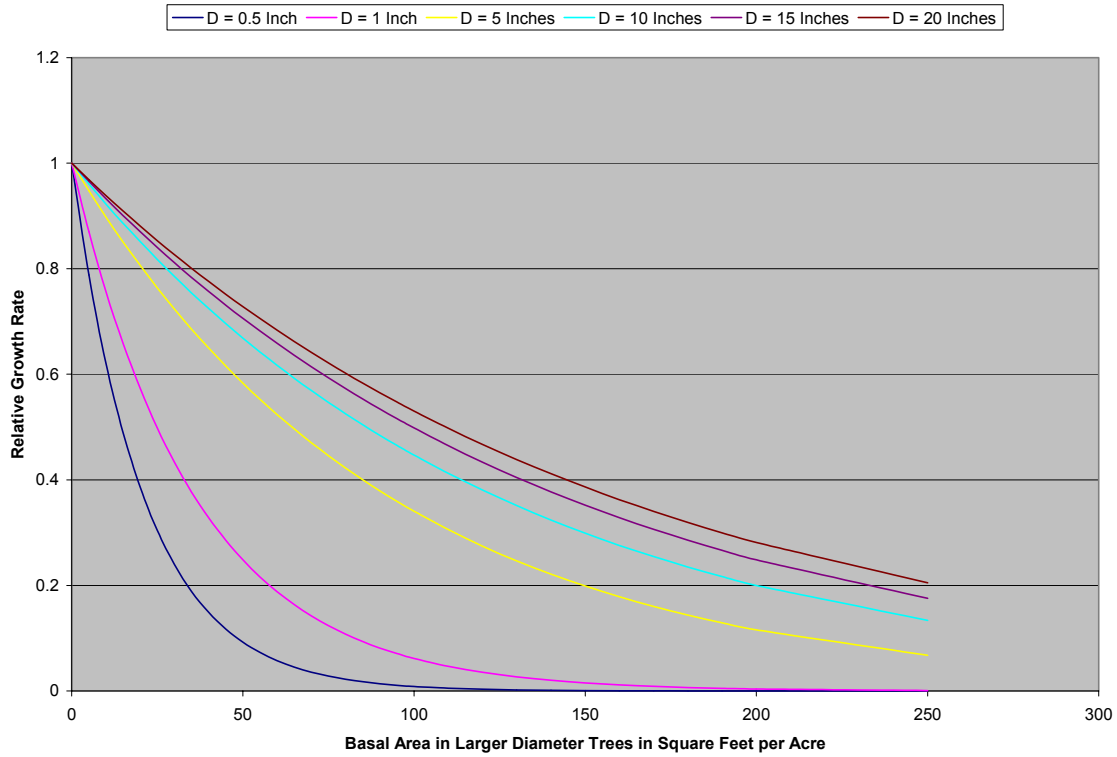

Figure 9.4 Multiplicative modifier for adjusting the predicted maximum ΔD to the plot's measured BA. Parameters of the model were determined using the weighted summation method.

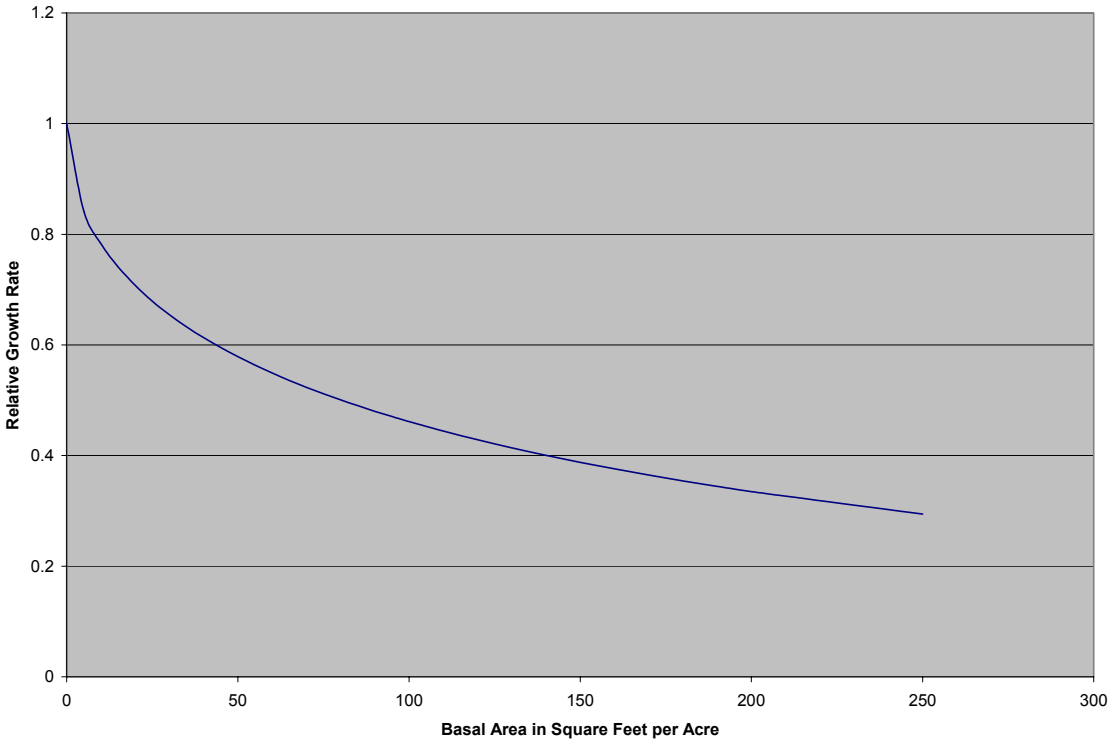

9.6 Literature Cited

Cao, Q.V. 2000. Prediction of annual diameter growth and survival for individual trees from periodic measurements. Forest Science 46: 127-131.

Gould, P.J., D.D. Marshall, and C.A. Harrington. 2008. Prediction of growth and mortality of Oregon white oak in the Pacific Northwest. Western Journal of Applied Forestry 23: 26-33.

Hann, D.W. and M.L. Hanus. 2002. Enhanced diameter-growth-rate equations for undamaged and damaged trees in southwest Oregon. Forest Research Lab., Oregon State University, Corvallis, Oregon. Research Contribution 39. 54p.

Hann, D.W. and D.R. Larsen. 1991. Diameter growth equations for fourteen tree species in southwest Oregon. Oregon State University, Forest Research Laboratory, Corvallis, Oregon. Research Bulletin 69. 18p.

Hann, D.W. D.D. Marshall and M.L. Hanus. 2003. Equations for predicting height-to-crown-base, 5-year diameter growth rate, 5-year height growth rate, 5-year mortality rate and maximum size-density trajectory for Douglas-fir and western hemlock in the coastal region of the Pacific Northwest. Forest Research Lab., Oregon State University, Corvallis, Oregon. Research Contribution 40. 83p.

Hann, D.W., D.D. Marshall, and M.L. Hanus. 2006. Re-analysis of the SMC-ORGANON equations for diameter-growth rate, height-growth rate, and mortality rate equations of Douglas-fir. Forest Research Lab., Oregon State University, Corvallis, Oregon. Research Contribution 49. 24.

Hann, D.W., D.D. Marshall, and M.L. Hanus. 2007. Reanalysis of the Western Hemlock Diameter-growth-rate Equation in SMC-ORGANON. College of Forest Resources, University of Washington, Seattle, Washington. SMC Working Paper 5. 23p.

Johnson, G. 2002. Diameter growth prediction equation. ORGANON calibration for western hemlock project, Willamette Industries. Internal Report. 21p.

McDill, M.E. and R.L. Amateis. 1993. Fitting discrete-time dynamic models having any time interval. Forest Science 39: 499-519.

Weiskittel, A.R., D.W. Hann, D.E. Hibbs, T.Y. Lam, and A.A. Bluhm. 2009. Modeling top height growth of red alder plantations. Forest Ecology and Management 258: 323-331.

Zumrawi, A.A. and D.W. Hann. 1993. Diameter growth equations for Douglas-fir and grand fir in the western Willamette Valley of Oregon. Forest Research Lab., Oregon State University, Corvallis, Oregon. Research Contribution 4. 6p.

10.0 Annual Height Increment Equation for Red Alder

The height growth rate (ΔH) equation used in RAP-ORGANON is a direct and indirect function of tree and plot attributes (Hann and Ritchie 1988, Ritchie and Hann 1990, Johnson 2000, Hann and Hanus 2002, Hann et al. 2003, and Hann et al. 2006). The tree attributes include total height (H), crown ratio (CR), and crown closure at the tip of the tree (CCH). The plot attribute is site index [red alder site index (SI) in this case]. The combination of H and SI are used to determine the tree's potential height growth rate (POTΔH), as a function of growth effective age, from the top height growth equation of Weiskittel et al. (2009), which is illustrated in Figure 10.1. The remaining attributes are used to predict a modifier equation that transforms the potential estimate to an estimate of tree's actual height growth rate.

Figure 10.1 Graph of the potential annual height increment (POTΔH) plotted across growth effective age for SI values of 30, 60, and 90 feet. POTΔH is predicted from the Weiskittel et al. (2009) top height growth equation.

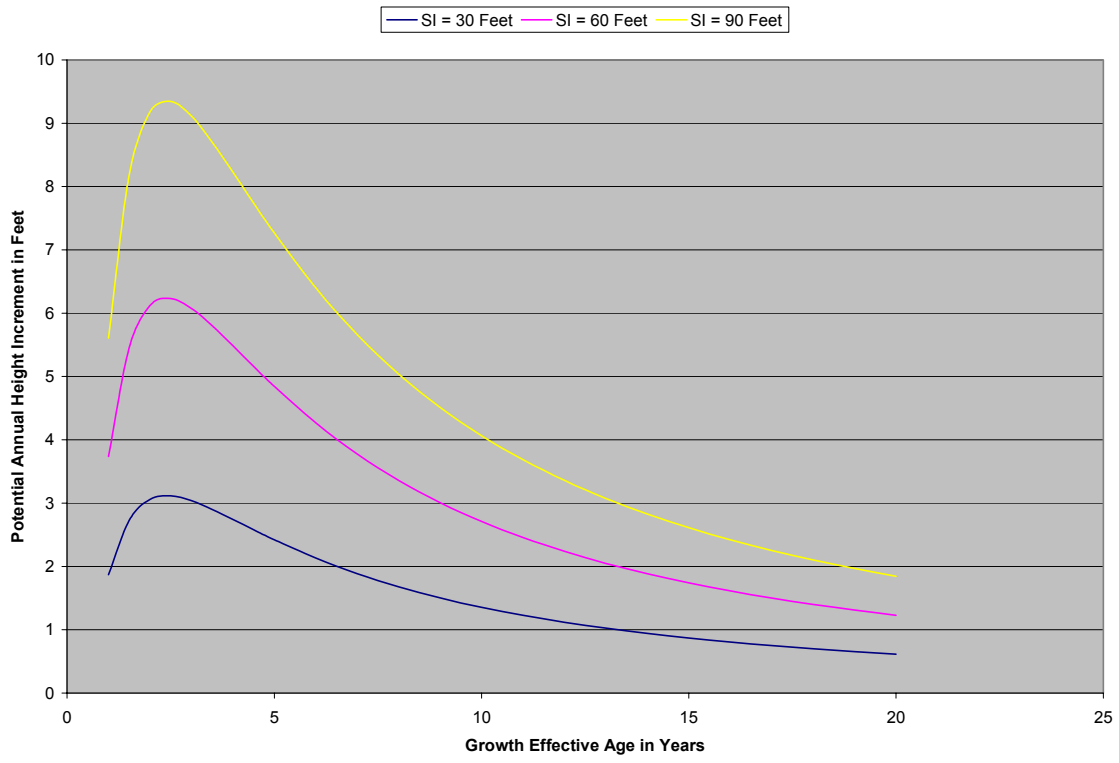

The definition of these variables depended upon the specific approach used to estimate the parameters. Three different approaches were used to fit the modifier equation the control plot data:

1. A weighted nonlinear regression fit to periodic annual increment (PAI) data, where the periodic annual variables were determined for the central year of the growth period using linear interpolation. The predictor variables used in this analysis were H, CR, and CCH at the start of the central, annual growth period, POTΔH for the growth period, and RASI of

the plot. As with the development of previous ORGANON height growth rate equations, the weight used in this approach was $POT\Delta H^2$. Weighting was accomplished by dividing both sides of the equation by $POT\Delta H$.

2. An unweighted nonlinear regression fit to the periodic data by applying the summation of annual growth predictions procedure used by Cao (2000). The predictor variables needed in this analysis were $POT\Delta H_S$, $POT\Delta H_E$, H_S, H_E, CR_S, CR_E, CCH_S, and CCH_E, where a subscript of S indicates the variable at the start of the variable length growth period and a subscript of E indicates the variable at the end of the variable length growth period. Linear interpolation was used to calculate the value of each predictor variable at the start of every annual growth period in the measurement period. The initial parameter estimates for the annual ΔH equation were then used to predict each year's ΔH and the values summed to provide an estimate of the periodic growth rate. The objective of the nonlinear regression analysis was to find the parameters of the annual ΔH equation that minimized the squared difference between the predicted and actual periodic growth rate.

3. A weighted nonlinear regression fit to the periodic data by applying a modification of the summation of annual growth predictions procedure used by Cao (2000). The approach is the same as #2 except each observation was weighted by dividing both sides of the equation by the sum of all predicted annual $POT\Delta H$ in the measurement period.

10.1 Data

A description of the control plots employed to form the modeling data set used in approach #1 is found in Table 10.1, and a description of the modeling data set used in approaches #2 and #3 is found in Table 10.2. A validation data set was created by including all measurements on the treatment plots that had not yet received their treatments. Therefore, the validation data set averaged smaller trees than the modeling data set. A description of the validation data set used in approach #1 is found in Table 10.3, and a description of the validation data set used in approaches #2 and #3 is found in Table 10.4.

Table 10.1 Descriptive statistics for the modeling data set used in the central PAI procedure to fit the annual ΔH equations for plantation grown red alder.

Attribute	Mean	Minimum	Maximum	Std. Deviation
Tree Level Attributes: N = 31,997				
ΔH (ft.)	3.42	-7.2	12.13	1.66
$POT\Delta H$ (ft.)	4.24	0.63	8.57	1.43
H (ft.)	29.19	5.3	76.8	11.41
CR	0.7539	0.0523	1.0000	0.1856
CCH (%)	19.32	0.00	197.26	24.99
Plot Level Attribute: N = 196				
SI (ft.)	64.1	32.2	89.9	10.25

Table 10.2 Descriptive statistics for the modeling data set used in the summation procedures to fit the annual ΔH equations for plantation grown red alder.

Attribute	Mean	Minimum	Maximum	Std. Deviation
Tree Level Attributes: N = 31,997				
$POT\Delta H_S$ (ft.)	4.64	0.7	8.8	1.55
$POT\Delta H_E$(ft.)	3.46	0.5	8.5	1.21
H_S (in.)	25.45	4.6	74.1	11.85
H_E (in.)	36.35	5.6	84.0	11.01
CR_S	0.8112	0.0234	1.0000	0.1986
CR_E	0.6463	0.0209	1.0000	0.2168
CCH_S (%)	16.86	0.00	222.35	23.41
CCH_E (%)	24.00	0.00	233.53	31.59
Plot/Measurement Level Attribute: N = 600				
LEN (yrs.)	3.33	1.00	7.00	0.82
Plot Level Attribute: N = 196				
SI (ft.)	64.1	32.2	89.9	10.25

Table 10.3 Descriptive statistics for the validation data set used to evaluate the PAI procedure's annual ΔH equations for plantation grown red alder.

Attribute	Mean	Minimum	Maximum	Std. Deviation
Tree Level Attributes: N = 39,355				
ΔH (ft.)	3.79	-6.5	11.3	1.49
POTΔH (ft.)	4.51	1.13	7.97	1.01
H (ft.)	25.19	5.0	71.0	8.63
CR	0.7800	0.1517	1.0000	0.1507
CCH (%)	19.26	0.00	182.44	21.94
Plot Level Attribute: N = 217				
SI (ft.)	60.8	33.6	86.9	9.13

Table 10.4 Descriptive statistics for the validation data set used to evaluate the summation procedures' annual ΔH equations for plantation grown red alder.

Attribute	Mean	Minimum	Maximum	Std. Deviation
Tree Level Attributes: N = 39,355				
$POT\Delta H_S$ (ft.)	5.01	1.2	8.3	1.11
$POT\Delta H_E$(ft.)	3.59	0.6	7.9	0.92
H_S (in.)	20.71	4.6	67.6	8.78
H_E (in.)	33.47	4.6	77.8	9.22
CR_S	0.8659	0.0814	1.0000	0.1637
CR_E	0.6206	0.0484	1.0000	0.1957
CCH_S (%)	16.16	0.00	191.47	19.64
CCH_E (%)	25.09	0.00	220.24	30.45
Plot/Measurement Level Attribute: N = 401				
LEN (yrs.)	3.80	1.00	14.00	1.58
Plot Level Attribute: N = 217				
SI (ft.)	60.8	33.6	86.9	9.13

10.2 Data Analysis and Results

The general model form from Hann et al. (2006) was used to predict ΔH of red alder growing in plantations. The equation is a product of POTΔH and a modifier equation (MOD):

$\Delta H = POT\Delta H \times MOD + \varepsilon_{\Delta H}$

Where,

$$MOD = b_0(e^{b_1+b_2CCH} + (e^{b_3CCH^{0.5}} - e^{b_1+b_2CCH})e^{-(1.0-CR)^2 e^{b_4CCH^{0.5}}}$$

The resulting parameters and their standard errors are found in Table 10.5. Each set of parameters was evaluated for how well they characterized the modeling data using both the central PAI method modeling data set and the summation method modeling data set. Each set of parameters was then validated by determining how well they characterized their respective validation data sets.

Table 10.5 Parameter estimates and their standard errors (in parentheses) for the red alder plantation annual ΔH equation by parameter estimation procedure.

Parameter	Weighted Central PAI Procedure	Unweighted Summation Procedure	Weighted Summation Procedure
b_0	1.07563185 (0.004232771)	1.0002764167 (0.0037601738)	1.0476380753 (0.0042298975)
b_1	-0.254739839 (0.02525384)	-0.0389491614 (0.0190624666)	-0.2109222796 (0.0237370949)
b_2	-0.0128743358 (0.001282122)	-0.0137069834 (0.0005511120)	-0.0134163653 (0.0010933858)
b_3	-0.070294082 (0.001259503)	-0.0510931238 (0.0011535441)	-0.0609398629 (0.0013363562)
b_4	0.120539836 (0.01963069)	0.2058143848 (0.0109072936)	0.1469442410 (0.0166954912)

10.3 Model Evaluations

For the central PAI analysis, the annual height growth rate was predicted for each observation and the residual of predicted ΔH minus actual ΔH was then calculated. The mean residual (a measure of bias), the root mean square error (RMSE, a measure of accuracy), and the adjusted coefficient of determination (R_a^2) were then calculated from the residuals. The results are found in Table 10.6. Surprisingly, the parameters fit using the weighted summation procedure had the best values for all three evaluation statistics. The weighted central PAI procedure provided somewhat better fit statistics than the unweighted summation procedure.

Table 10.6 Evaluation fit statistics for unweighted residuals (predicted minus actual) from estimating the central PAI procedure data set using the annual ΔH model form and parameters estimated using the three alternative parameter estimation procedures.

Estimation Procedure	Bias	RMSE	R_a^2
Weighted Central PAI	+0.0133	1.0567	0.5957
Unweighted Summation	-0.0196	1.0555	0.5966
Weighted Summation	+0.0130	1.0545	0.5974

For the summation data set analysis, the annual height growth rate equations were used to predict the periodic increment for the various growth periods found in the data set. This was done using the same linear interpolation procedures as was used in the parameter estimation process. Length of the growth periods varied from one to eleven years. For each growth period, the mean residual, the standard deviation of the residuals (a measure of precision), and the R_a^2 were then calculated from the periodic residuals. The results were summarized by growth period and are presented in Table 10.7. In general, the three procedures produced similar fit statistics. Overall, the weighted summation procedure had slightly better fit statistics, followed closely by the unweighted summation procedure.

Table 10.7 Evaluation fit statistics for unweighted residuals (predicted minus actual) from estimating the summation procedure data set using the annual ΔH model form and parameters estimated using the three alternative parameter estimation procedures.

Length of Growth Period (yrs.)	Number of Observation	Weighted Central PAI Procedure	Unweighted Summation Procedure	Weighted Summation Procedure
Bias (ft.)				
1	330	-0.0468	-0.2064	-0.0838
2	579	+0.4377	+0.3137	+0.4160
3	24127	+0.0211	-0.1084	+0.0112
4	4171	+0.4506	+0.3934	+0.4754
5	2391	-0.1961	-0.1695	-0.2369
6	313	+0.3381	+0.1073	+0.2948
7	66	+0.1287	+0.5358	+0.1080
Standard Deviation of Residuals (ft.)				
1	348	1.4158	1.4120	1.4147
2	753	2.9983	2.9911	2.9886
3	23480	3.2396	3.2025	3.2174
4	4244	4.1126	4.1218	4.1256
5	1471	4.2295	4.2407	4.2274
6	383	3.4587	3.4870	3.4731
7	66	3.4049	3.3938	3.3984
R_a^2				
1	348	0.2155	0.2039	0.2148
2	753	0.4723	0.4801	0.4767
3	23480	0.5873	0.5963	0.5930
4	4244	0.3326	0.3316	0.3276
5	1471	0.3904	0.3876	0.3905
6	383	0.1947	0.1884	0.1898
7	66	0.1819	0.1679	0.1854

10.4 Model Validations

For the central PAI validation, the periodic annual diameter growth rate was predicted for each observation in the validation data set and the residual of predicted ΔD minus actual ΔD was then calculated. The mean residual (a measure of bias), the root mean square error (RMSE, a measure of accuracy), and the adjusted coefficient of determination (R_a^2) were then calculated from the residuals. The results are found in Table 10.8. The parameters fit using the weighted central PAI procedure had the best fit statistics by a very small margin over the weighted summation procedure.

Table 10.8 Validation fit statistics for unweighted residuals (predicted minus actual) from estimating the central PAI procedure data set using the annual ΔH model form and parameters estimated using the three alternative parameter estimation procedures.

Estimation Procedure	Bias	RMSE	R_a^2
Weighted Central PAI	-0.1482	1.0484	0.5066
Unweighted Summation	-0.1586	1.0592	0.4963
Weighted Summation	-0.1351	1.0490	0.5060

For validations using the summation method data set, the annual diameter growth rate equations were used to predict the periodic increment for the various growth periods found in the validation data set. This was done using the same linear interpolation procedures as was used in the parameter estimation process. Length of the growth periods varied from one to fourteen years. For each growth period, the mean residual, the standard deviation of the residuals (a measure of precision), and the R_a^2 were then calculated from the periodic residuals. The results were summarized by growth period and are presented in Table 10.9. Again, the weighted summation procedure had the best overall fit statistics, followed by the unweighted summation procedure.

Table 10.9 Validation fit statistics for unweighted residuals (predicted minus actual) from estimating the summation procedure data set using the annual ΔH model form and parameters estimated using the three alternative parameter estimation procedures.

Length of Growth Period (yrs.)	Number of Observation	Weighted Central PAI Procedure	Unweighted Summation Procedure	Weighted Summation Procedure
Bias (ft.)				
1	155	-0.7175	-0.8223	-0.7428
2	3091	-1.6413	-1.7290	-1.6434
3	24367	-0.4002	-0.4502	-0.3540
4	7069	+0.5144	+0.4739	+0.5223
5	2812	-0.0562	-0.0704	-0.0958
6	1057	-2.7851	-2.9100	-2.7831
9	385	-0.9292	-1.0381	-0.9661
11	220	+0.5023	+0.1886	+0.4418
12	72	+1.4726	+1.2894	+1.3897
14	127	+3.3556	+3.2961	+3.3466
Standard Deviation of Residuals (ft.)				
1	155	1.4419	1.3932	1.4200
2	3091	2.5902	2.6029	2.5840
3	24367	3.2320	3.2078	3.2194
4	7069	3.4140	3.4068	3.4211
5	2812	3.6718	3.6660	3.6551
6	1057	4.0049	3.9939	3.9948
9	385	6.2699	6.3443	6.3234
11	220	3.5710	3.3710	3.4991
12	72	3.2538	3.1308	3.1681
14	127	5.0375	5.1123	5.0850
R_a^2				
1	155	-0.4559	-0.4697	-0.4417
2	3091	0.1947	0.1637	0.1968
3	24367	0.4296	0.4357	0.4359
4	7069	0.4591	0.4632	0.4566
5	2812	0.6908	0.6917	0.6934
6	1057	0.5561	0.5445	0.5578
9	385	0.6200	0.6091	0.6130
11	220	0.7339	0.7667	0.7455
12	72	0.0560	0.1518	0.1144
14	127	-0.0660	-0.0765	-0.0782

10.5 Discussion

The results of this study indicate that the central PAI procedure provided predictions that are close to those from the two summation procedures, particularly the weighted summation procedure. This finding contradicts the results reported in McDill and Amateis (1993) and Cao (2000). McDill and Amateis (1993) examined alternative methods of interpolating multiple year

growth intervals to obtain estimates of annual growth rate. These methods included an "averaging" method and a "midpoint" method. Both methods used average growth rate over the measurement interval as an estimate of the annual response variable. The averaging method used predictor variables at the start of the measurement period and the midpoint method uses predictor variables at the center of the measurement period (similar to the central PAI procedure used in this study). McDill and Amateis (1993) found that both procedures produced bias estimates of annual growth rate, and Cao (2000) found that the averaging method was biased in comparison to his unweighted summation method.

One possible explanation for the difference in findings is whether or not age wasa used as a predictor variable in the equation. Both McDill and Amateis (1993) and Cao (2000) used age as predictor variables in their equations, while this study does not. The implication of these results is that the change in growth rate may be more linear over change in tree and/or stand size than it is over change in tree or stand age.

Another factor that might explain the difference in findings is the observation that the top height growth equations used to define potential ΔH peaks at an age of about 3-years from seed (Weiskittel 2009). The ages of all measurements used in this study were greater than 3-years, eliminating predictions of potential ΔH from the most nonlinear portion of the top height growth equation, making the linear interpolation assumption more reasonable.

The results of these analyses indicate that the parameters derived from the weighted summation procedure are the best for characterizing both the central PAI method data set and the summation method data set. A graph of this modifier equation can be found in Figure 10.2.

Figure 10.2 Graph of the multiplicative modifier equation on POTΔH for predicting ΔH plotted across CR for CCH values of 0, 1, 5, 20, 50, and 100 percent. POTΔH is predicted from the Weiskittel et al. (2009) top height growth equation.

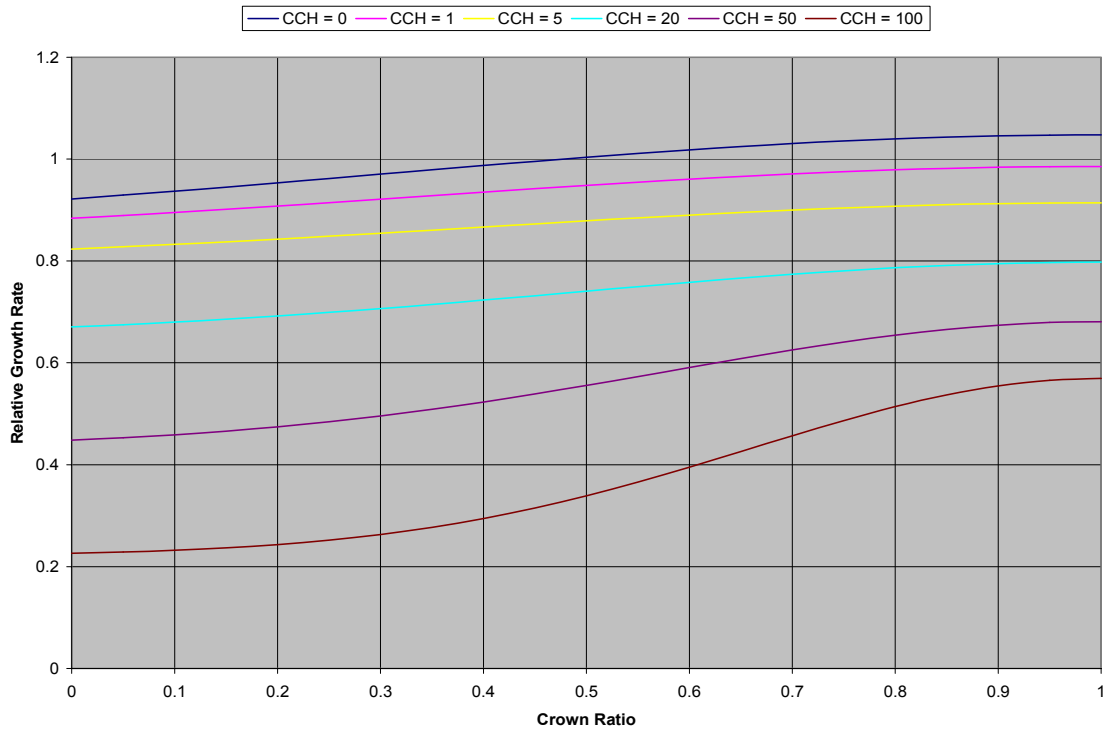

10.6 Literature Cited

Cao, Q.V. 2000. Prediction of annual diameter growth and survival for individual trees from periodic measurements. Forest Science 46: 127-131.

Hann, D.W. and M.L. Hanus. 2002. Enhanced height-growth-rate for undamaged and damaged trees in southwest Oregon. Forest Research Lab., Oregon State University, Corvallis, Oregon. Research Contribution 41. 38p.

Hann, D.W. and M.W. Ritchie. 1988. Height growth rate of Douglas-fir: A comparison of model forms. Forest Science 34: 165-175.

Hann, D.W. D.D. Marshall and M.L. Hanus. 2003. Equations for predicting height-to-crown-base, 5-year diameter growth rate, 5-year height growth rate, 5-year mortality rate and maximum size-density trajectory for Douglas-fir and western hemlock in the coastal region of the Pacific Northwest. Forest Research Lab., Oregon State University, Corvallis, Oregon. Research Contribution 40. 83p.

Hann, D.W., D.D. Marshall, and M.L. Hanus. 2006. Re-analysis of the SMC-ORGANON equations for diameter-growth rate, height-growth rate, and mortality rate equations of Douglas-fir. Forest Research Lab., Oregon State University, Corvallis, Oregon. Research Contribution 49. 24.

Johnson, G. 2000. Height growth equation. ORGANON calibration for western hemlock project, Willamette Industries. Internal Report. 9p.

McDill, M.E. and R.L. Amateis. 1993. Fitting discrete-time dynamic models having any time interval. Forest Science 39: 499-519.

Ritchie, M.W. and D.W. Hann. 1990. Height growth rate equations for six conifer species in southwest Oregon. Oregon State University, Forest Research Laboratory, Corvallis, Oregon. Research Paper 54. 12p.

Weiskittel, A.R., D.W. Hann, D.E. Hibbs, T.Y. Lam, and A.A. Bluhm. 2009. Modeling top height growth of red alder plantations. Forest Ecology and Management 258: 323-331.

11.0 Annual Crown Recession Equation for Red Alder

The crown recession rate (ΔHCB) used in ORGANON is an indirect approach that uses a static HCB equation to predict HCB at the start and end of the growth period and then uses the difference as an estimate of ΔHCB. Hann and Hanus (2004) evaluated this approach versus a dynamic equation that directly predicts ΔHCB and found that the indirect method was unbiased but less precise than the direct approach. The objective of this analysis was to develop a direct dynamic equation for ΔHCB that could then be compared to the traditional indirect approach when the equations are inserted into RAP-ORGANON.

The direct ΔHCB functions of Maguire and Hann (1990) and Hann and Hanus (2004) used both tree and plot attributes. The tree attributes included predicted height growth rate (PΔH), crown ratio (CR), crown length (CL), and, possibly, growth effective age which can be computed without knowing the tree's or stand's actual age. The plot attributes included crown competition factor (CCF) and, possibly, the total number of years since seed for the plantation (TAGE). The definition of these variables depends upon the specific approach used to estimate the parameters. In this study, the estimator of PΔH is the one that was found best in the ΔH analysis (i.e., the parameters that were estimated by the weighted summation method). Three different approaches were used to estimate the parameters from the control plots data:

1. A weighted nonlinear regression fitted to periodic annual increment (PAI) data, where the periodic annual variables were determined for the central year of the growth period using linear interpolation. The predictor variables used in this analysis were PΔH, CL, CCF, GEA, or TAGE at the start of the central, annual growth period. As with the ΔHCB equations developed by Maguire and Hann (1990) and Hann and Hanus (2004), the weight used in this approach was $(CL + P\Delta H)^2$. Weighting was accomplished by dividing both sides of the equation by (CL + PΔH).

2. An unweighted nonlinear regression fit to the periodic data using the summation of annual predictions procedure used by Cao (2000). The predictor variables needed in this analysis were $P\Delta H_S$, $P\Delta H_E$, CR_S, CR_E, CL_S, CL_E, CCF_S, CCF_E, GEA_S, GEA_E, or $TAGE_S$ and $TAGE_E$, where a subscript of "S" indicates the variable at the start of the variable length measurement period and a subscript of "E" indicates the variable at the end of the variable length measurement period. Linear interpolation was used to calculate the value of each predictor variable at the start of every annual growth period in the measurement period. The initial parameter estimates for the annual ΔHCB equation were then used to predict each year's ΔHCB and the values summed to provide an estimate of the periodic crown recession rate. The objective of the nonlinear regression analysis was to find the parameters of the annual ΔHCB equation that minimized the squared difference between the predicted and actual periodic crown recession rate.

3. A weighted nonlinear regression fit to the periodic data using a modification of the summation of annual predictions procedure used by Cao (2000). The approach is the same as #2 except each observation was weighted by dividing both sides of the equation by the sum of (CL + PΔH) values in the measurement period.

11.1 Data

Because the definition of HCB differed between the two major data sets, the crown recession model was developed from the subset of the data that was collected using the "¾" rule (see section 8.0). A description of the control plot data employed to form the modeling data set that was used in approach #1 is found in Table 11.1. A description of the modeling data set used in approaches #2 and #3 is found in Table 11.2.

Table 11.1 Descriptive statistics for the modeling data set used in the central PAI procedure to fit the annual ΔHCB equations for plantation grown red alder.

Attribute	Mean	Minimum	Maximum	Std. Deviation
Tree Level Attributes: N = 11,230				
ΔHCB (ft.)	1.67	-5.00	10.80	1.72
PΔH (ft.)	3.28	0.47	7.59	1.52
CL (ft.)	19.97	0.63	51.7	8.76
CR	0.7273	0.0523	0.9908	0.1790
GEA (yr.)	7.02	1.83	22.80	3.48
Plot/Measurement Level Attribute: N = 321				
CCF (%)	223.72	10.69	670.20	169.60
TAGE (yr.)	9.1	4.5	15	3.3

Table 11.2 Descriptive statistics for the HSC modeling data set used in developing the summation procedures to fit the annual ΔHCB equations for plantation grown red alder.

Attribute	Mean	Minimum	Maximum	Std. Deviation
Tree Level Attributes: N = 11,230				
ΔHCB (ft.)	5.59	-25.0	40.0	5.96
$P\Delta H_S$ (ft.)	3.66	0.44	8.49	1.69
$P\Delta H_E$ (ft.)	2.53	0.34	6.04	1.21
CL_S (ft.)	18.43	0.30	57.1	9.64
CL_E (ft.)	23.10	0.30	61.7	9.21
CR_S	0.7549	0.0234	0.9927	0.1775
CR_E	0.6753	0.0234	0.9939	0.2187
GEA_S (yr.)	6.04	1.5	22.1	3.21
GEA_E (yr.)	8.84	1.9	32.4	4.01
Plot/Measurement Level Attribute: N = 321				
CCF_S (%)	200.09	4.81	673.401	170.79
CCF_E (%)	270.78	18.17	664.46	175.20
$TAGE_S$ (yr.)	7.97	4.0	13.0	3.04
$TAGE_E$ (yr.)	11.20	6.0	18.0	3.51
LEN (yr.)	3.24	1.00	5.00	0.71

Two validation data sets were created by including all measurements on the treatment plots that had not yet received their treatments. Therefore, the validation data sets averaged smaller trees

than the modeling data sets. A description of the validation data set used in approach #1 is found in Table 11.3. A description of the validation data set used in approaches #2 and #3 is found in Table 11.4.

Table 11.3 Descriptive statistics for the HSC validation data set used to evaluate the central PAI procedure's annual ΔHCB equations of plantation grown red alder.

Attribute	Mean	Minimum	Maximum	Std. Deviation
Tree Level Attributes: N = 7,377				
ΔHCB (ft.)	1.67	-1.53	10.60	1.46
PΔH (ft.)	4.05	1.43	6.51	0.79
CL (ft.)	13.95	1.35	44.27	4.91
CR	0.7824	0.1644	0.9824	0.1064
GEA (yr.)	4.64	1.80	15.43	1.67
Plot/Measurement Level Attribute: N = 96				
CCF (%)	215.56	61.29	487.21	94.27
TAGE (yr.)	6.2	4.0	12.0	1.8

Table 11.4 Descriptive statistics for the HSC validation data set used to evaluate the summation procedures' annual ΔHCB equations for plantation grown red alder.

Attribute	Mean	Minimum	Maximum	Std. Deviation
Tree Level Attributes: N = 7,377				
ΔHCB (ft.)	7.76	-4.6	43.9	8.43
$P\Delta H_S$ (ft.)	4.74	1.62	7.57	0.98
$P\Delta H_E$ (ft.)	2.81	0.53	5.02	0.80
CL_S (ft.)	10.67	0.6	49.3	4.82
CL_E (ft.)	20.36	2.3	55.7	6.60
CR_S	0.8321	0.0814	0.9883	0.1053
CR_E	0.7097	0.1553	1.0000	0.1831
GEA_S (yr.)	3.15	1.6	12.5	0.98
GEA_E (yr.)	7.18	2.1	29.2	3.01
Plot/Measurement Level Attribute: N = 96				
CCF_S (%)	137.56	39.42	487.21	90.78
CCF_E (%)	348.22	101.92	563.88	123.00
$TAGE_S$ (yr.)	4.53	4.0	10.0	1.23
$TAGE_E$ (yr.)	8.87	5.0	18.0	3.04
LEN (yr.)	4.33	1.0	14.0	2.83

11.2 Data Analysis and Results

Only a hand full of studies has explored the direct, nonspatial modeling of ΔHCB. Most of these were compared in Hann and Hanus (2004). Numerous modifications to the basic model forms found to be best in Hann and Hanus (2004) were explored to determine if further improvements could be made. In addition, the model forms used in Garber et al. (2008) were also examined.

This led to the following general model form for predicting ΔHCB of red alder growing in plantations:

$$\Delta HCB = \frac{(CL + P\Delta H)^{b_1}}{1.0 + e^{b_2 + b_3 X_1 + b_4 X_2^{b_5} + b_6 X_3 + b_7 X_4}} + \varepsilon_{\Delta HCB}$$

Where,

X_1 = ln(CR)

X_2 = CR

X_3 = GEA or TAGE

X_4 = ln(CCF + 1.0)

The resulting parameters and their standard errors for the equation with TAGE are found in Table 11.5. The resulting parameters and their standard errors for the equation with GEA are found in Table 11.6. Each set of parameters was evaluated for how well they characterized the modeling data using both the modeling data set for central PAI method and modeling data set for the summation method. Each set of parameters was then validated by determining how well they characterized their respective validation data sets.

Table 11.5. Parameter estimates and their standard errors (in parentheses) for the red alder plantation ΔHCB equation with TAGE by parameter estimation procedure.

Parameter	Weighted Central PAI Procedure	Unweighted Summation Procedure	Weighted Summation Procedure
b_1	0.545425068 (0.01517984)	0.3442053099 (0.0039253997)	0.7374535173 (0.0269536524)
b_2	3.99861543 (0.1362829)	7.6269495390 (0.8815276825)	3.4614649396 (0.1309499470)
b_3	-1.24030707 (0.1038381)	-4.033712491 (0.5764435780)	-0.5680935469 (0.0856820011)
b_4	5.80378650 (0.3730760)	6.2822530362 (0.7348660158)	3.0098998107 (0.1760548607)
b_5	8.84670718 (0.5426171)	3.1879346100 (0.5371539655)	7.0831395083 (0.6046341165)
b_6	0.115437331 (0.005402653)	0.0195744407 (0.0088573027)	0.0992286447 (0.0037978418)
b_7	-1.05840405 (0.04225245)	-2.453873954 (0.1189008269)	-0.6753368214 (0.0283170606)

Table 11.6 Parameter estimates and their standard errors (in parentheses) for the red alder plantation ΔHCB equation with GEA by parameter estimation procedure.

Parameter	Weighted Central PAI Procedure	Unweighted Summation Procedure	Weighted Summation Procedure
b_1	0.512201507 (0.01549502)	0.3414098304 (0.0037204820)	0.8262156107 (0.0366235567)
b_2	4.60162015 (0.1595692)	8.0614123644 (0.9992208917)	4.0867738376 (0.1311533940)
b_3	-1.80237600 (0.1268554)	-4.397001890 (0.6449398876)	-0.6873315869 (0.0831751935)
b_4	6.09697269 (0.4148633)	6.6389905998 (0.8576567340)	2.8593138798 (0.1908428082)
b_5	9.06857199 (0.5772720)	3.0153613105 (0.5342893749)	7.8354198003 (0.6849236625)
b_6	0.0720336609 (0.004712209)	0.0 (NA	0.0700692943 (0.0037012161)
b_7	-1.15230096 (0.05018275)	-2.582727032 (0.1263938710)	-0.6458862494 (0.0268879876)

11.3 Model Evaluations

For the central PAI analysis, the annual ΔHCB rate was predicted for each observation and the residual of predicted ΔHCB minus actual ΔHCB was then calculated. The mean residual (a measure of bias), the root mean square error (RMSE, a measure of accuracy), and the adjusted coefficient of determination (R_a^2) were then calculated from the residuals. The results are found in Table 11.7 for the equations with TAGE and in Table 11.8 for the equations with GEA. The bias statistics for both model forms were within the measurement precision of ΔHCB. In general, the R_a^2 statistics were largest for the weighted central PAI estimation method and the lowest for the weighted summation estimation method. The R_a^2 statistic for unweighted summation estimation method was highest for the equation with TAGE, and the R_a^2 statistic for weighted central PAI estimation method was the highest for the equation with GEA. Contrary to the previous study of Hann and Hanus (2004), the unweighted summation analysis did not find the GEA variable to be statistically significant.

Table 11.7 Evaluation fit statistics for unweighted residuals (predicted minus actual) from estimating the central PAI data set using the annual ΔHCB model form with TAGE and parameters estimated using the three alternative parameter estimation procedures.

Estimation Procedure	Bias (ft.)	RMSE (ft.)	R_a^2
Weighted Central PAI	-0.0390	1.3380	0.3968
Unweighted Summation	-0.0346	1.3375	0.3973
Weighted Summation	-0.0598	1.3511	0.3850

Table 11.8 Evaluation fit statistics for unweighted residuals (predicted minus actual) from estimating the central PAI data set using the annual ΔHCB model form with GEA and parameters estimated using the three alternative parameter estimation procedures.

Estimation Procedure	Bias (ft.)	RMSE (ft.)	R_a^2
Weighted Central PAI	-0.0239	1.3279	0.4058
Unweighted Summation	-0.0492	1.3381	0.3967
Weighted Summation	-0.0687	1.3468	0.3889

For the summation method data set analysis, the annual crown recession rate equations were used to predict the periodic increment for the various growth periods found in the data set. This was done using the same linear interpolation procedures used in the parameter estimation process. Length of the growth periods varied from one to eleven years. For each growth period, the mean residual, the standard deviation of the residuals (a measure of precision), and the R_a^2 were then calculated from the periodic residuals. The results were summarized by growth period and are presented in Table 11.9 for the equations with TAGE and in Table 11.10 for the equations with GEA. The evaluation statistics vary substantially between model form and length of growth period. Concentrating on the growth periods with the largest number of observations (i.e., growth periods with either three or five years in length), the bias statistics seem to be about the same for the three parameter estimation methods and the two model forms, while the R_a^2 statistics are largest for the unweighted summation method. The equations with GEA seemed to have somewhat larger R_a^2 statistics that the equations with TAGE.

Table 11.9 Evaluation fit statistics for unweighted residuals (predicted minus actual) from estimating the summation procedure data set using the ΔHCB model form with TAGE and parameters estimated using the three alternative parameter estimation procedures.

Length of Growth Period (yrs.)	Number of Observation	Weighted Central PAI Procedure	Unweighted Summation Procedure	Weighted Summation Procedure
Bias (ft.)				
1	19	+0.0858	+0.3031	-0.0587
2	137	+0.0362	+0.4247	-0.4097
3	9536	-0.1498	-0.3437	-0.1131
5	1538	-1.8386	+0.8918	-2.2550
Standard Deviation of Residuals (ft.)				
1	19	2.6538	2.6791	2.5693
2	137	3.5315	3.6226	3.4708
3	9536	4.0777	4.0297	4.0832
5	1538	7.2873	6.8966	7.0920
R_a^2				
1	19	-0.2684	-0.3088	-0.1883
2	137	-0.0924	-0.1652	-0.0698
3	9536	0.3857	0.3966	0.3844
5	1538	0.0085	0.1512	0.0279

Table 11.10 Evaluation fit statistics for unweighted residuals (predicted minus actual) from estimating the summation procedure data set using the ΔHCB model form with GEA and parameters estimated using the three alternative parameter estimation procedures.

Length of Growth Period (yrs.)	Number of Observation	Weighted Central PAI Procedure	Unweighted Summation Procedure	Weighted Summation Procedure
Bias (ft.)				
1	19	+0.1898	+0.3148	-0.0413
2	137	+0.2574	+0.4149	-0.3345
3	9536	-0.2025	-0.4026	-0.2083
5	1538	-0.8388	+1.0061	-1.5694
Standard Deviation of Residuals (ft.)				
1	19	2.7649	2.6856	2.6852
2	137	3.6324	3.6322	3.5703
3	9536	4.0642	4.0276	4.0866
5	1538	7.3662	6.8721	7.1546
R_a^2				
1	19	-0.3822	-0.3164	-0.2975
2	137	-0.1614	-0.1706	-0.1263
3	9536	0.3891	0.3956	0.3823
5	1538	0.0352	0.1533	0.0583

11.4 Model Validations

For the central PAI analysis, the annual ΔHCB rate was predicted for each observation and the residual of predicted ΔHCB minus actual ΔHCB was then calculated. The mean residual (a measure of bias), the root mean square error (RMSE, a measure of accuracy), and the adjusted coefficient of determination (R_a^2) were then calculated from the residuals. The results are found in Table 11.11 for the equations with TAGE and in Table 11.12 for the equations with GEA. The bias statistics for both model forms were within the measurement precision of the ΔHCB. In general, the R_a^2 statistics were largest for the weighted central PAI estimation method and the lowest for the unweighted summation estimation method. The one exception was the equation with TAGE fit to the HSC data set in which the weighted summation estimation method was highest value for R_a^2. For the HSC data set, the equation with GEA had higher R_a^2 statistics for the equations fit with the weighted central PAI and the unweighted summation method (the latter equation did not include GEA).

Table 11.11 Validation fit statistics for unweighted residuals (predicted minus actual) from estimating the central PAI data set using the annual ΔHCB model form with TAGE and parameters estimated using the three alternative parameter estimation procedures.

Estimation Procedure	Bias (ft.)	RMSE (ft.)	R_a^2
Weighted Central PAI	+0.2183	1.1042	0.4298
Unweighted Summation	+0.1150	1.1653	0.3649
Weighted Summation	+0.0956	1.0996	0.4345

Table 11.12. Validation fit statistics for unweighted residuals (predicted minus actual) from estimating the HSC central PAI data set using the annual ΔHCB model form with GEA and parameters estimated using the three alternative parameter estimation procedures.

Estimation Procedure	Bias (ft.)	RMSE (ft.)	R_a^2
Weighted Central PAI	+0.0976	1.0984	0.4357
Unweighted Summation	+0.0775	1.1602	0.3705
Weighted Summation	-0.0942	1.1209	0.4125

For the summation method data set analysis, the annual crown recession rate equations were used to predict the periodic increment for the various growth periods found in the data set. This was done using the same linear interpolation procedures used in the parameter estimation process. Length of the growth periods varied from one to eleven years. For each growth period, the mean residual, the standard deviation of the residuals (a measure of precision), and the R_a^2 were then calculated from the periodic residuals. The results were summarized by growth period and are presented in Table 11.13 for the equations with TAGE and in Table 11.14 for the equations with GEA. The evaluation statistics vary substantially between model form and length of growth period. Concentrating on the growth periods with the largest number of observations (i.e., growth periods with two, three, or six years in length), the bias statistics seem to be about the same for the three parameter estimation methods and the two model forms, while the R_a^2 statistics are smallest for the unweighted summation method. The equations with TAGE seemed to have somewhat larger R_a^2 statistics that the equations with GEA.

Table 11.13 Validation fit statistics for unweighted residuals (predicted minus actual) from estimating the summation procedure data set using the ΔHCB model form with TAGE and parameters estimated using the three alternative parameter estimation procedures.

Length of Growth Period (yrs.)	Number of Observation	Weighted Central PAI Procedure	Unweighted Summation Procedure	Weighted Summation Procedure
Bias (ft.)				
1	155	-0.0881	-0.3355	+0.0275
2	2916	+0.6697	+0.6161	+0.6281
3	1964	+0.1111	-0.0414	+0.0331
4	36	-0.5233	-3.9806	-0.8900
5	588	-2.6856	-4.2717	-3.4930
6	914	-1.3245	-2.8840	-2.3305
9	385	+1.6967	+0.6676	-0.4027
11	220	+2.5229	+2.7136	-0.2598
12	72	-4.8136	-5.3567	-7.5468
14	127	-2.1839	+1.0219	-5.4475
Standard Deviation of Residuals (ft.)				
1	155	1.3177	1.2183	1.2762
2	2916	2.1490	2.1558	2.0894
3	1964	4.2809	4.5866	4.2970
4	36	3.5786	3.3422	3.5005
5	588	4.4699	4.5166	4.4191
6	914	4.9156	4.8819	4.8757
9	385	7.2705	6.9874	6.8070
11	220	5.1544	4.3318	4.9912
12	72	6.8284	5.4418	6.6958
14	127	7.2976	6.4437	6.8735
R_a^2				
1	155	-0.1301	-0.0351	-0.0557
2	2916	0.0932	0.1003	0.1481
3	1964	0.3572	0.2626	0.3527
4	36	-0.1841	-1.4851	-0.1823
5	588	-0.1488	-0.6334	-0.3408
6	914	-0.0558	-0.3099	-0.1898
9	385	-0.1403	-0.0079	0.0489
11	220	0.0375	0.2361	0.2706
12	72	-2.9971	-2.3466	-4.8477
14	127	-0.6799	-0.2318	-1.2323

Table 11.14 Validation fit statistics for unweighted residuals (predicted minus actual) from estimating the summation procedure data set using the ΔHCB model form with GEA and parameters estimated using the three alternative parameter estimation procedures.

Length of Growth Period (yrs.)	Number of Observation	Weighted Central PAI Procedure	Unweighted Summation Procedure	Weighted Summation Procedure
Bias (ft.)				
1	155	-0.2167	-0.3973	-0.1345
2	2916	+0.4229	+0.5146	+0.2624
3	1964	-0.2360	-0.1561	-0.4575
4	36	-1.7832	-4.0768	-2.3885
5	588	-3.5272	-4.4210	-4.7399
6	914	-2.1463	-3.0494	-3.5587
9	385	+1.1401	+0.4390	-1.6851
11	220	+2.7696	+2.5170	-1.0488
12	72	-5.0429	-5.6028	-8.7447
14	127	-1.4629	+0.8346	-6.3651
Standard Deviation of Residuals (ft.)				
1	155	1.2814	1.2147	1.2423
2	2916	2.1228	2.1551	2.0830
3	1964	4.3389	4.5792	4.3813
4	36	3.6141	3.3431	3.6180
5	588	4.6189	4.5130	4.6639
6	914	5.1408	4.8875	5.2130
9	385	7.7384	6.9973	7.3298
11	220	5.3114	4.3004	5.3650
12	72	6.8093	5.4065	6.7562
14	127	8.6525	6.4115	8.3848
R_a^2				
1	155	-0.0943	-0.0588	-0.0116
2	2916	0.1615	0.1214	0.2112
3	1964	0.3381	0.2642	0.3198
4	36	-0.4776	-1.5577	-0.7151
5	588	-0.4272	-0.6869	-0.8690
6	914	-0.2643	-0.3522	-0.6234
9	385	-0.2516	-0.0055	-0.1572
11	220	-0.0487	0.2742	0.1273
12	72	-3.1129	-2.4807	-6.0221
14	127	-1.2284	-0.2096	-2.2155

11.5 Discussion

The results indicated that weighted central PAI estimation method produced parameters that were better fits to both the evaluation and validation central PAI data sets than the other two parameter estimation methods. The results are less clear for the summation data sets. The unweighted summation estimation method produced parameters that were better fits to the

evaluation summation data set. For the validation summation data set, the weighted central PAI estimation method seemed to produce slightly better results than the weighted summation estimation method. The equations incorporating GEA were better than the equations incorporating TAGE.

The results of this study indicate that the central PAI procedure provided predictions that are better than those from the two summation procedures. This finding contradicts the results reported in McDill and Amateis (1993) and Cao (2000). McDill and Amateis (1993) examined alternative methods of interpolating multiple year growth intervals to obtain estimates of annual growth rate. These methods included an "averaging" method and a "midpoint" method. Both methods use average growth rate over the measurement interval as an estimate of the annual response variable. The averaging method uses predictor variables at the start of the measurement period and the midpoint method uses predictor variables at the center of the measurement period (similar to the central PAI procedure used in this study). McDill and Amateis (1993) found that both procedures produced bias estimates of annual growth rate, and Cao (2000) found that the averaging method was biased in comparison to his unweighted summation method.

Given the results of these analyses, it was decided to evaluate using the parameter estimates from the weighted central PAI procedure in RAP-ORGANON. Graphs of predictions from the equation with TAGE are found in Figures 11.1 to 11.5. Graphs of predictions from the equation with GEA are found in Figures 11.6 to 11.10. Figures 11.1 and 11.6 show the maximum predicted ΔHCB plotted across (CL + PΔH). Figures 11.2, 11.3, 11.4, and 11.5 show the multiplicative modifier for TAGE values of 5, 10, 15, and 20 years, respectively, that adjusts the predicted maximum ΔHCB to the tree's CR and the plot's CCF. Figures 11.7, 11.8, 11.9, and 11.10 show the multiplicative modifier for GEA values of 5, 10, 15, and 20 years, respectively, that adjusts the predicted maximum ΔHCB to the tree's CR and the plot's CCF.

The shapes of the modifiers, where relative ΔHCB peaks across CR and is reduced by increasing CCF, agree with the previous findings of Maguire and Hann (1990) and Hann and Hanus (2004). The peak in the modifiers occurs at CR values of 0.66 and 0.69 for the equations using TAGE and GEA, respectively. The peaks in CR found by Hann and Hanus (2004) ranged from 0.62 for a similar equation with TAGE to 0.64 for a similar equation with GEA.

Figure 11.1 Maximum predicted ΔHCB for the equation with TAGE. Parameters of the equation were determined using the central weighted PAI method.

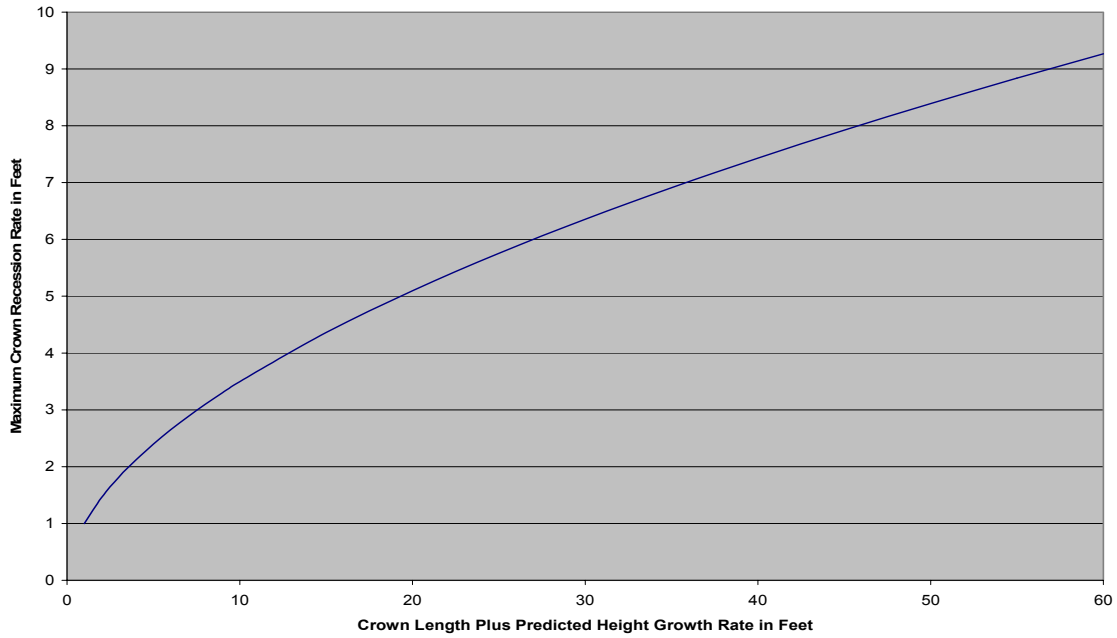

Figure 11.2 Multiplicative modifier for adjusting the predicted maximum ΔHCB to the tree's measured CR, the plot's measured CCF, and a TAGE of 5 years for the ΔHCB equation developed using TAGE. Parameters of the equation were determined using the central weighted PAI method.

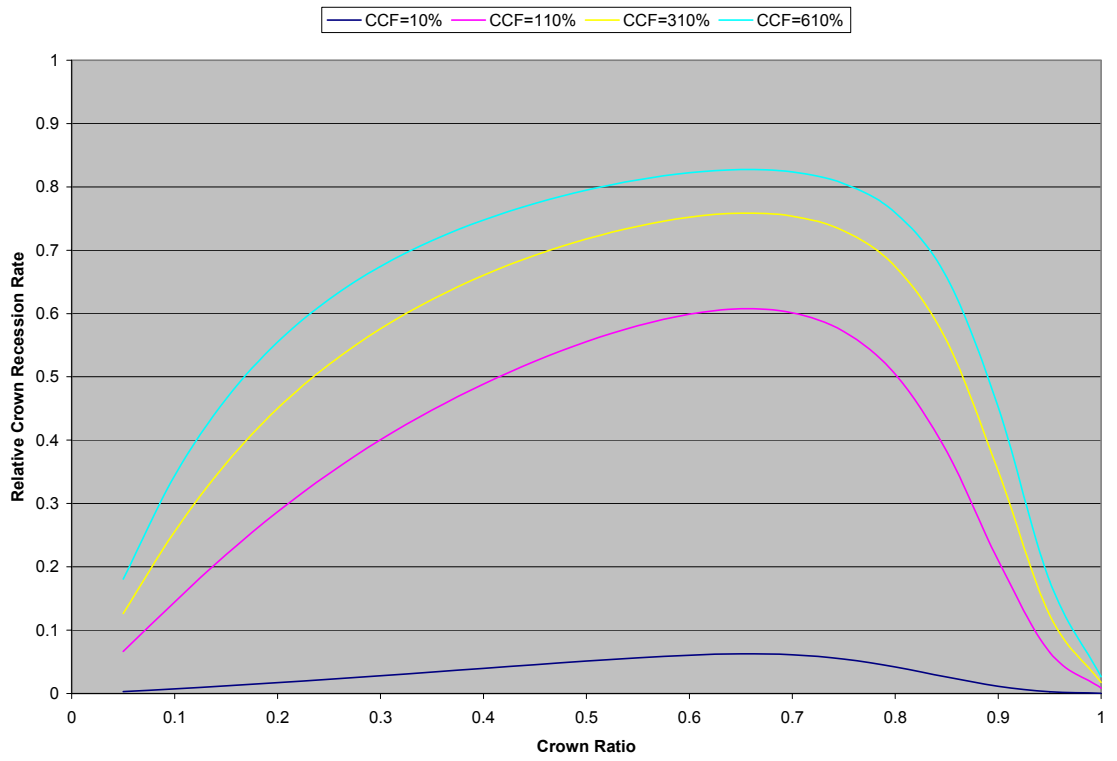

Figure 11.3 Multiplicative modifier for adjusting the predicted maximum ΔHCB to the tree's measured CR, the plot's measured CCF, and a TAGE of 10 years for the ΔHCB equation developed using TAGE. Parameters of the equation were determined using the central weighted PAI method.

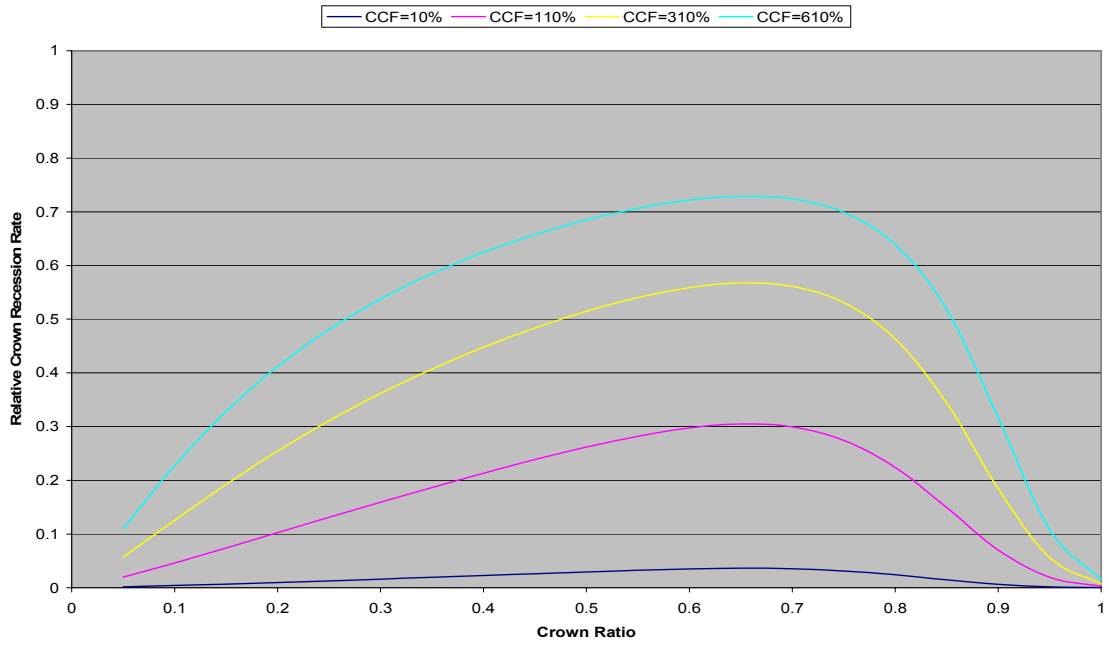

Figure 11.4 Multiplicative modifier for adjusting the predicted maximum ΔHCB to the tree's measured CR, the plot's measured CCF, and a TAGE of 15 years for the ΔHCB equation developed using TAGE. Parameters of the equation were determined using the central weighted PAI method.

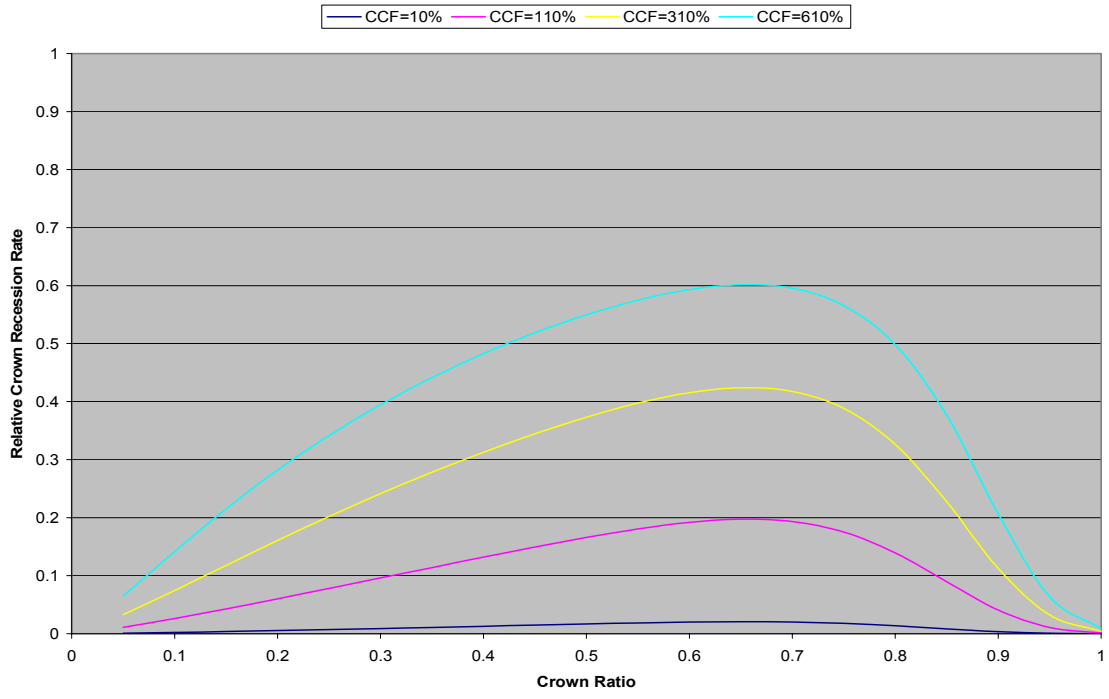

Figure 11.5 Multiplicative modifier for adjusting the predicted maximum ΔHCB to the tree's measured CR, the plot's measured CCF, and a TAGE of 20 years for the ΔHCB equation developed using TAGE. Parameters of the equation were determined using the central weighted PAI method.

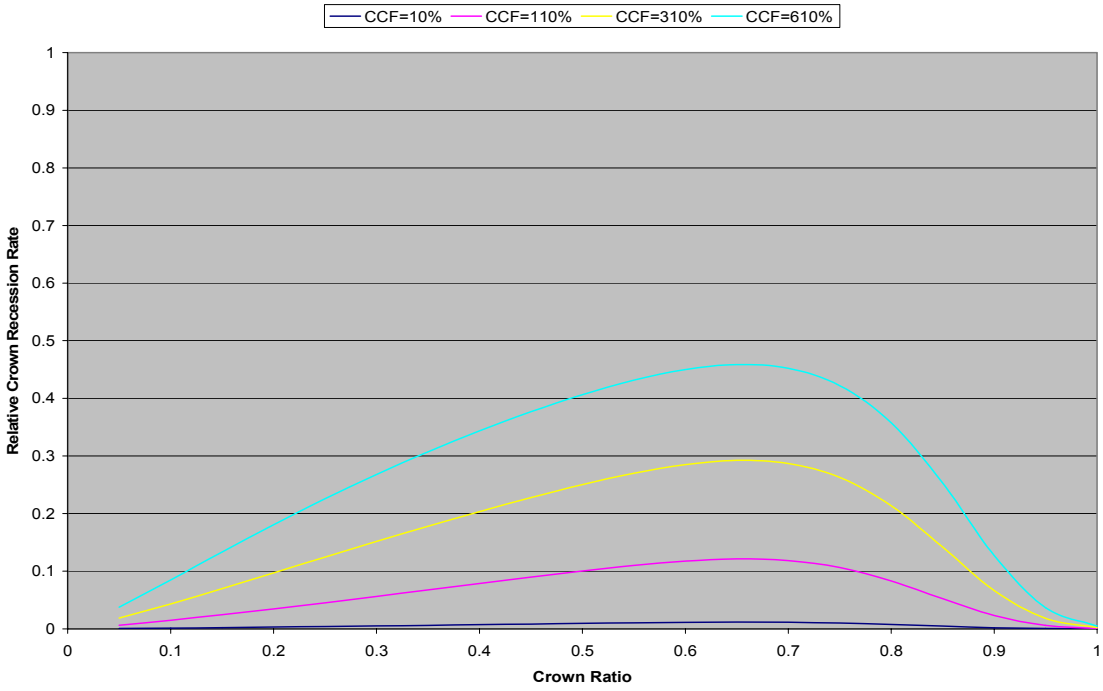

Figure 11.6 Maximum predicted ΔHCB for the equation with GEA. Parameters of the equation were determined using the central weighted PAI method.

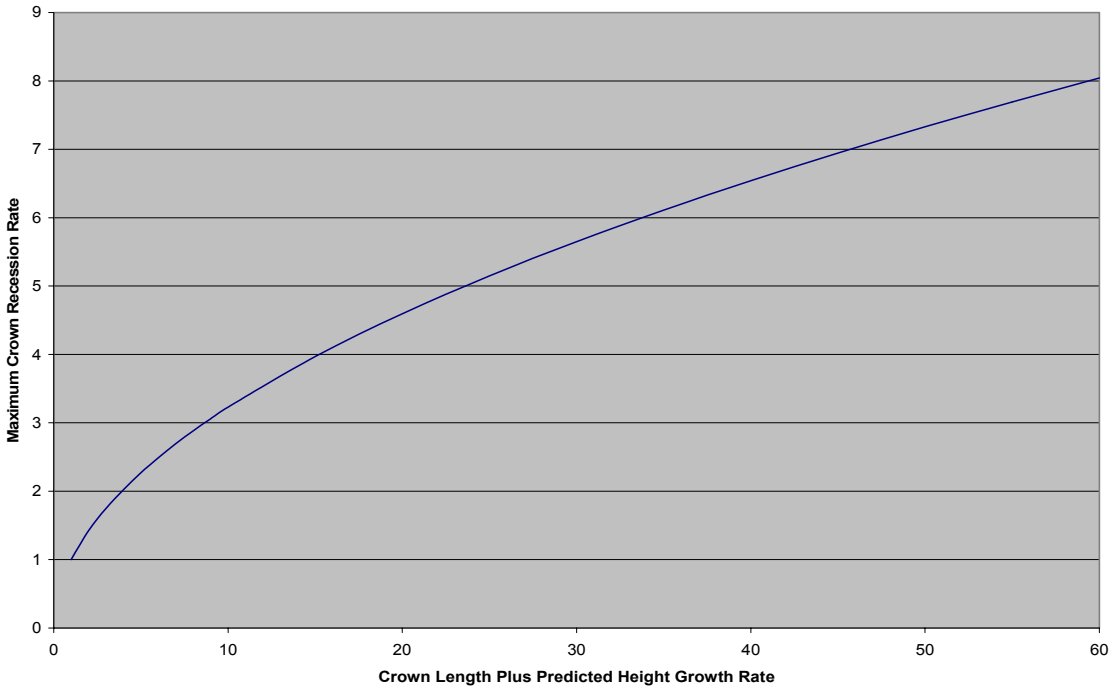

Figure 11.7 Multiplicative modifier for adjusting the predicted maximum ΔHCB to the tree's measured CR, the plot's measured CCF, and a GEA of 5 years for the ΔHCB equation developed using GEA. Parameters of the equation were determined using the central weighted PAI method.

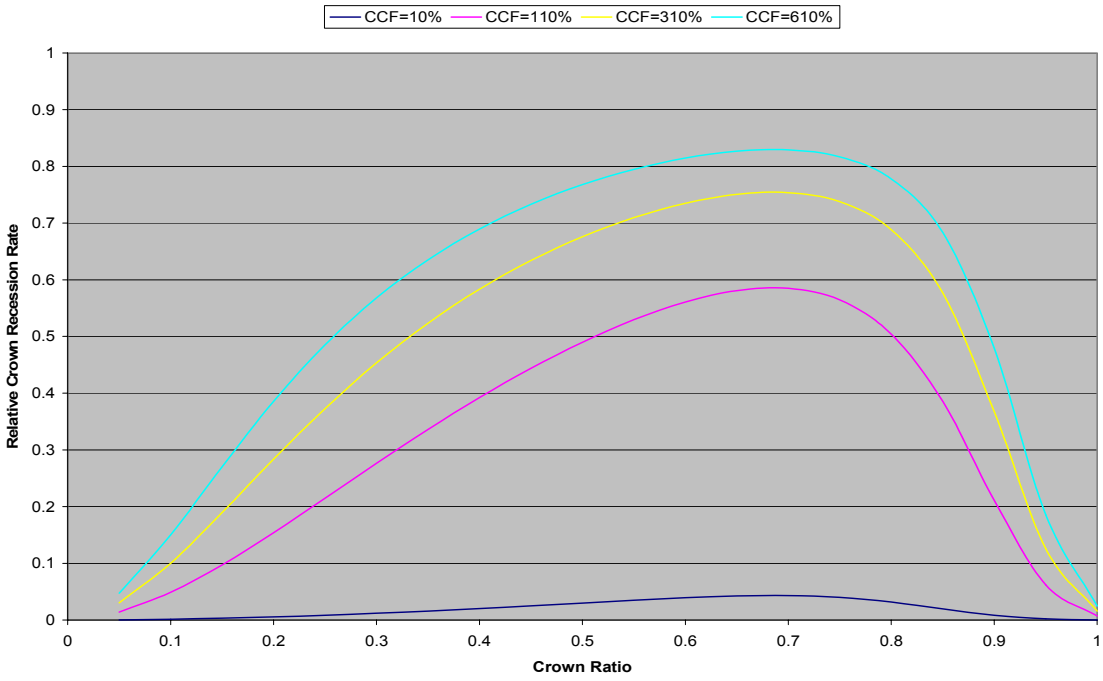

Figure 11.8 Multiplicative modifier for adjusting the predicted maximum ΔHCB to the tree's measured CR, the plot's measured CCF, and a GEA of 10 years for the ΔHCB equation developed using GEA. Parameters of the equation were determined using the central weighted PAI method.

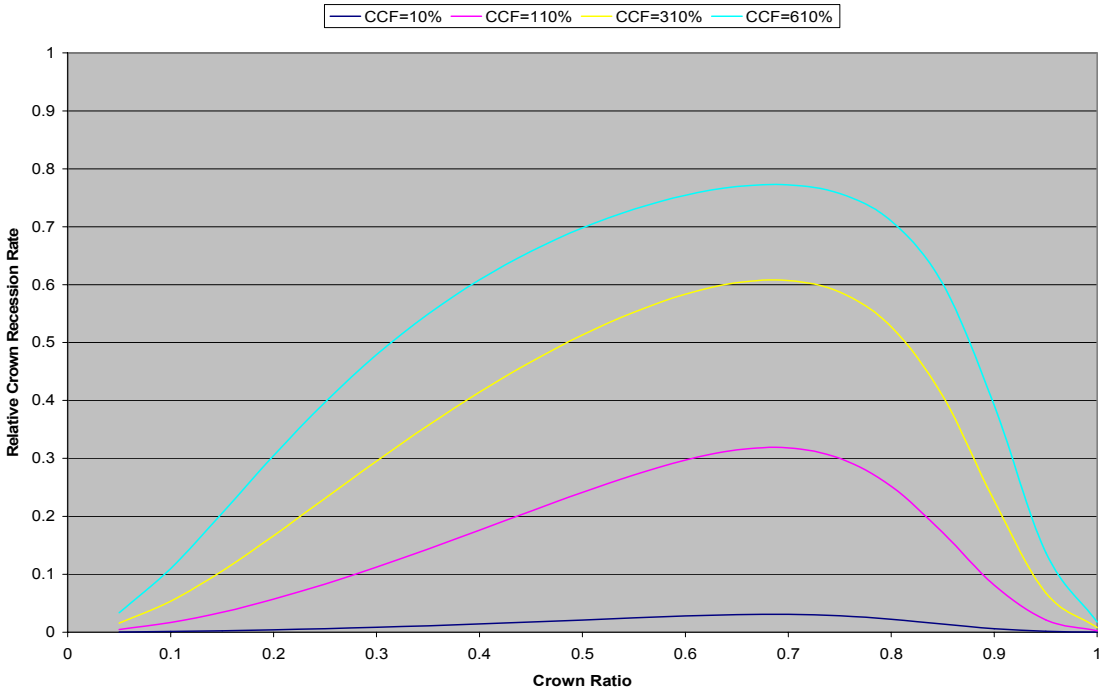

Figure 11.9 Multiplicative modifier for adjusting the predicted maximum ΔHCB to the tree's measured CR, the plot's measured CCF, and a GEA of 15 years for the ΔHCB equation developed using GEA. Parameters of the equation were determined using the central weighted PAI method.

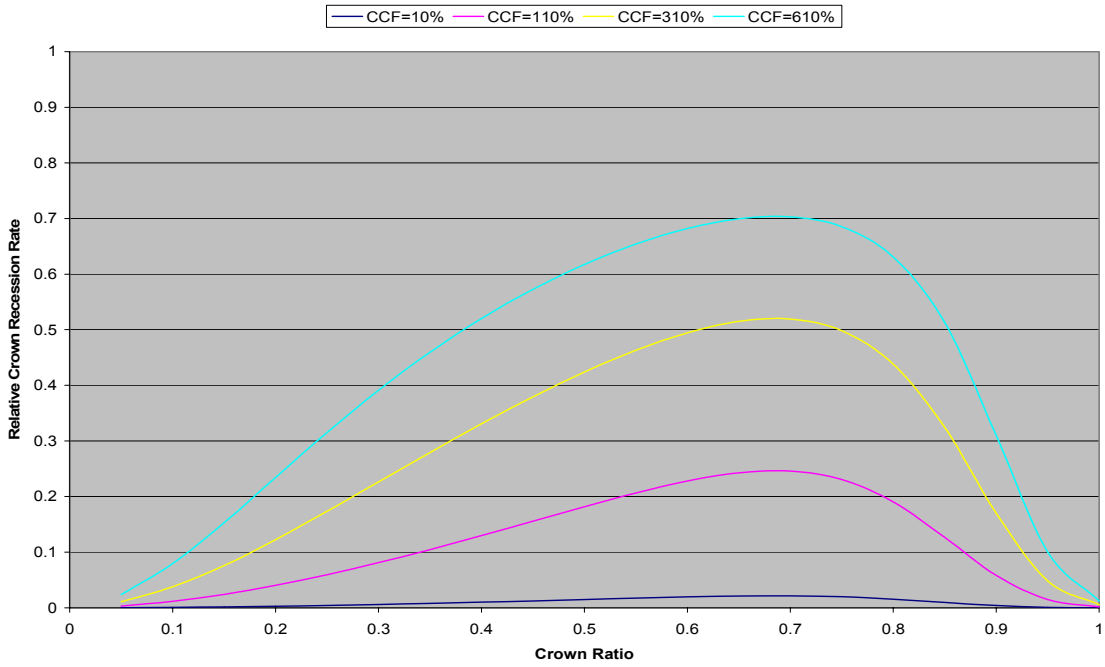

Figure 11.10 Multiplicative modifier for adjusting the predicted maximum ΔHCB to the tree's measured CR, the plot's measured CCF, and a GEA of 20 years for the ΔHCB equation developed using GEA. Parameters of the equation were determined using the central weighted PAI method.

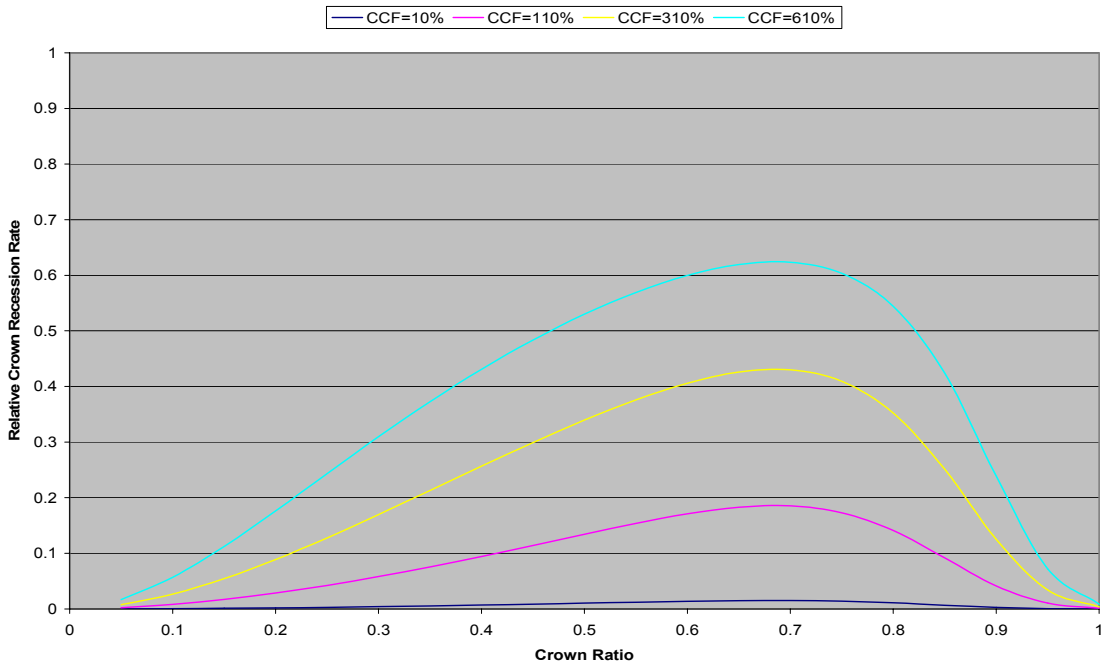

11.6 Literature Cited

Cao, Q.V. 2000. Prediction of annual diameter growth and survival for individual trees from periodic measurements. Forest Science 46: 127-131.

Garber, S.M., R.A. Monserud, and D.A. Maguire. 2008. Crown recession patterns in three conifer species of the Northern Rocky Mountains. Forest Science 54: 633-646.

Hann, D.W. and M.L. Hanus. 2004. Evaluation of nonspatial approaches and equation forms used to predict tree crown recession. Canadian Journal of Forest Research 34: 1993-2003.

Maguire, D.A and D.W. Hann. 1990. Constructing models for direct prediction of 5-year crown recession in southwestern Oregon Douglas-fir. Canadian Journal of Forest Research 20: 1044-1052.

McDill, M.E. and R.L. Amateis. 1993. Fitting discrete-time dynamic models having any time interval. Forest Science 39: 499-519.

12.0 Annual Mortality Rate Equation for Red Alder

The annual mortality rate equation in ORGANON predicts the annual probability of mortality (PM) for a specified sample tree. It is used to reduce each sample tree's expansion factor over time. The objective of this analysis was to develop a PM equation that can be inserted into RAP-ORGANON.

Previous PM equations in ORGANON (e.g., Hann and Wang 1990, Hann and Hanus 2001, Hann et al. 2003, Hann et al. 2006, Gould et al. 2008) had used both tree and plot attributes. The tree attributes used in these studies included a dichotomous mortality variable (MORT) indicating whether the tree died before the end of the growth period (MORT = 1 if died in growth period, = 0 if survived the growth period), diameter at breast height (D), crown ratio (CR), predicted crown ratio (PCR), a dichotomous CR variable indicating whether the tree had a measured CR (I_{CR} = 1 if CR is measured, = 0 if not), and basal area per acre in larger diameter trees (BAL). The plot attributes used in these studies included site index (SI; red alder SI in this study), length of growth period in years (PLEN), the expansion factor (EF) of all sample trees on a plot, and basal area per acre (BA).

12.1 Data

The modeling data set was created from the control plot data, and the validation data set was created by including all measurements on the treatment plots that had not yet received their treatments. The attributes used to create the predictor variables were those that were measured at the start of each variable length growth period. Description of the modeling data set is found in Table 12.1. Description of the validation data set is found in Table 12.2.

Table 12.1 Descriptive statistics for the data set used to fit and evaluate the annual PM equations for plantation grown red alder.

Attribute	Mean	Minimum	Maximum	Std. Deviation
Subsampled Tree Level Attributes: N = 57,377				
CR	0.7753	0.0209	1.00	0.1991
PCR	0.7769	0.2004	1.00	0.1797
Tree Level Attributes: N = 109,287				
D (in.)	3.02	0.1	12.1	1.76
BAL ($ft.^2$/ac.)	26.53	0.00	127.30	25.74
PCR	0.6884	0.1933	1.00	0.2013
Plot/Measurement Level Attribute: N = 664				
BA ($ft.^2$/ac.)	36.39	0.05	127.47	31.68
PLEN (years)	3.17	1	7	0.95
Plot Level Attribute: N = 196				
SI (ft.)	64.1	32.2	89.9	10.25
EF (#/Ac.)	3.39	2.00	4.16	0.67

Table 12.2 Descriptive statistics for the data set used to validate the annual PM equations for plantation grown red alder.

Attribute	Mean	Minimum	Maximum	Std. Deviation
Subsampled Tree Level Attributes: N = 69,890				
CR	0.7967	0.0306	1.00	0.1915
PCR	0.8001	0.3150	1.00	0.1710
Tree Level Attributes: N = 78,316				
D (in.)	2.21	0.2	9.6	1.39
BAL ($ft.^2$/ac.)	16.25	0.00	91.66	17.64
PCR	0.7876	0.3150	1.00	0.1732
Plot/Measurement Level Attribute: N = 405				
BA ($ft.^2$/ac.)	28.06	0.66	91.69	23.54
PLEN (years)	3.82	1	14	1.62
Plot Level Attribute: N = 221				
SI (ft.)	60.8	33.6	86.9	9.13
EF (#/Ac.)	3.61	2.00	4.60	0.56

12.2 Data Analysis

The following general model form was used to characterize the PM of red alder growing in plantations:

$$PM = \left[1.0 + e^{-Z}\right]^{-1} + \varepsilon_{PM}$$

Nineteen Z-functions were examined in the analysis and are described in Table 12.3. The first five Z-functions were developed sequentially by starting with an intercept term only (Z-function #1), adding DBH (Z-function #2), then adding BAL (Z-function #3), then adding SI (Z-function #4), and finally adding BA (Z-function #5). This analysis showed that BA was "significant" to predicting PM if CR was not in the model. Z-function #6 was the function with CR that Hann et al. (2006) used for the SMC-ORGANON Douglas-fir equations. It substituted a scaled PCR value for CR when CR was not measured. Errors-in-variables theory (Fuller 1987, Carroll et al. 1995) would indicate that this approach could produce a biased predictor of PM. Therefore, Z-function #7 was added to examine whether allowing separate parameters on CR and PCR would improve predictions. Z-functions #8 and #9 explored whether adding additional DBH terms would improve predictions. Z-functions #10, #11, #12, and #14 explored minor adjustments to the exponents of Z-function #5. Z-function #13 substituted a BAL transformation found to be useful in modeling ΔD for the BAL terms used Z-function #5. Finally, Z-functions #15 through #19 explored minor adjustments to the exponents of Z-function #13.

Table 12.3 Description of the Z-functions evaluated for predicting the probability of annual mortality (PM) in plantation red alder. Tree and stand attributes forming the Z-function include diameter at breast height (DBH), measured crown ratio (CR), predicted crown ratio (PCR), an indicator variable (I_{CR}) that is 1.0 if the tree had a measured CR and 0.0 if it had not been measured, red alder site index (RASI), basal area per acre in larger diameter trees (BAL), and basal area per acre (BA).

Z-Function	Model Form
1	$Z=b_0$
2	$Z=b_0+b_1D$
3	$Z=b_0+b_1D+b_3BAL$
4	$Z=b_0+b_1D+b_3BAL+b_4SI$
5	$Z=b_0+b_1D+b_3BAL+b_4\ RASI+b_4BA$
6	$Z=b_0+b_1D+b_2[I_{CR}\cdot CR+(I_{CR}-1)\cdot PCR]+b_3BAL+b_4\ SI$
7	$Z=b_0+b_{0,1}I_{CR}+b_1D+b_2PCR+b_{2,1}I_{CR}\cdot CR+b_3BAL+b_4\ SI$
8	$Z=b_0+b_1D+b_3BAL+b_4SI+b_5BA+b_6D^2$
9	$Z=b_0+b_1D+b_3BAL+b_4SI+b_5BA+b_6/D$
10	$Z=b_0+b_1D^2+b_3BAL+b_4SI+b_5BA$
11	$Z=b_0+b_1D+b_3BAL^2+b_4SI+b_5BA$
12	$Z=b_0+b_1D+b_3BAL^{1/2}+b_4SI+b_5BA$
13	$Z=b_0+b_1D+b_3BAL/\ln(D+1.0)+b_4SI+b_5BA$
14	$Z=b_0+b_1D+b_3BAL+b_4SI\ +b_5BA^{1/2}$
15	$Z=b_0+b_1D+b_3BAL/\ln(DBH+1.0)+b_4SI^2+b_5BA$
16	$Z=b_0+b_1D+b_3BAL/\ln(D+1.0)+b_4SI^{1/2}+b_5BA$
17	$Z=b_0+b_1D+b_3BAL/\ln(D+1.0)+b_4SI+b_5BA^{1/2}$
18	$Z=b_0+b_1D+b_3BAL/\ln(D+1.0)+b_4SI^2+b_5BA^{1/2}$
19	$Z=b_0+b_1D+b_3BAL/\ln(D+1.0)+b_4SI^{1/2}+b_5BA^{1/2}$

The regression coefficients were estimated using the maximum likelihood estimation procedures of SAS (e.g., Hann and Hanus 2001, Hann et al. 2006). The dichotomous survival variable was used as the dependent variable. The variable lengths of the growth periods in the data required that the parameters be estimated using the following formulation (Flewelling and Monserud 2002):

$$PS = \left[1.0 + e^{Z}\right]^{-PLEN} + \varepsilon_{PS}$$

Where,

PS = The annual probability of survival

The regression coefficients of the Z function are identical for both the PM and the PS equations. Because the sample trees have unequal sampling probabilities caused by the use of different plot sizes in the modeling data sets, each observation was weighted by EF. The parameters of the PM/PS equation were determined using maximum likelihood estimation.

12.3 Evaluation, Validation, and Results

12.3.1 Evaluation and Validation Statistics

Three statistics were used in model evaluation and model validation:

1. The size of Pearson's chi-square "goodness of fit" (or "lack of fit") statistic (Hamilton 1974, Hann et al. 2003, Hann et al. 2006) for both predicted mortality rate and predicted survival rate.

2. The number and statistical significance of runs in the sign of the residuals (Draper and Smith 1998) for the classes formed to calculate the Pearson's chi-square statistics.

3. A comparison of the actual and predicted total annual mortality rate and a comparison of the actual and predicted total annual survival rate.

Chi-Square Statistic and Test

The chi-square "goodness of fit" statistic was calculated for each of the attributes that formed the predictor variables (i.e., D, CR/PCR, BAL, SI, and BA). For each variable, the sample trees were divided into 40 classes and then the actual annual number of trees dying (O_i) and the predicted annual number of trees dying (E_i) were determined for each class with non-zero entries. These values were then used in the following formulas:

$$\chi^2 = \sum_{i=1}^{nc} \frac{(O_i - E_i)^2}{E_i}$$

Where,

nc = Number of non-zero classes

A small value for the chi-square statistic indicates a good fit to the data. If the assumptions of the test are met, then the chi-square statistics is approximately chi-square distributed. A significance test at α=0.01 can be formed by comparing the statistic against a critical chi-squared value (Snedecor and Cochran 1980). The degrees-of-freedom for the tests is calculated as the number of non-zero cells minus the number of parameters estimate for the PM equation.

Runs Statistic and Test

The chi-square test takes into account the size of the differences between predicted and actual values but not the signs of those differences. The runs statistic and associated test evaluates whether the signs of the average residuals for the predictor variable classes formed to calculate the chi-square statistics are random over the predictor variable classes. Therefore, the runs test is another aspect to testing whether the model fits the data set well. To calculate the runs test, one needs to count the number of plus signs for the average residuals of a chi-square class (nc_1), the number of negative signs for the average residuals of a chi-square class (nc_2), and the number of runs (r). These are then used to form the following z-statistic (not to be confused with the Z-functions used in the morality equations):

$z = (r-\mu \pm ½)/\sigma$

Where,

$$\mu = (2nc_1nc_2)/(nc_1+nc_2) + 1$$
$$\sigma = [2nc_1nc_2(2nc_1nc_2-nc_1-nc_2)]/[(nc_1+nc_2)^2(nc_1+nc_2-1)]$$

The sign on the ½ term in the z-statistic equation is positive if $r < \mu$ and negative if $r > \mu$. The resulting z-statistic is a unit normal deviate and can be tested against critical values of 1.960 for $\alpha = 0.05$ and 2.576 for $\alpha = 0.01$.

Actual and Predicted Annual Rates of Mortality and Survival

The actual and predicted rates of mortality and survival are confounded by the usage of different plot sizes and lengths of growth periods. The following methods were used to estimate the total actual and total predicted annual mortality and survival rates per acre across all sample trees (n) in either the modeling or validation data sets:

$$TAMORT = \sum_{i=1}^{n} \frac{MORT_i}{PLEN_i} \; EF_i$$

$$PTAMORT = \sum_{i=1}^{n} \frac{(1.0 - (1.0 - PPM_i)PLEN_i)}{PLEN_i} \; EF_i$$

$$TASURV = \sum_{i=1}^{n} \frac{1.0 - MORT_i}{PLEN_i} \; EF_i$$

$$PTASURV = \sum_{i=1}^{n} \frac{\left((1.0 - PPM_i)PLEN_i\right)}{PLEN_i} \; EF_i$$

Where,

TAMORT = Actual total annual mortality rate per acre summed across all sample trees for a given Z=function.

PTAMORT = Predicted total annual mortality rate per acre summed across all sample trees for a given Z=function.

TASURV = Actual total annual survival rate per acre summed across all sample trees for a given Z=function.

PTASURV = Predicted total annual survival rate per acre summed across all sample trees for a given Z=function.

PPM_i = Predicted probability of mortality for the i^{th} tree for a given Z-function..

Ideally, TAMORT should equal PTAMORT and TASURV should equal PTASURV.

12.3.2 Preliminary Evaluation

The nineteen Z-functions listed in Table 12.3. were evaluated on both the modeling data set and validation data set by:

1. Calculating the annual probability of mortality chi-square statistics for each of the five tree and stand attributes used to form the predictor variables. The results are presented in Table 12.4 for the modeling data set and Table 12.5 for the validation data set.

2. For both data sets, the chi-square statistics for each attribute were then ranked from 1 to 19 with a rank of 1 given for the equation with the smallest chi-square statistic and a rank of 19 given for the equation with the largest chi-square statistic (noted in bold in the tables are the equations with smallest five values of the chi-square statistic for each attribute).

3. For a given data set, the rank values were averaged across the attributes for a given equation and the resulting averages ranked from 1 to 19 with a rank of 1 given for the equation with the smallest average of individual ranks and a rank of 19 given for the equation with the largest average of individual ranks. The resulting rankings of the averages by data set for each Z-function are found in Table 12.6.

4. Finally, the two data set rankings were themselves averaged across the two data sets and the five models with the lowest average rankings were selected for further evaluation (Table 12.6). Noted in bold in Table 12.6 are the Z-functions with the five smallest rankings for each data set and combined.

Table 12.4 Evaluation Chi-square statistics for alternative Z-functions used to predict annual probability of mortality (PM). Tree and stand attributes forming the Z-function include diameter at breast height (D), crown ratio (CR), red alder site index (SI), basal area per acre in larger diameter trees (BAL), and basal area per acre (BA). Noted in bold for each attribute are the Z-functions with the five smallest Chi-square values.

Z-Function	D	CR	SI	BAL	BA
1	1392.9	9675.9	558.8	13600.6	3061.6
2	641.9	10665.6	843.6	15724.1	6621.3
3	279.4	241.5	296.9	267.4	386.6
4	269.3	265.4	**207.9**	272.2	374.3
5	248.8	251.7	219.1	263.7	393.8
6	273.3	**162.3**	**188.2**	274.5	354.4
7	258.0	**174.9**	**184.4**	222.3	277.9
8	128.5	249.2	**193.8**	328.3	500.7
9	251.2	250.1	**215.1**	274.3	407.3
10	1068.4	278.2	242.3	212.2	286.7
11	187.5	278.3	226.7	311.7	518.4
12	274.0	187.4	297.8	**161.5**	**249.7**
13	**86.3**	180.9	286.1	**155.6**	**237.4**
14	302.0	195.0	292.2	**158.5**	**251.0**
15	**85.2**	178.8	259.4	**156.5**	**237.7**
16	**86.8**	181.9	306.4	**155.4**	**237.5**
17	**102.4**	**177.0**	368.0	180.9	254.7
18	**101.0**	**175.3**	324.2	181.4	253.9
19	102.8	**177.9**	400.8	181.1	255.6

Table 12.5 Validation Chi-square statistics for alternative Z-functions used to predict annual probability of mortality (PM). Tree and stand attributes forming the Z-function include diameter at breast height (D), crown ratio (CR), red alder site index (SI), basal area per acre in larger diameter trees (BAL), and basal area per acre (BA). Noted in bold for each attribute are the Z-functions with the five smallest Chi-square values.

Z-Function	D	CR	SI	BAL	BA
1	811.9	3487.2	696.7	2753.0	964.3
2	1094.2	3728.6	1298.5	3402.7	1935.1
3	**166.2**	469.0	432.7	236.6	**258.0**
4	198.4	468.8	**251.8**	**212.6**	**243.3**
5	175.6	462.3	**268.1**	**222.0**	**258.5**
6	190.8	**180.9**	**245.4**	**215.4**	290.8
7	267.4	**175.5**	**258.3**	262.8	366.9
8	**76.1**	445.7	307.5	264.2	314.2
9	**159.0**	457.5	269.8	**225.3**	**263.9**
10	759.4	530.7	**257.9**	**214.9**	**258.4**
11	**93.8**	503.5	288.0	288.9	319.8
12	338.4	**406.6**	313.5	262.7	293.7
13	177.5	425.1	320.6	244.6	284.5
14	353.6	421.3	303.2	231.7	281.5
15	**170.0**	425.4	310.1	245.5	284.8
16	181.0	425.1	328.6	244.0	283.9
17	329.2	**421.1**	400.2	346.7	433.1
18	321.6	**421.1**	375.9	346.6	432.0
19	332.8	421.3	415.5	346.5	433.0

Table 12.6 Overall rankings of alternative Z-functions from the evaluation and validation Chi-square statistics. A Ranking value of 1 indicates the Z-function had the smallest overall sum of Chi-square values across all tree and stand attributes, and a ranking of 19 indicates the Z-function had the largest overall sum of Chi-square values across all tree and stand attributes. Noted in bold are the five Z-functions with the five smallest ranking values.

Z-Function	Evaluation Rankings	Validation Rankings	Combined Rankings
1	18	18	18
2	19	19	19
3	16	11	16
4	13	**2**	6.5
5	11	**4**	6.5
6	7	**1**	**1**
7	**4**	**5.5**	**2.5**
8	12	12	15
9	14	**3**	8.5
10	15	**5.5**	11
11	17	14	17
12	9	13	13
13	**1.5**	9.5	**4**
14	10	7	8.5
15	**1.5**	8	**2.5**
16	**3**	9.5	**5**
17	6	16	13
18	**5**	15	10
19	8	14	13

Two of the selected Z-functions (#6 and #7) included CR/PCR as predictor variables, while the other selected Z-functions (#13, #15, and #16) included BA as a predictor variable instead of CR/PCR. As with previous ORGANON modeling efforts, attempts to incorporate BA into Z-functions #6 and #7 were unsuccessful. Therefore, one has a choice of having a PM model with either CR or BA. CR has proved to be a strong predictor variable in PM equations (Hann and Wang 1990, Hann and Hanus 2001). If, however, it is subsampled in the modeling data set, then its usage raises concerns about bias due to errors-in-variables. These concerns can be avoided if a model without CR, but including BA, were used instead. The resulting parameters and their standard errors for the five selected Z-functions are found in Table 12.7. The five selected Z-functions were then subjected to more intense evaluation.

Table 12.7 Parameter estimates and their standard errors for the five selected Z-functions used to predict PM of plantation red alder.

Parameter	Estimate	Standard Error
Z-Function #6: $Z=b_0+b_1D+b_2[I_{CR}\cdot CR+(I_{CR}-1)\cdot PCR]+b_3BAL+b_4$ SI		
b_0	-4.333150734	0.0806035836
b_1	-.9856713799	0.0097097801
b_2	-2.583317081	0.0750503833
b_3	0.0394546978	0.0005181476
b_4	0.0369852164	0.0011128827
b_5	0.0	NA
Z-Function #7: $Z=b_0+b_{0,1}I_{CR}+b_1D+b_2PCR+b_{2,1}I_{CR}\cdot CR+b_3BAL+b_4$ SI		
b_0	-5.245052994	0.0924940126
$b_{0,1}$	-1.274659249	0.0386653861
b_1	-.9832557816	0.0099512828
b_2	-.8225083414	0.1101458574
$b_{2,1}$	-2.369065043	0.0749857578
b_3	0.0419691572	0.0006263719
b_4	0.0359741649	0.0011671766
b_5	0.0	NA
Z-Function #13: $Z=b_0+b_1D+b_3BAL/\ln(D+1.0)+b_4SI+b_5BA$		
b_0	-7.028355251	0.0780392609
b_1	-.7578758271	0.0208119800
b_2	0.0	NA
b_3	0.0390248377	0.0010380751
b_4	0.0342389444	0.0011153301
b_5	0.0219542504	0.0010397355
Z-Function #15: $Z=b_0+b_1D+b_3BAL/\ln(D+1.0)+b_4SI^2+b_5BA$		
b_0	-5.954004078	0.0497095209
b_1	-.7614732473	0.0208233209
b_2	0.0	NA
b_3	0.0389346344	0.0010376696
b_4	0.0002671114	0.0000084185
b_5	0.0221915506	0.0010399943
Z-Function #16: $Z=b_0+b_1D+b_3BAL/\ln(D+1.0)+b_4SI^{1/2}+b_5BA$		
b_0	-9.136760996	0.1453409375
b_1	-.7557373634	0.0208047560
b_2	0.0	NA
b_3	0.0390513830	0.0010381229
b_4	0.5387649062	0.0179942418
b_5	0.0218569376	0.0010394545

12.3.3 Model Evaluations

The five selected Z-functions were evaluated by predicting both the PPM and the probability of survival (PPS) for each tree and using these predictions to calculate the three evaluation statistics. Past studies have fit either PPM or PPS equations and that choice can have an impact

upon the resulting evaluation statistics even though the two predictions are mirrors of each other. Table 12.8 presents the PPM chi-square values, critical chi-square statistics for $\alpha = 0.01$, number of runs in residuals, runs test z-statistics, and number of cells used to calculate all statistics, and Table 12.9 presents the same values for PPS. Calculated chi-square values greater than the critical chi-square statistics indicates a lack of fit to the data. Noted in bold are the Z-functions with the smallest Chi-square values, the largest number of runs, or a significant runs test z-statistic at $\alpha = 0.01$. Table 12.12 presents the total actual and predicted annual mortality rates and survival rates by Z-function used to make the predictions. Noted in bold is the Z-function with the predicted value that is closest to the actual value. The values in Table 12.12 are for trees with both measured and predicted CR. To evaluate whether the two sources of CR affect the predictions, Table 12.13 presents the total actual and predicted annual mortality rates and survival rates by Z-function used to make the predictions for just those trees with measured CR.

Table 12.8. Evaluation chi-square values, critical chi-square statistics for $\alpha = 0.01$, number of runs in residuals, runs test z-statistics, and number of cells used to calculate all statistics for the five selected Z-functions used to predict annual probability of mortality (PM). Tree and stand attributes forming the Z-function include diameter at breast height (D), crown ratio (CR), red alder site index (SI), basal area per acre in larger diameter trees (BAL), and basal area per acre (BA). Noted in bold are the Z-functions with the smallest Chi-square values, the largest number of runs, or a significant runs test z-statistic at $\alpha = 0.01$.

Z-Function	D	CR	SI	BAL	BA
Chi-Square Values					
6	273.3	**162.3**	188.2	274.5	354.4
7	258.0	174.9	**184.4**	222.3	277.9
13	86.3	180.9	286.1	155.6	**237.4**
15	**85.2**	178.8	259.4	156.5	237.7
16	86.8	181.9	306.4	**155.4**	237.5
Critical Chi-Square Statistic for $\alpha = 0.01$					
6,13,15,16	36.2	57.3	27.7	57.3	37.6
7	33.4	54.8	24.7	54.8	34.8
Number of Runs in Residuals					
6	4	9	8	17	**14**
7	4	9	8	**18**	**14**
13	**8**	**11**	**9**	16	**14**
15	**8**	**11**	8	16	**14**
16	**8**	**11**	**9**	16	**14**
Runs Test z-Statistic					
6	**-3.55**	**-3.30**	-0.28	-1.11	+0.01
7	**-3.55**	**-3.07**	-0.28	-0.57	+0.01
13	-1.86	**-3.01**	-0.19	-1.24	+0.07
15	-1.86	**-3.01**	-0.54	-1.24	+0.07
16	-1.86	**-3.01**	-0.19	-1.24	+0.07
Number of Cells					
All	24	40	18	40	25

Table 12.9. Evaluation chi-square values, critical chi-square statistics for α = 0.01, number of runs in residuals, runs test z-statistics, and number of cells used to calculate all statistics for the five selected Z-functions used to predict annual probability of survival (PS). Tree and stand attributes forming the Z-function include diameter at breast height (D), crown ratio (CR), red alder site index (SI), basal area per acre in larger diameter trees (BAL), and basal area per acre (BA). Noted in bold are the Z-functions with the smallest Chi-square values, the largest number of runs, or a significant runs test z-statistic at α = 0.01.

Z-Function	D	CR	SI	BAL	BA
Chi-Square Values					
6	2.3	5.6	**2.3**	4.6	6.2
7	2.2	**4.3**	2.4	3.9	5.0
13	**0.9**	8.5	2.7	3.7	**4.9**
15	**0.9**	8.4	2.7	**3.6**	**4.9**
16	**0.9**	8.5	2.7	3.7	5.0
Critical Chi-Square Statistic for α = 0.01					
6,13,15,16	57.3	57.3	33.4	57.3	37.6
7	54.8	54.8	30.6	54.8	34.8
Number of Runs in Residuals					
6	5	10	**10**	17	**14**
7	5	10	**10**	**18**	**14**
13	**11**	**11**	**10**	16	**14**
15	**11**	**11**	**10**	16	**14**
16	**11**	**11**	**10**	16	**14**
Runs Test z-Statistic					
6	**-4.96**	**-3.30**	-0.51	-1.11	+0.01
7	**-4.96**	**-3.07**	-0.51	-0.57	+0.01
13	**-3.04**	**-3.01**	-0.62	-1.24	+0.07
15	**-3.04**	**-3.01**	-0.62	-1.24	+0.07
16	**-3.04**	**-3.01**	-0.62	-1.24	+0.07
Number of Cells					
All	40	40	22	40	25

Two of the Z-functions have CR/PCR but no BA predictor variables and they will be referred to as "CR/PCR models." The other three Z-functions have BA but no CR/PCR predictor variables and they will be referred to as "BA models."

Examination of the PPM chi-square values in Table 12.8 shows that the CR/PCR models had smaller values for SI and slightly smaller values for CR, while the BA models had smaller values for D and BAL and slightly smaller values for BA. All of the chi-square values in Table 8 indicate a lack of fit to the data at α = 0.01. The number of runs was generally larger for the BA models. The runs test indicated possible non-random trends in the average residuals over D for the CR/PCR models at α = 0.01 and possible non-random trends in the average residuals over CR for all models at α = 0.01. Examination of the total actual and predicted annual mortality rates in Table 12.12 indicated that the CR/PCR models came closer to predicting the actual values. The same result occurred when the comparison was restricted to trees with measured CR (Table 12.13).

Examination of the PPS chi-square values in Table 12.9 showed that the CR/PCR models had smaller values for CR and slightly smaller values for SI, while the BA models had smaller values for D slightly smaller values for BAL and BA. All of the chi-square values in Table 9 indicate the models demonstrated no lack of fit to the data at $\alpha = 0.01$. The number of runs were larger generally larger for the BA models. The runs test indicated possible non-random trends in the average residuals over D and CR at $\alpha = 0.01$ for all models. Examination of the total actual and predicted annual survival rates in Table 12 indicated that the CR/PCR models came closer to predicting the actual values.

For the CR/PCR models, Z-function #7 had the smallest PPM chi-square values for four of the five attributes (Table 12.8), and it had the smallest PPS chi-square values for four of the five attributes (Table 12.9). The differences in the PPM and PPS chi-square values for the BA models were very small (Tables 12.8 and 12.9), with Z-function #15 holding a slight edge over the other two Z-functions. Differences in the number of runs and the runs test z-statistic were very small within each category of Z-function (Tables 12.8 and 12.9). For the total actual and predicted annual mortality and survival rates in Table 12.12, Z-function #6 came closest to both actual values for the CR/PCR models and Z-function #16 came closest to both actual values for the BA models. The same result occurred when the comparison was restricted to trees with measured CR (Table 12.13).

12.3.4 Model Validations

The five selected Z-functions were validated by predicting both PPM and PPS for each tree and using these predictions to calculate the three evaluation statistics. Table 12.10 presents the PPM chi-square values, critical chi-square statistics for $\alpha = 0.01$, number of runs in residuals, runs test z-statistics, and number of cells used to calculate all statistics, and Table 12.11 presents the same values for PPS. Chi-square values greater than the critical chi-square statistics indicates a lack of fit to the data. Noted in bold are the Z-functions with the smallest Chi-square values, the largest number of runs, or a significant runs test z-statistic at $\alpha = 0.01$. Table 12.12 presents the total actual and predicted annual mortality rates and survival rates by Z-function used to make the predictions. Noted in bold is the Z-function with the predicted value that is closest to the actual value. The values in Table 12.12 are for trees with both measured and predicted CR. To evaluate whether the two sources of CR affect the predictions, Table 12.13 presents the total actual and predicted annual mortality rates and survival rates by Z-function used to make the predictions for just those trees with measured CR.

Table 12.10 Validation chi-square values, critical chi-square statistics for α = 0.01, number of runs in residuals, runs test z-statistics, and number of cells used to calculate all statistics for the five selected Z-functions used to predict annual probability of mortality (PM). Tree and stand attributes forming the Z-function include diameter at breast height (D), crown ratio (CR), red alder site index (SI), basal area per acre in larger diameter trees (BAL), and basal area per acre (BA). Noted in bold are the Z-functions with the smallest Chi-square values, the largest number of runs, or a significant runs test z-statistic at α = 0.01.

Z-Function	D	CR	SI	BAL	BA
Chi-Square Values					
6	190.8	180.9	**245.4**	**215.4**	290.8
7	267.4	**175.5**	258.3	262.8	366.9
13	177.5	425.1	320.6	244.6	284.5
15	**170.0**	425.4	310.1	245.5	284.8
16	181.0	425.1	328.6	244.0	**283.9**
Critical Chi-Square Statistic for α = 0.01					
All	37.6	56.1	33.4	59.9	36.2
Number of Runs in Residuals					
6	3	**8**	**8**	11	7
7	3	7	**8**	11	5
13	**7**	6	**8**	10	**8**
15	**7**	6	**8**	**12**	**8**
16	**7**	6	**8**	10	**8**
Runs Test z-Statistic					
6	**-3.41**	**-3.16**	-0.15	**-2.67**	-1.19
7	**-3.41**	**-3.45**	-0.15	**-2.67**	-2.05
13	-1.49	**-4.00**	-0.15	-2.39	-0.68
15	-1.49	**-4.00**	-0.15	-1.80	-0.86
16	-1.49	**-4.00**	-0.15	-2.39	-0.68
Number of Cells					
All	20	34	17	37	19

Table 12.11 Validation chi-square values, critical chi-square statistics for $\alpha = 0.01$, number of runs in residuals, runs test z-statistics, and number of cells used to calculate all statistics for the five selected Z-functions used to predict annual probability of survival (PS). Tree and stand attributes forming the Z-function include diameter at breast height (D), crown ratio (CR), red alder site index (SI), basal area per acre in larger diameter trees (BAL), and basal area per acre (BA). Noted in bold are the Z-functions with the smallest Chi-square values, the largest number of runs, or a significant runs test z-statistic at $\alpha = 0.01$.

Z-Function	D	CR	SI	BAL	BA
Chi-Square Values					
6	**1.3**	5.8	**2.1**	**8.8**	**4.0**
7	2.0	**5.1**	**2.1**	10.3	4.9
13	1.5	12.2	2.5	16.2	4.9
15	1.5	12.2	2.5	16.1	4.8
16	1.6	12.1	2.5	16.3	4.9
Critical Chi-Square Statistic for $\alpha = 0.01$					
All	62.4	62.4	37.6	59.9	36.2
Number of Runs in Residuals					
6	6	**11**	**10**	11	7
7	6	10	**10**	11	5
13	**10**	9	**10**	10	**8**
15	**10**	9	**10**	**12**	**8**
16	**10**	9	**10**	10	**8**
Runs Test z-Statistic					
6	**-4.53**	**-2.73**	+0.20	-2.67	-1.19
7	**-4.53**	**-3.00**	+0.20	-2.67	-2.05
13	**-2.86**	**-3.55**	+0.20	-2.39	-0.68
15	**-2.86**	**-3.55**	+0.20	-1.80	-0.86
16	**-2.86**	**-3.55**	+0.20	-2.39	-0.68
Number of Cells					
All	39	39	20	37	19

Table 12.12 Total actual and predicted annual mortality rates and survival rates by the selected five Z-functions for the evaluation data set and the validation data set. Noted in bold is the Z-function with the predicted value that is closest to the actual value.

Z-function	Actual Annual Mortality	Predicted Annual Mortality	Actual Annual Survival	Predicted Annual Survival
Evaluation Data Set				
6	4,446.7	**4,554.8**	353,073.1	**352,965.0**
7	4,446.7	4,580.1	353,073.1	352,939.7
13	4,446.7	4,585.2	353,073.1	352,934.5
15	4,446.7	4,585.2	353,073.1	352,934.6
16	4,446.7	4,584.7	353,073.1	352,935.0
Validation Data Set				
6	2,230.5	2,157.8	282,455.7	282,528.4
7	2,230.5	2,152.3	282,455.7	282,533.9
13	2,230.5	2,220.7	282,455.7	282,465.4
15	2,230.5	2,208.0	282,455.7	282,478.1
16	2,230.5	**2,228.1**	282,455.7	**282,458.1**

Table 12.13 Total actual and predicted annual mortality rates by the selected five Z-functions for the trees in the evaluation data set and the validation data set with measured crown ratios. Noted in bold is the Z-function with the predicted value that is closest to the actual value.

Z-function	Evaluation Data Set Actual Annual Mortality	Evaluation Data Set Predicted Annual Mortality	Validation Data Set Actual Annual Mortality	Validation Data Set Predicted Annual Mortality
6	1889.5	**1907.0**	1883.5	1861.7
7	1889.5	1941.8	1883.5	1817.9
13	1889.5	1831.8	1883.5	**1884.1**
15	1889.5	1828.5	1883.5	1873.0
16	1889.5	1832.6	1883.5	1890.2

Examination of the PPM chi-square values in Table 12.10 shows that the CR/PCR models had smaller values for SI and CR, while the BA models had smaller values for D and BA. The result was mixed for BAL with the CR/PCR models having the smallest and largest values. All of the chi-square values in Table 12.10 indicated a lack of fit to the data at $\alpha = 0.01$. The number of runs were larger generally larger for the BA models. The runs test indicated possible non-random trends in the average residuals over D and over BAL for the CR/PCR models at $\alpha = 0.01$ and possible non-random trends in the average residuals over CR for all models at $\alpha = 0.01$. Examination of the total actual and predicted annual mortality rates in Table 12.12 indicated that the BA models came closer to predicting the actual values. The same result occurred when the comparison was restricted to trees with measured CR (Table 12.13).

Examination of the PPS chi-square values in Table 12.11 shows that the CR/PCR models had smaller values for CR and for BAL and slightly smaller values for SI. The results for D and for BA were mixed with the CR/PCR models having the smallest and largest values. All of the chi-square values in Table 12.11 indicated that the models demonstrated no lack of fit to the data at $\alpha = 0.01$. The number of runs were larger generally larger for the BA models. The runs test indicate possible non-random trends in the average residuals over D and CR at $\alpha = 0.01$ for all models. Examination of the total actual and predicted annual survival rates in Table 12.12 indicated that the BA models came closer to predicting the actual values.

For the CR/PCR models, Z-function #6 had the smallest PPM chi-square values for four of the five attributes (Table 12.10), and it had the smallest PPS chi-square values for four of the five attributes (Table 12.11). The differences in the PPM and PPS chi-square values for the BA models were very small (Tables 10 and 11), with Z-function #16 holding a slight edge over the other two Z-functions. Differences in the number of runs and the runs test z-statistic were very small within each category of Z-function (Tables 12.10 and 12.11). For the total actual and predicted annual mortality and survival rates in Table 12.12, Z-function #6 came closest to both actual values for the CR/PCR models and Z-function #16 came closest to both actual values for the BA models. When the comparison was restricted to trees with measured CR, Z-function #6 came closest to the actual value for the CR/PCR models and Z-function #13 came closest to actual value for the BA models (Table 12.13).

12.4 Discussion

The fact that the chi-square value consistently indicated a lack of fit when predicting PM and then indicated no lack of fit when predicting PS demonstrates a weaknesses of using that value for statistically testing the fit of a mortality/survival equation to the data. This result may be one reason why expressing the equation in its PS form is so popular. However, the usage of the chi-square statistic as a ranking devise is probability still helpful in comparing alternative model forms (Z-functions).

Examining the chi-square and runs test results, the CR/PCR model with Z-function #7 was the overall best Z-function based upon the evaluation data set results and Z-function #6 was the overall best based upon the validation data set results. For the BA models, Z-function #15 was the overall best Z-function for both data sets, with Z-function #16 proving to be slightly better than Z-function #13 for both data sets.

Examining the comparisons of actual to predicted total annual mortality and survival rates, the CR/PCR model with Z-function #6 was the overall best Z-function for both data sets. In addition, Z-function #6 predicted the total annual mortality rate best for the subset of the modeling data that was composed of just those trees with measured CR. It is believed that these results indicate that bias due to errors-in-variables may not be a serious problem with Z-function #6. For the BA models, Z-function #16 was the overall best Z-function for both data sets and Z-function #13 proved to be better than Z-function #15.

These results lead to the conclusion that Z-function #6 was the best CR/PCR model for predicting PM/PS and that Z-function #16 was the best BA model for predicting PM/PS. Graphs of annual PPM from the mortality model using Z-function #6 are displayed in Figures 12.1 through 12.4. Graphs of annual PPM from the mortality model using Z-function #16 are displayed in Figures 12.5 through 12.8. Figures 12.1 and 12.5 show annual PPM values for a simulated open grown tree, in which BAL is set to zero and BA is set to the basal area of the tree, plotted across D and for SI of 30, 60, and 90 feet. Figures 12.2 through 12.4 and 12.6 through 12.8 show annual PPM plotted across CR for BAL values of 0, 20, 40, 60, 80, 100, and 120 ft^2 when SI has been fixed to 60 feet and D fixed to three values of 1.0, 5.0, and 9.0 inches. Figures 12.2 and 12.6 show the resulting predictions when D is fixed at 1.0 inches. Figures 12.3 and 12.7 show the resulting predictions when D is fixed at 5.0 inches. Finally, and Figures 12.4 and 12.8 show the resulting predictions when D is fixed at 9.0 inches.

Examination of these graphs indicates that both models predict near zero PM when D approaches 9.0 inches. One would expect PM to first decline and then increase over D (Hann and Hanus 2001). Attempts to incorporate this behavior were attempted (e.g., Z-function #8) but they resulting in models with poorer fits to the data and that predicted a 100% probability of mortality when D exceeded approximately 20 inches. Unlike the ΔD and ΔH data sets in which the range of the modeling data sets fully incorporated the peak of those values (and therefore allowed characterization of those peaks), the PM modeling data set is still too young to display the expected U-shaped behavior over D. It is critical, therefore, to continue to remeasure the red alder installations in order to ultimately solve this problem.

Because of this limitation, the only correction to the lack of mortality and resulting unreasonable increases in BA over time will come as a result of the usage of the “Limit on Maximum SDI”

option in ORGANON. This problem should also lead to a restriction on the upper age for projections from RAP-ORGANON (probably 20 to 25 years from seed).

Of the final two PM models under consideration, the model with Z-function #6 predicts somewhat more mortality than the model with Z-function #16. Z-function #16 is probability best for characterizing the current modeling data set, but Z-function #6 might extrapolate somewhat better and its model form is consistent with the other versions of ORGANON. Therefore, the model with Z-function #6 will be selected for evaluation in RAP-ORGANON.

Figure 12.1 Predicted annual probability of mortality using Z-function # 6 for an open grown tree (i.e., CR = 0.0 and BAL = 0.0) plotted across D and for SI of 30, 60, and 90 feet.

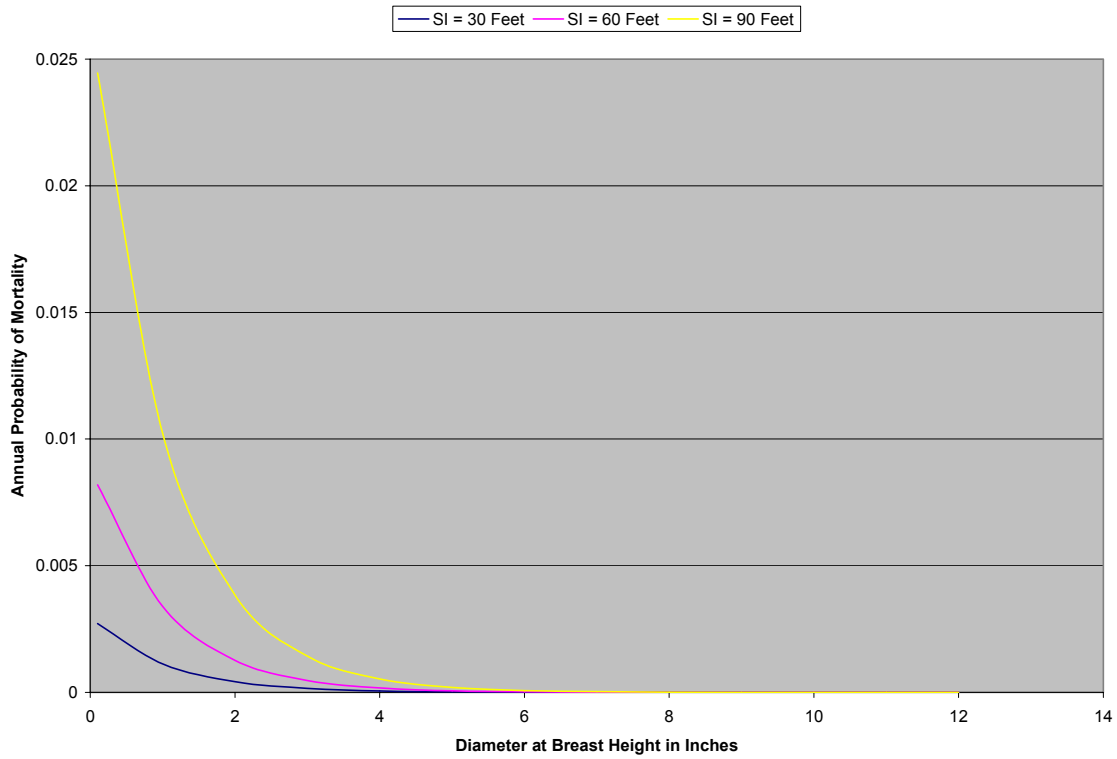

Figure 12.2 Predicted annual probability of mortality using Z-function # 6 plotted across CR for BAL of 0, 20, 40, 60, 80, 100, and 120 ft^2 and with D = 1.0 inches and SI = 60 feet.

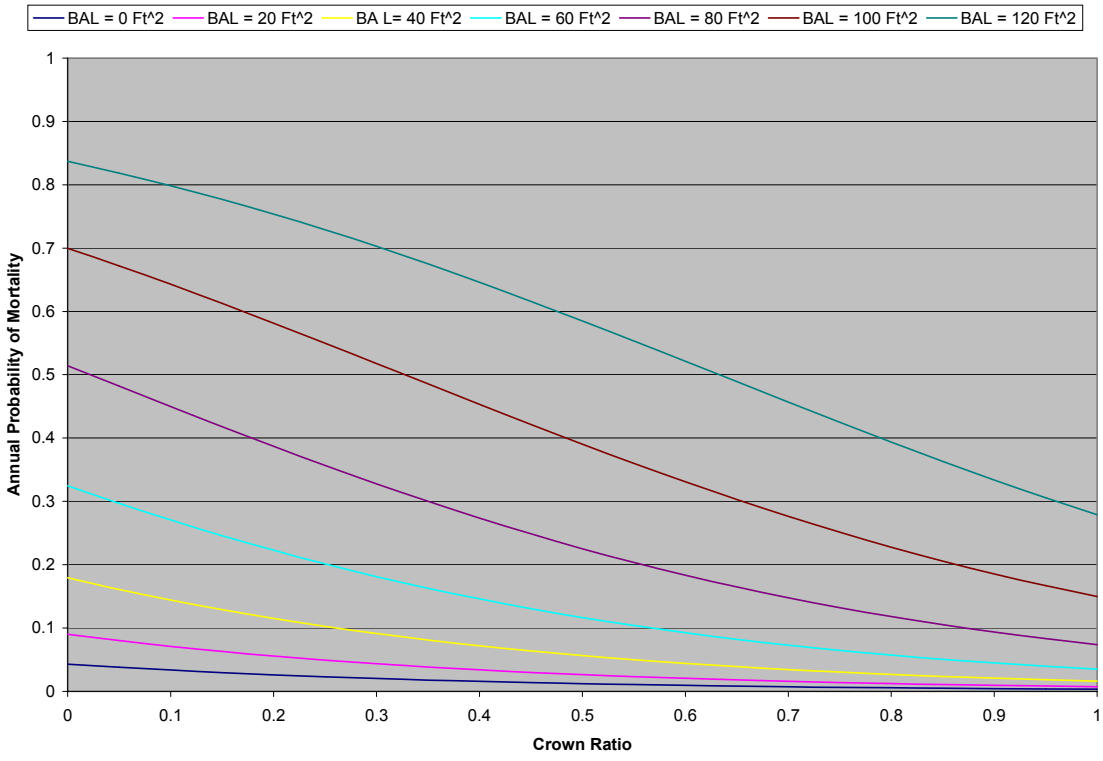

Figure 12.3 Predicted annual probability of mortality using Z-function # 6 plotted across CR for BAL of 0, 20, 40, 60, 80, 100, and 120 ft^2 and with D = 5.0 inches and SI = 60 feet.

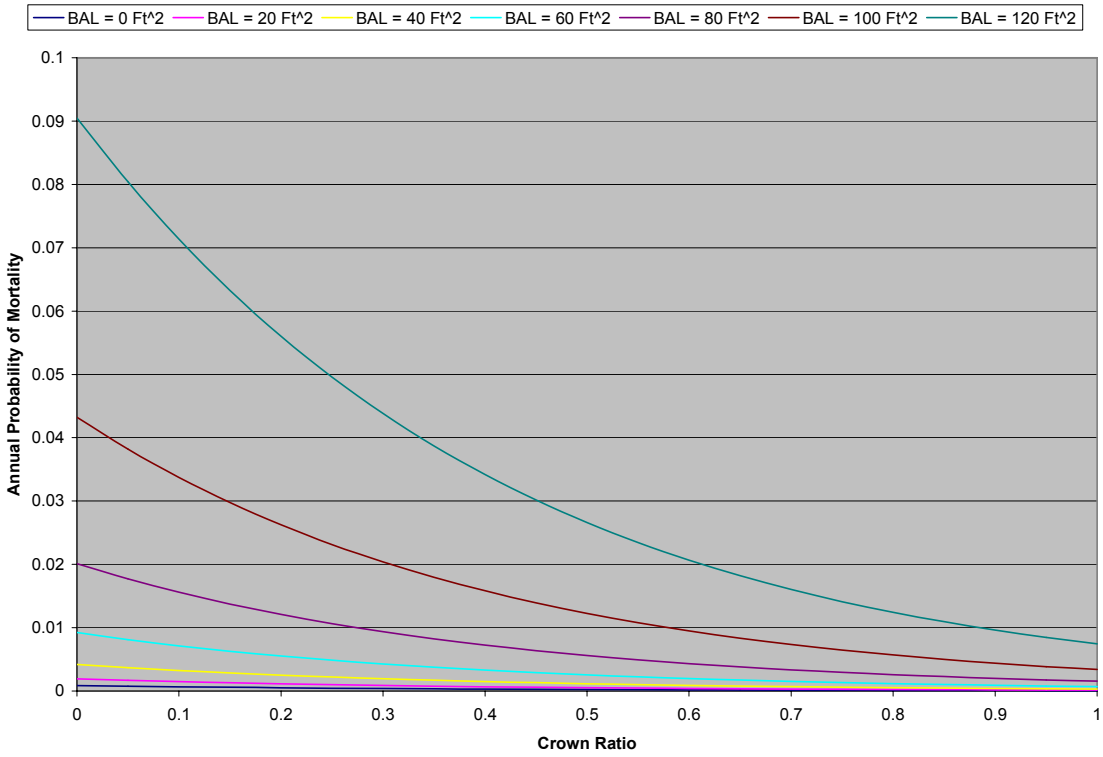

Figure 12.4 Predicted annual probability of mortality using Z-function # 6 plotted across CR for BAL of 0, 20, 40, 60, 80, 100, and 120 ft^2 and with D = 9.0 inches and SI = 60 feet.

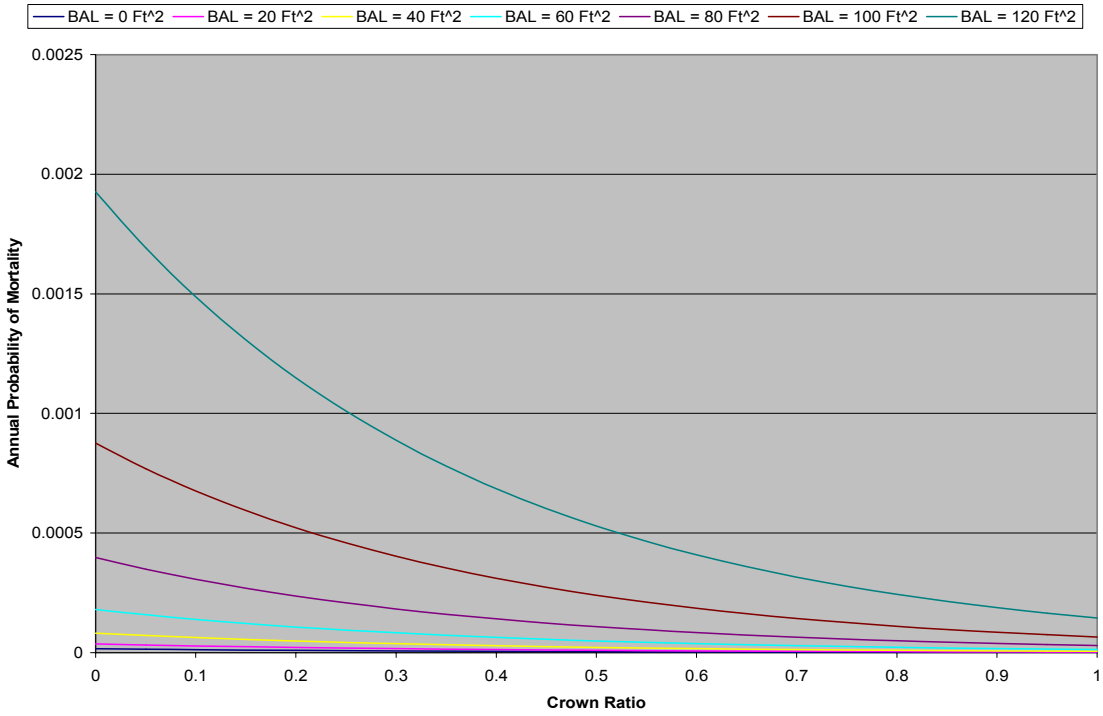

Figure 12.5 Predicted annual probability of mortality using Z-function # 16 for an open grown tree (i.e., BAL = 0.0 and BA = 0.005454154·DBH^2) plotted across D and for SI of 30, 60, and 90 feet.

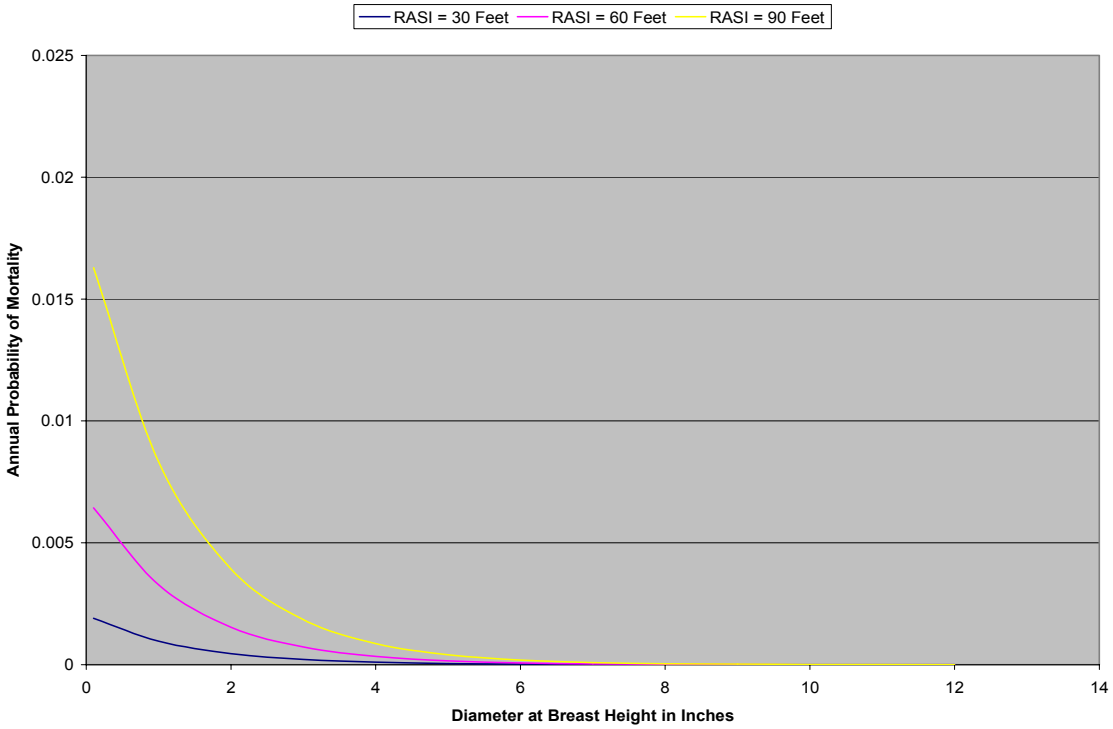

Figure 12.6 Predicted annual probability of mortality using Z-function # 16 plotted across relative BAL (i.e., BAL/BA) for BA of 10, 30, 50, 70, 90, 110, and 130 ft^2 and with D = 1.0 inches and SI = 60 feet.

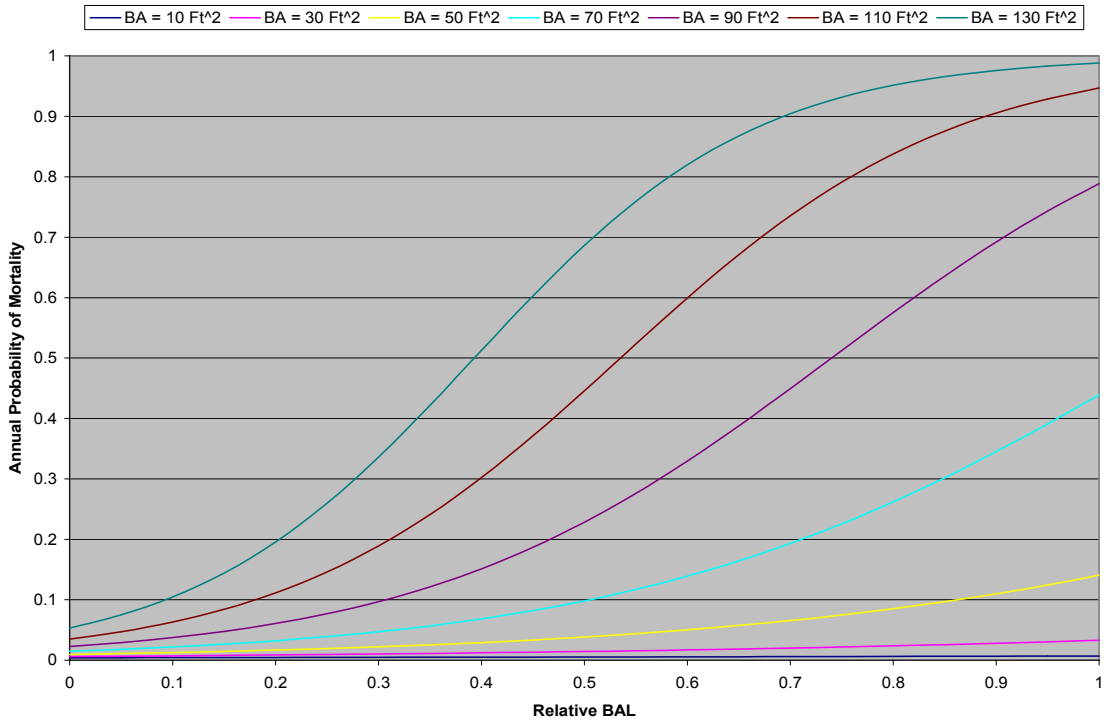

Figure 12.7 Predicted annual probability of mortality using Z-function # 16 plotted across relative BAL (i.e., BAL/BA) for BA of 10, 30, 50, 70, 90, 110, and 130 ft^2 and with D = 5.0 inches and SI = 60 feet.

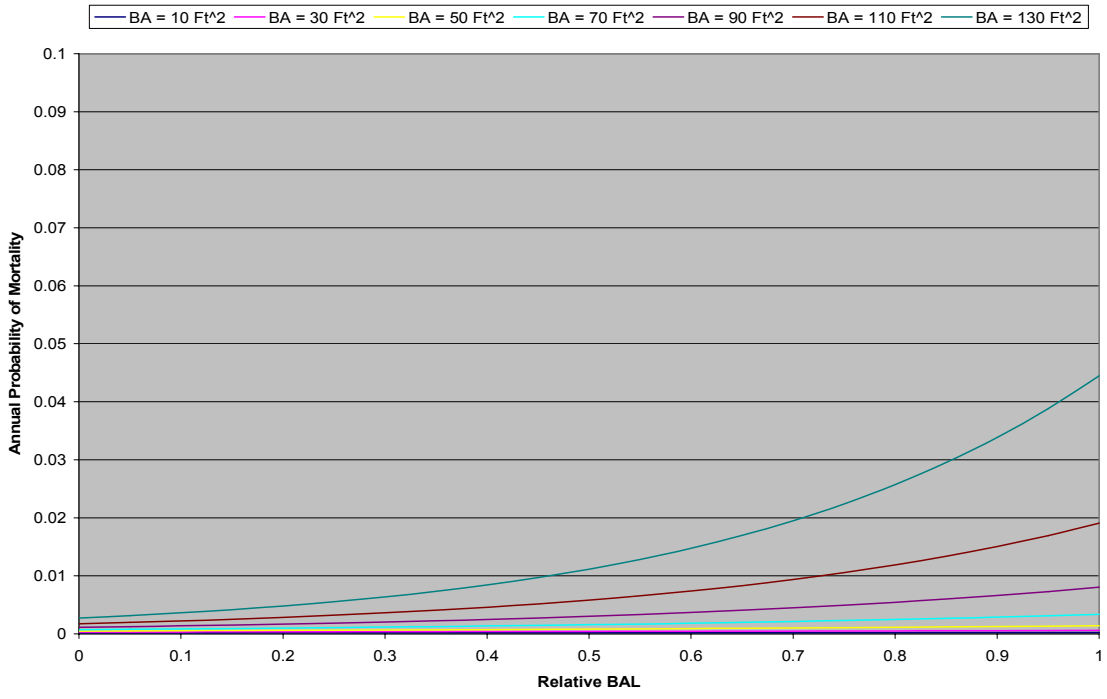

Figure 12.8 Predicted annual probability of mortality using Z-function # 16 plotted across relative BAL (i.e., BAL/BA) for BA of 10, 30, 50, 70, 90, 110, and 130 ft^2 and with D = 9.0 inches and SI = 60 feet.

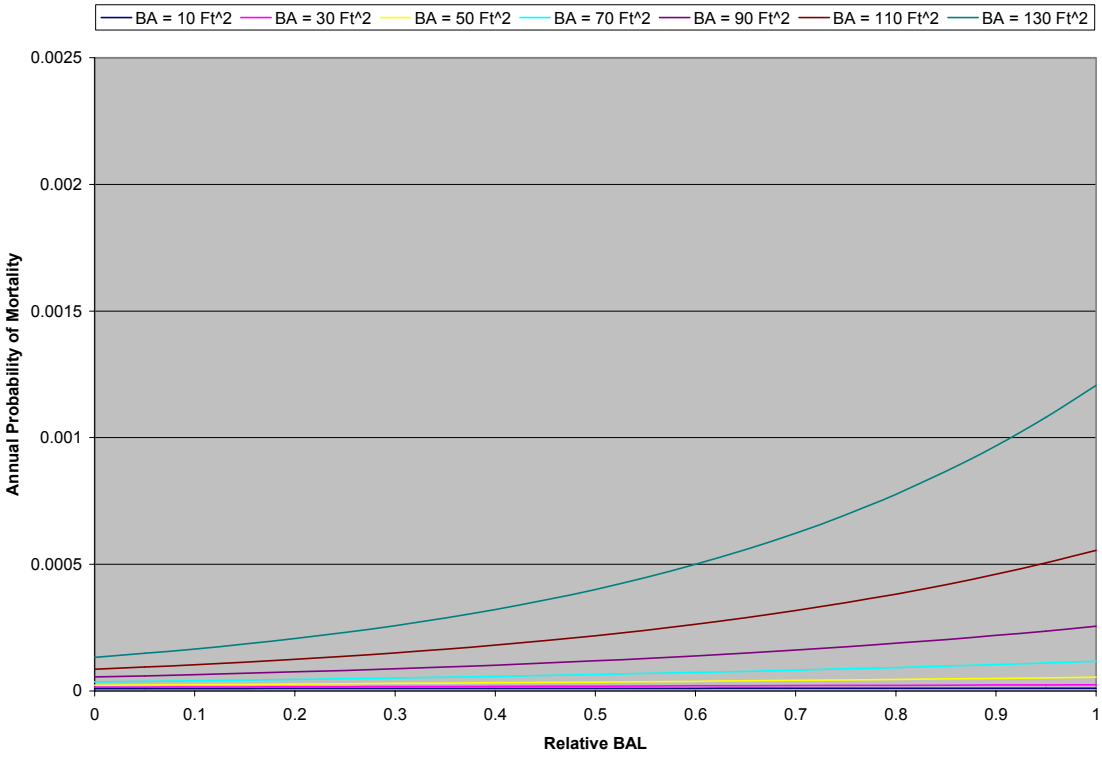

12.5 Literature Cited

Carroll, R.J., D. Ruppert, and L.A. Stefanski. 1995. *Measurement Error in Nonlinear Models.* Chapman & Hall, New York, New York. 305p.

Draper, N.R. and H. Smith. 1998. Applied Regression Analysis. Third Edition. John Wiley & Sons, New York. 706p.

Flewelling, J.W. and R.A. Monserud. 2002. Comparing methods for modeling tree mortality, pp. 168-177 in Second Forest Vegetation Simulator Conference, N.L. Crookston and R.N. Havis, compilers, USDA Forest Service, Rocky Mountain Research Station, Fort Collins, Colorado. Proceedings RMRS-P-25. 208p.

Fuller, W.A. 1987. *Measurement Error Models*. John Wiley & Sons, New York, New York. 440p.

Gould, P.J., D.D. Marshall, and C.A. Harrington. 2008. Prediction of growth and mortality of Oregon white oak in the Pacific Northwest. Western Journal of Applied Forestry 23: 26-33.

Hamilton, D.A., Jr. 1974. Event probabilities estimated by regression. USDA Forest Service, Intermountain Forest and Range Experiment Station, Ogden, Utah. Research Paper INT-152. 18p.

Hann, D.W. and M.L. Hanus. 2001. Enhanced mortality equations for trees in the mixed conifer zone of southwest Oregon. Forest Research Lab., Oregon State University, Corvallis, Oregon. Research Contribution 34. 34p.

Hann, D.W. and C.-H. Wang. 1990. Mortality equations for individual trees in southwest Oregon. Oregon State University, Forest Research Laboratory, Corvallis, Oregon. Research Bulletin 67. 17p.

Hann, D.W. D.D. Marshall and M.L. Hanus. 2003. Equations for predicting height-to-crown-base, 5-year diameter growth rate, 5-year height growth rate, 5-year mortality rate and maximum size-density trajectory for Douglas-fir and western hemlock in the coastal region of the Pacific Northwest. Forest Research Lab., Oregon State University, Corvallis, Oregon. Research Contribution 40. 83p.

Hann, D.W., D.D. Marshall, and M.L. Hanus. 2006. Re-analysis of the SMC-ORGANON equations for diameter-growth rate, height-growth rate, and mortality rate equations of Douglas-fir. Forest Research Lab., Oregon State University, Corvallis, Oregon. Research Contribution 49. 24.

Snedecor, G.W., and W.G. Cochran. 1980. Statistical Methods, Seventh Edition. The Iowa State Press, Ames, Iowa. 507p.

13.0 Maximum Size-Density Trajectory for Red Alder

The maximum size-density trajectory is used as an option in RAP-ORGANON to restrict stand development in a manner that keeps the stand on or below the maximum size-density trajectory as it develops over time (Hann and Wang 1990, Hann et al. 2003).

13.1 Data Analysis and Results

The following is the maximum size-density trajectory equation used in ORGANON:

$$\ln(QMD_i)=a_1-a_2\cdot\ln(N_i)-(a_1\cdot a_4)\cdot(N_i/N_0)^{a3}$$

Where,

QMD_i = The quadratic mean diameter at the i^{th} measurement

N_i = The number of trees per acre at the i^{th} measurement

N_0 = The number of trees per acre at the first measurement

Two data sets were available for estimating the parameters of the maximum size-density trajectory:

1. The 196 control plots
2. The measurements taken on the treatment plots before the treatments were applied to the plots.

The first step of the analysis was to ascertain whether the plots in these data sets had developed enough so that their most recent measurements fell on the maximum size-density line. Two methods were used to assess this situation.

The first involved calculating the stand density index (SDI) values for each measurement on each plot. This was done using both Reineke's (1933) exponential parameter and Puettmann et al.'s (1993) exponential parameter for red alder. It was expected that stands with measurements falling on the maximum size-density line would have near constant SDI values in the later measurements. Examination of the data indicated that there were no plots in which the last two values of SDI were near the same.

The second method involved calculating the following slope value using all consecutive pairs of measurements available on each plot:

$$\text{Slope} = [\ln(QMD_{i+1})-\ln(QMD_i)]/[\ln(N_{i+1})-\ln(N_i)]$$

It was expected that stands with measurements falling on or near the maximum size-density line would have values of slope values between −0.5 and −1.0 for at least the last measurement. None of the treatment plots and only 15 of the 196 control plots had last pair of measurements that met this criterion.

The 15 control plots were then used to estimate the parameters of the maximum size-density trajectory but the resulting values were not reasonable. The value of a_2 was then fixed to

Reineke's (1933) value of 0.62305 and the remaining parameters estimated but again the remaining parameters were unreasonable. The same was true when the slope parameter of Puettmann et al. (1993) was used. This led to the conclusion that the data sets had not developed far enough for them to be useful in estimating the parameters of the maximum size-density trajectory of red alder plantation.

The data from the 15 plots were then tested against the parameter estimates of Puettmann et al. (1993):

$a_1 = 5.96$
$a_2 = 0.64$
$a_3 = 3.88$
$a_4 = 0.07$

This was done by fitting the following equation to the data from the 15 control plots:

$$\ln(QMD_i)=b_1\cdot[5.96-0.64\times\ln(N_i)-(5.96\times0.07)\times(N_i/N_0)^{3.88}]$$

The expectation was that b_1 would take a value of one if the Puettmann et al. (1993) parameters provide a reasonable fit to the data. The value of b_1 was calculated to be 0.939502932 with a standard error of 0.02893281. The t-statistic for a t-test of b_1 being one was 2.09095 which is significant at $\alpha = 0.05$ but not $\alpha = 0.01$. Therefore, it was decided to use the Puettmann et al. (1993) parameters for the RAP version of ORGANON.

13.2 Literature Cited

Hann, D.W. and C.-H. Wang. 1990. Mortality equations for individual trees in southwest Oregon. Oregon State University, Forest Research Laboratory, Corvallis, Oregon. Research Bulletin 67. 17p.

Hann, D.W. D.D. Marshall and M.L. Hanus. 2003. Equations for predicting height-to-crown-base, 5-year diameter growth rate, 5-year height growth rate, 5-year mortality rate and maximum size-density trajectory for Douglas-fir and western hemlock in the coastal region of the Pacific Northwest. Forest Research Lab., Oregon State University, Corvallis, Oregon. Research Contribution 40. 83p.

Puettmann, K.J., D.W. Hann, and D.E. Hibbs. 1993. Evaluation of the size-density relationships for pure red alder and Douglas-fir stands. Forest Science 39: 7-27.

Reineke, L.H. 1933. Perfecting a stand-density index for even-aged forests. Journal of Agricultural Research 46: 627-638.

14.0 Residual Equations for the Red Alder Annual Diameter Increment and Height Increment Equations

ORGANON has an option of record tripling in order to increase variability into the user's tree list. This pseudo random feature is particularly useful for small tree lists (Stage 1973). ORGANON triples the tree list first based upon diameter increment and then upon height increment resulting in a nine times increase in the length of the tree list at the end of each growth cycle. Tripling continues until the expanded tree list reaches the maximum length of 2000 records. If a tripling of every tree record would increase the tree list above 2000 records, then tripling every other tree record will be used if that strategy would keep the resulting expanded tree list below 2000.

Performing tripling requires models for predicting the means for the lower 1/3 and upper 1/3 residuals of annual diameter increment or annual height increment. These annual residual equations were developed using the annual central PAI control plot data sets and associated three sets of parameter estimates develop for both equations. The residuals for the middle 1/3 of the residuals is formed by summing together the predictions from the lower and upper 1/3 residuals equations.

14.1 Data Analysis and Results

For diameter increment, the model form for the residual models was:

$$\Delta DRES_{i,j} = MWRES_i \cdot P\Delta D_j^{0.5}$$

Where,

$\Delta DRES_{i,j}$ = The i^{th} type of annual diameter increment residual for the j^{th} tree
$MWRES_i$ = Mean weighted annual residual for the i^{th} type of residual
$P\Delta D_j$ = The predicted diameter increment for the j^{th} tree
i = 1 if a lower residual and 2 if an upper residual

The resulting values of $MWRES_i$ for the diameter increment equations are found in Table 14.1. A graph of the predicted upper and lower residual models for the ΔD model fit using the weighted summation procedure is found in Figure 14.1.

Table 14.1 Red alder mean weighted residuals for the lower 1/3 of the ΔD residuals ($MWRES_1$) and the upper 1/3 of the ΔD residuals ($MWRES_2$) by the ΔD parameter estimation procedure.

Type of Residual	Weighted Central PAI Procedure	Unweighted Summation Procedure	Weighted Summation Procedure
$MWRES_1$	-0.20579103	-0.20655398	-0.20610321
$MWRES_2$	+0.21302679	+0.21184136	+0.21278486

Figure 14.1 Predicted upper and lower residual models for the plantation red alder diameter increment (ΔD) model fit using the weighted summation procedure and plotted over predicted diameter increment (PΔD).

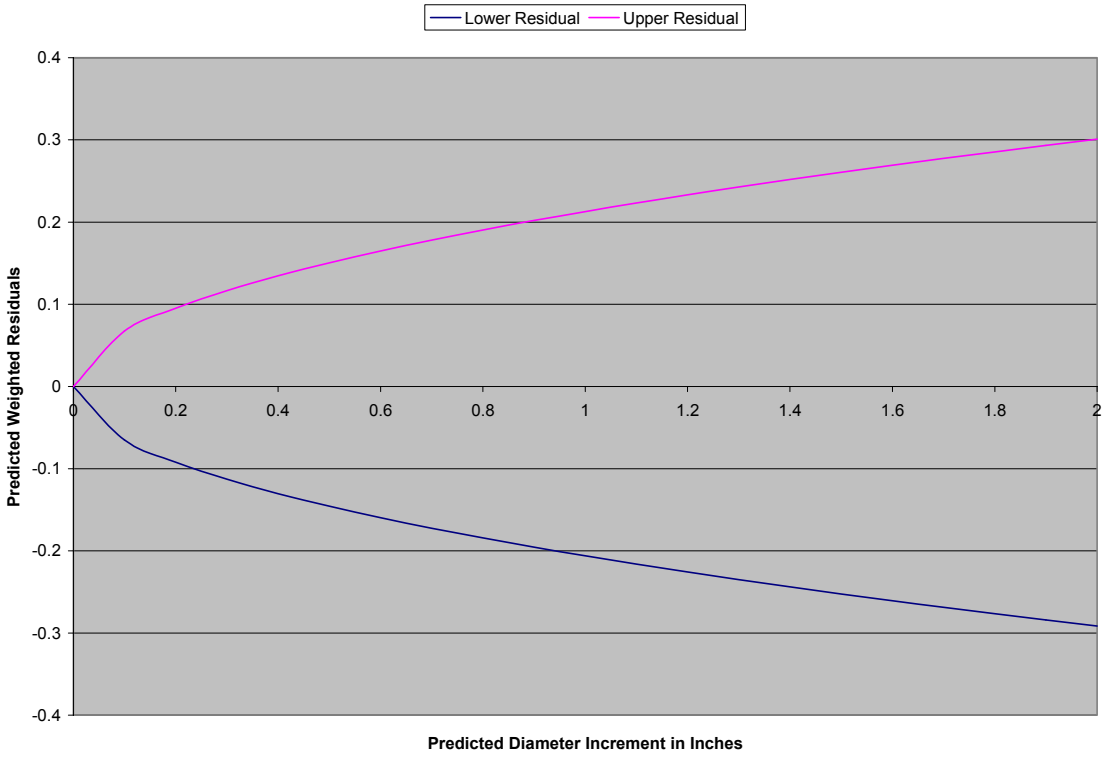

For the height increment equation, the model form for the residual models was:

$$\Delta HRES_{i,j} = b_{0,i} + b_{1,i} \cdot P\Delta H_j + b_{2,i} \cdot P\Delta H_j^2$$

Where,

$\Delta HRES_{i,j}$ = The i^{th} type of annual height increment residual for the j^{th} tree
$b_{k,i}$ = The k^{th} parameter for the i^{th} type of residual
$P\Delta H_j$ = The predicted height increment for the j^{th} tree

The values of $b_{k,i}$ for the height increment equations were fit using ordinary least squares regression and the resulting values and their standard errors are found in Table 14.2. A graph of the predicted upper and lower residual models for the ΔH model fit using the weighted summation procedure is found in Figure 14.2.

Table 14.2 Red alder parameter estimates and their standard errors (in parentheses) for predicting the lower 1/3 of the annual ΔH residuals ($b_{k,1}$) and the upper 1/3 of the annual ΔH residuals ($b_{k,2}$) by the ΔH parameter estimation procedure.

Type of Residual	Weighted Central PAI Procedure	Unweighted Summation Procedure	Weighted Summation Procedure
Lower Residuals Equation			
$b_{0,1}$	-0.606131769 (0.04526508)	-0.537333398 (0.04764439)	-0.565597958 (0.04624062)
$b_{1,1}$	-0.235444538 (0.02671925)	-0.274029519 (0.02872595)	-0.259956282 (0.02750199)
$b_{2,1}$	+0.0246201751 (0.003634941)	+0.0294187634 (0.004010644)	+0.0276968137 (0.003781465)
Upper Residuals Equation			
$b_{0,2}$	+0.799898611 (0.04191868)	+0.945013941 (0.03965116)	+0.866609308 (0.04034583)
$b_{1,2}$	+0.144453996 (0.02456621)	+0.0556682415 (0.02329508)	+0.100265352 (0.02376177)
$b_{2,2}$	-0.0189371133 (0.00333982)	-0.00785224482 (0.003178838)	-0.0135706039 (0.003240367)

Figure 14.2 Predicted upper and lower residual models for the plantation red alder height increment (ΔH) model fit using the weighted summation procedure and plotted over predicted height increment (PΔH).

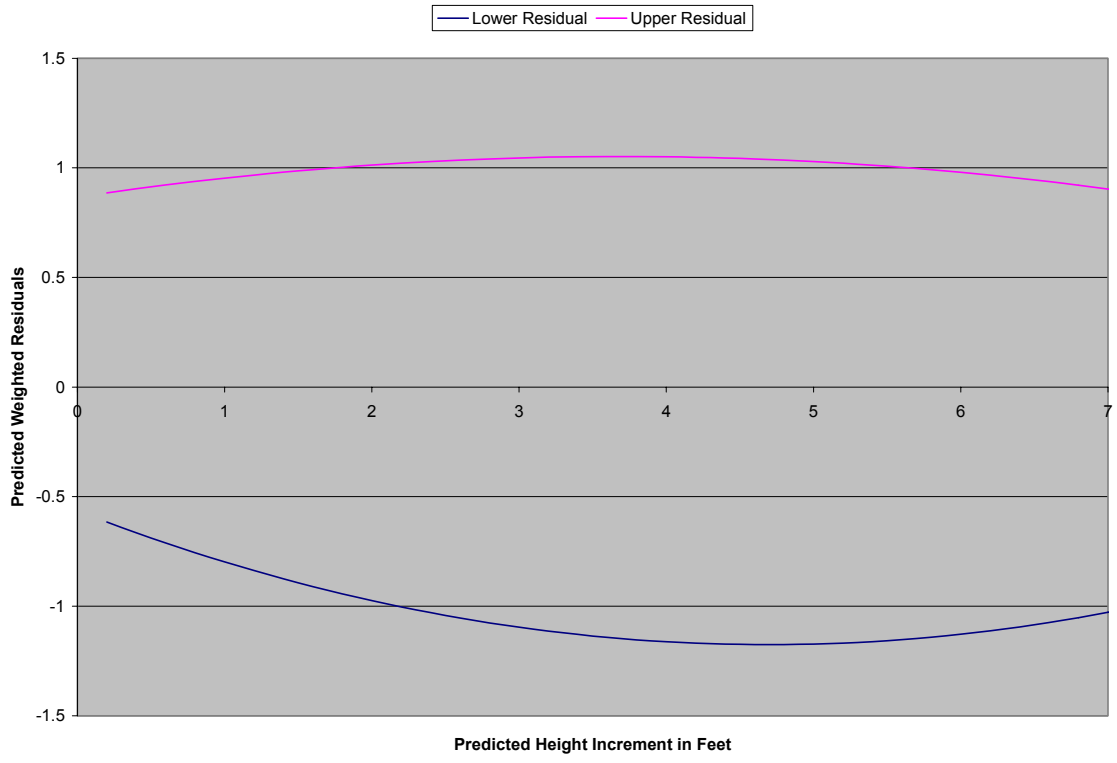

14.3 Discussion

The residual models for both diameter increment and height increment follow the same trends as found in previous versions of ORGANON. The absolute values of the diameter increment residual equations monotonically increase as PΔD increases and the inequity of the $MWRES_i$ values indicate a slight, positive skewness. The absolute value of the height increment residual equations first increases, peaks, and then declines as PΔD increases, with the peaks occurring within the range of PΔD found in the data set. This behavior may be in part attributed to the size of errors that occur in measuring tree height while the tree is standing. Larsen et al. (1987) found that measurement errors increase with tree height. The largest values of ΔH occur in very young, short dominant trees with smallest amounts of measurement error. The effect of measurement error in the dependent variable is an increase in the residual variance (Kmenta 1986). Therefore, the smallest contribution of measurement error to the residual error will occur in the fastest growing trees that happen to be the shortest trees.

14.4 Literature Cited

Kmenta, J. 1986. Elements of Econometrics, Second Edition. Macmillian Publishing Company, New York. 786p.

Larsen, D.R., D.W. Hann and S.C. Stearns-Smith. 1987. Accuracy and precision of the tangent method of measuring tree height. Western Journal of Applied Forestry 2: 26-28.

Stage, A.R. 1973. PROGNOSIS model for stand development. USDA Forest Service, Intermountain Forest and Range Experiment Station, Ogden, Utah. Research Paper INT 137. 32p.

15.0 Effects of Thinning upon Red Alder Diameter Increment, Height Increment, Crown Recession, and Mortality Rate Equations

A properly applied thinning that does not damage the residual trees will increase the diameter increment of the residual trees because of the increased availability of moisture, nutrients, and light (Oliver and Larson, 1996, Tappeiner et al., 2007). Thinning may increase, decrease, or maintain the height increment of the residual trees depending upon tree species, crown class, age, and density of the stand before thinning (Oliver and Larson, 1996, Tappeiner et al., 2007). The increase in growing space from thinning will lead to an increase in crown width, a reduction in crown recession, and an increase in crown length if height increment is still significant (Oliver and Larson, 1996, Tappeiner et al., 2007). Moreover, the improvement of the light environment will increase foliage density within the crown (Oliver and Larson, 1996, Tappeiner et al., 2007). Finally, a properly applied thinning should reduce the probability of mortality for the residual trees. How quickly these responses will be manifested in the residual trees will depend upon stand structure and tree species, crown size, and crown class of the trees before thinning, with the duration of thinning responses extending well beyond crown closure (Oliver and Larson, 1996).

Tree level models, such as RAP-ORGANON, that incorporate one- and two-sided measures of competition and a measure of crown size into their equations for untreated stands will inherently produce a thinning response that is sensitive to both the intensity and the type of thinning. Intensity of thinning is reflected in the size of reduction in the competition measures, and type of thinning is reflected in the relative reduction in the two measures of competition often expressed in tree level models. For example, thinning from below will reduce just the two-sided measure of competition, while thinning from above will reduce both resulting in larger predicted responses from thinning from above than thinning from below. Furthermore, use of crown size variables in the prediction equations will also provide differential response due to type of thinning if the understory trees have smaller crowns than the overstory trees. On the other hand, smaller size trees can be predicted to have larger potential increments, particularly if a potential times modifier approach is used for the basic untreated equation.

These predicted thinning responses may not fully characterize the actual thinning response. Thinning modifiers can be important in tree level models because: (1) crown density often increases after thinning, (2) damaged trees, which can reduce diameter increment (Hann and Hanus, 2002a) and height increment (Hann and Hanus, 2002b), are often removed in thinning and, as a result, the population is modified, (3) thinning shock can occur after treatment, (4) thinning can increase the susceptibility of the residual stand to damaging agents such as wind and snow, and (5) the dynamics of diameter increment, height increment, and crown recession can accelerate after thinning. The last possibility is of particular concern if the measurement intervals used to collect the modeling data are particularly long resulting in larger changes in those attributes over the growth period than would be predicted by the untreated equations.

The RAP-ORGANON model includes equations for predicting the development of untreated stands. Furthermore, all of the dynamic equations incorporate measures of competition. Therefore, the RAP-ORGANON equations developed using untreated data will predict a response to thinnings because of the reduction in competition. Whether or not this predicted behavior is adequate to characterize the effects of thinning depends upon the species; the type, timing, and intensity of thinning; and the particular dynamic equation being examined. Hann et al. (2003) found that ORGANON's predicted thinning response from the untreated diameter

increment and height increment equations of Douglas-fir and western hemlock were inadequate for characterizing the full response to thinning. They also found that the untreated mortality rate equations for both species adequately characterized the mortality rate after thinning. These results were for five-year growth periods in which the predictor variables were measured at the start of the growth period. Therefore, any large thinning induced changes to the dynamics of how the untreated trees' predictor variables (such as height to crown base) change over the growth period might not be adequately reflected in those start of growth period values for thinned trees. However, such problems might be reduced or eliminated with shorter growth periods.

Hann et al. (2003) found that the effects of thinning could be adequately characterized by stand level predictor variable of proportion of the basal area removed in the thinning (PREM) and the number of years since the thinning (YT). For the diameter increment (ΔD) and height increment (ΔH) equations the multiplicative thinning modifier (TMOD) took the general form:

$$TMOD_{j,k} = 1.0 + b_1 (PREM_{j,k})^{b_2} e^{b_3 YT_{j,k}} \qquad \text{Equation (15.1)}$$

Hann et al. (2003) reported that the modifier predicted an increase in diameter increment and a decrease in height increment after thinning for both conifer species. Most of the effect was gone after 10 years for both the diameter increment and height increment equations.

While the modifier equation could be fit to individual tree data, the fact that the predictor variables use only stand level attributes would result in inflated number of degrees of freedom and, therefore, under estimated variances of the resulting parameters. Therefore, the red alder thinning analyses used stand level data sets to estimate the parameters and standard errors of the parameters. For ease of analysis, the ΔD and ΔH data sets were developed using the central PAI type data sets rather than the summation data sets used to develop the tree level equations for untreated plots.

For the ΔD, ΔH, and crown recession (ΔHCB) equations, the basic relationship to be estimated from the treatment plot data is:

$TI_{i,j,k} = (TMOD_{j,k})\ (UI_{i,j,k})$

Where,

$TI_{i,j,k}$ = Measured thinning increment for tree i, plot j, and measurement k.
$TMOD_{j,k}$ = Thinning modifier value for plot j and measurement k.
$UI_{i,j,k}$ = Adjusted and calibrated untreated increment prediction for tree i, plot j, and measurement k.

If $TMOD_{j,k}$ is one for a given plot and measurement, then $UI_{i,j,k}$ is adequate for predicting the response to thinning. However, if $TMOD_{j,k}$ varies across values of PREM and YT, then the $TMOD_{j,k}$ values can be used to develop an appropriate modifier equation.

15.1 Data

The following describes the steps taken to develop the ΔD modifier and ΔH modifier data sets:

1. Both of the tree level equations for untreated plots were fit using the weighted summation method so the first step of the analysis was to adjust the equations to the central PAI data sets using weighted simple linear regression through the origin. The weighting schemes used in these adjustments was the same as used in fitting the untreated equations.

2. The adjusted untreated equations were then calibrated to the data collected on each treatment plot before application of the treatments. The calibration factors were computed using the data from just the last growth period before treatment. Hann and Hanus (2002a) and Hann et al. (2003) found that this type of calibration reduced the variation caused by between plot differences in the ΔD or ΔH. As in step #1, weighted simple linear regression through the origin was used to calculate these plot level calibrations.

3. The plot level calibrated untreated equations were then used to predict the post treatment increments (i.e., $UI_{i,j,k}$) for all trees and all growth periods for each of the treated plots.

4. The values of $TI_{i,j,k}$ and $UI_{i,j,k}$ were then used to calculate $TMOD_{j,k}$ using the following equation and the same weights ($w_{i,j,k}$) used to estimate the parameters of the untreated equations:

$$TMOD_{j,k} = \frac{\sum_{i=1}^{n_{j,k}} (w_{i,j,k})(UI_{i,j,k})(TI_{i,j,k})}{\sum_{i=1}^{n_{j,k}} (w_{i,j,k})(UI_{i,j,k})^2}$$

5. The resulting values of $TMOD_{j,k}$ are the response variables used in developing the TMOD prediction equations. The consequent ΔD data set for fitting Equation (15.1) is described in Table 15.1 and the consequent ΔH data set for fitting Equation (15.1) is described in Table 15.2.

Table 15.1 Descriptive statistics for the plantation grown red alder thinning data set used to fit the annual ΔD thinning modifier equation.

Attribute	Mean	Minimum	Maximum	Std. Deviation
Plot/Measurement Level Attributes: N = 308				
TMOD	0.9781015	0.364567	1.954348	0.2243839
PREM	0.5272255	0.005147	0.85601	0.1663362
YT (yrs.)	2.376623	0.0	11.0	2.467582
KNT	32.53571	2.0	75.0	9.91209

Table 15.2 Descriptive statistics for the plantation grown red alder thinning data set used to fit the annual ΔH thinning modifier equation.

Attribute	Mean	Minimum	Maximum	Std. Deviation
Plot/Measurement Level Attributes: N = 308				
TMOD	0.8866205	-0.21707	3.317576	0.479216
PREM	0.5272255	0.005147	0.85601	0.1663362
YT (yrs.)	2.376623	0.0	11.0	2.467582
KNT	32.53571	2.0	75.0	9.91209

The development of the ΔHCB thinning modifier data set was complicated by the fact that two model forms were used to characterize ΔHCB. As a result, two modifier data sets were developed, one for each of the model forms. Because the final untreated tree level parameters of both model forms were estimated using the weighted central PAI procedures, step #1 of above was not necessary. The final ΔHCB data set for fitting Equation (15.1) that was used with the basic equation containing TAGE is described in Table 15.3, and the final ΔHCB data set for fitting Equation (15.1) that was used with the basic equation containing GEA is described in Table 15.4.

Table 15.3 Descriptive statistics for the plantation grown red alder thinning data set used to fit the annual ΔHCB thinning modifier equation for the ΔHCB equation with TAGE.

Attribute	Mean	Minimum	Maximum	Std. Deviation
Plot/Measurement Level Attributes: N = 308				
TMOD	1.122082	-21.7262	19.69652	2.94829
PREM	0.5272255	0.005147	0.85601	0.1663362
YT (yrs.)	2.376623	0.0	11.0	2.467582
KNT	32.53571	2.0	75.0	9.91209

Table 15.4 Descriptive statistics for the plantation grown red alder thinning data set used to fit the annual ΔHCB thinning modifier equation for the ΔHCB equation with GEA.

Attribute	Mean	Minimum	Maximum	Std. Deviation
Plot/Measurement Level Attributes: N = 308				
TMOD	1.071299	-20.37439	18.11474	2.720868
PREM	0.5272255	0.005147	0.85601	0.1663362
YT (yrs.)	2.376623	0.0	11.0	2.467582
KNT	32.53571	2.0	75.0	9.91209

A completely different approach was used to form the annual probability of mortality (PM) thinning modifier data sets. Similar to the ΔHCB analysis, two model forms have been proposed for characterizing the PM of untreated stands: one using crown ratio variables but no basal area variable and the other using a basal area variable but no crown ratio variables. The mortality analysis was further complicated by the fact that a multiplicative modifier equation would not work with the logistic model form used to characterize tree mortality rate. Finally, the relative rarity of mortality on the plots meant that plot level calibrations would not be possible. Given these complications, the following approach was used to form the plot level thinning effects response variable.

First, the measured proportion of all trees on thinned plot "j" and measurement "k" dying over the growth period ($PPMT_{\bullet,j,k}$) was calculated by:

$$PPMT_{\bullet,j,k} = \frac{\sum_{i=1}^{n_{j,k}} (I_{i,j,k} \cdot EXPAN_{i,j,k})}{\sum_{i=1}^{n_{j,k}} EXPAN_{i,j,k}}$$

Where,

$I_{i,j,k}$ = Mortality indicator variable for j^{th} tree on the i^{th} thinned plot and k_{th} measurement
= 1.0 if the tree died in the growth period
= 0.0 if not

The measured proportion of all trees on thinned plot "i" surviving over the growth period ($PPST_{\bullet,j,k}$) was then calculated by:

$PPST_{\bullet,j,k} = 1.0 - PPMT_{\bullet,j,k}$

The measured proportion of all trees on thinned plot "i" surviving annually ($PST_{\bullet,j,k}$) was then calculated by:

$PST_{\bullet,j,k} = (PPST_{\bullet,j,k})^{1/LEN}$

Where,

LEN = Length of growth period in years

Finally, the response variable consisting of measured proportion of all trees on thinned plot "i" dying annually ($PMT_{\bullet,j,k}$) was calculated by:

$PMT_{\bullet,j,k} = 1.0 - PST_{\bullet,j,k\ i}$

Given the measured response variable for each plot, the model form used in the thinned stand mortality analysis was created in the following manner. First, the proportion of all trees on a thinned plot dying annually as predicted from the untreated plot equations ($PMC_{\bullet,j,k}$) was calculated by:

$$PMC_{\bullet,j,k} = \frac{\sum_{i=1}^{n_{j,k}} (PMC_{i,j,k} \cdot EXPAN_{i,j,k})}{\sum_{i=1}^{n_{j,k}} EXPAN_{i,j,k}}$$

Where,

$PMC_{i,j.k}$ = Predicted annual probability of mortality for tree "i" on thinned plot "j" and measurement "k" from the previously estimated untreated equations.

The predicted annual proportion of survival for all trees on thinned plot "j" and measurement "k" ($PSC_{\bullet,j,k}$) was then calculated by:

$PSC_{\bullet,j,k} = 1.0 - PMC_{\bullet,j,k}$

Given that $PMC_{\bullet,j,k}$ and $PSC_{\bullet,j,k}$ are known, the next step was to algebraically solve the following expression of the logistic equation for $e^{-ZC_{\bullet,j,k}}$:

$$PMC_{\bullet,j,k} = \frac{1.0}{1.0 + e^{-ZC_{\bullet,j,k}}}$$

The resulting solution was:

$$e^{-ZC_{\bullet,j,k}} = (PSC_{\bullet,J,K})/(PMC_{\bullet,J,K})$$

The resulting plot level equation used for modeling the effect of thinning upon predicted mortality rate was:

$$PMT_{\bullet,j,k} = \frac{1.0}{1.0 + e^{-ZC_{\bullet,j,k}} e^{-(b_0 + b_1(PREM_{j,k}) e^{b_2 YT_{j,k}})}} + \varepsilon_{j,k}$$

Another expression of the same equation would be:

$$PMT_{\bullet,j,k} = \frac{1.0}{1.0 + e^{-(ZC_{\bullet,j,k} + b_0 + b_1(PREM_{j,k}) e^{b_2 YT_{j,k}})}} + \varepsilon_{j,k} \qquad \text{Equation (15.2)}$$

If there is no thinning effect upon plot level rate of mortality, then $b_0 = b_1 = 0.0$ and:

$PMT_{\bullet,j,k} = PMC_{\bullet,j,k} + \varepsilon_{\bullet,j,k}$

The resulting $PMT_{\bullet,j,k}$ data set for fitting Equation (15.2) with the basic predictor variables using crown ratio predictor variables but not a basal area predictor variable is described in Table 15.5, and the resulting $PMT_{\bullet,j,k}$ data set for fitting Equation (2) with the basic predictor variables that use basal area but not crown ratio predictor variables is described in Table 15.6.

Table 15.5 Descriptive statistics for the plantation grown red alder thinning data set used to fit the PM thinning modifier equation.

Attribute	Mean	Minimum	Maximum	Std. Deviation
Plot/Measurement Level Attributes: N = 310				
PPMT	0.002728211	0.0	0.07168223	0.007065123
PPMC	0.001386901	0.00006188	0.01977899	0.001320336
PREM	0.5287288	0.005147	0.85601	0.1668466
YT (yrs.)	1.364516	0.0	9.0	2.140539
LEN (yrs.)	3.022581	1.0	5.0	0.9997442
KNT	80.59032	33.0	231.0	17.9143

Table 15.6 Parameter estimates, their standard errors, their t-statistics, and the probability that the parameter estimates are zero (P-Value) for the plantation grown red alder annual ΔD thinning modifier equation.

Parameter	Estimate	Standard Error	t-statistic	P-Value
b_1	-0.456273125	0.3047762	-1.50	0.13541
b_2	3.65818137	1.892551	1.93	0.05417
b_3	-0.489095418	0.3520848	-1.39	0.16580

15.2 Data Analysis, Results, and Discussion

15.2.1 Diameter Increment Equation

The first step of the analysis consisted of preparing three graphs:

1. Mean TMOD for all plots and measurements and the associated 99% confidence intervals for the mean values plotted over $YT_{j,k}$ (see Figure 15.1).
2. $TMOD_{j,k}$ for $YT_{j,k} = 0$ plotted over $PREM_{j,k}$ (see Figure 15.2).
3. $TMOD_{j,k}$ for $YT_{j,k} = 1$ plotted over $PREM_{j,k}$ (see Figure 15.3).

Figure 15.1 The average, upper 99% confidence interval, and lower 99% confidence interval for the weighted diameter increment modifier data plotted across number of years since thinning. The diameter increment equation was calibrated to the increment data from the last untreated growth period before being applied to the thinned data.

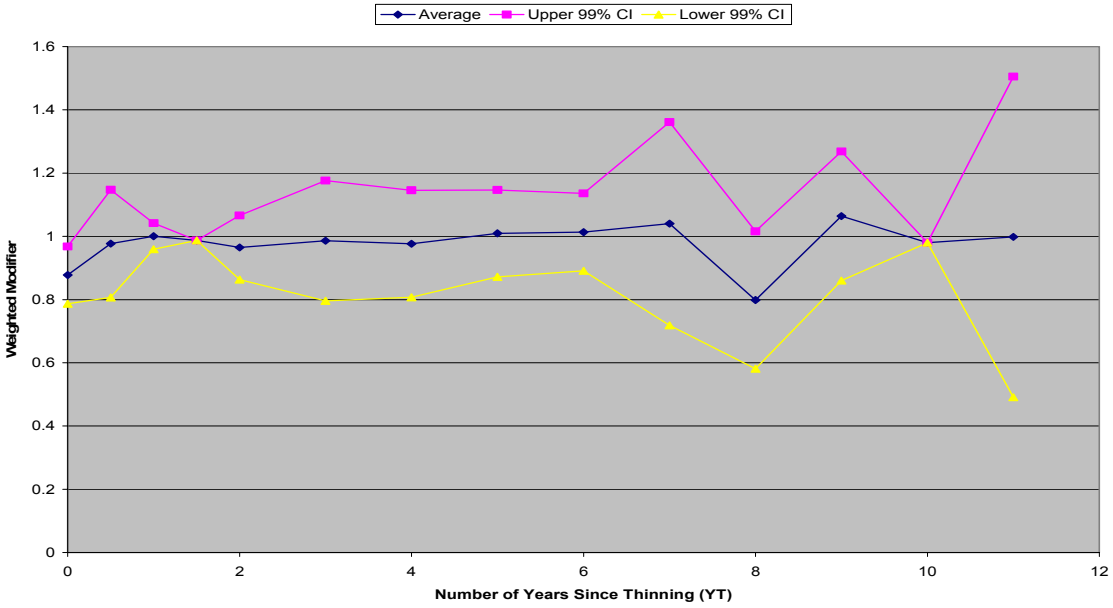

Figure 15.2 The weighted diameter increment thinning modifier data for the first year since thinning plotted across proportion of the basal area removed in thinning. The diameter increment equation was calibrated to the increment data from the last untreated growth period before being applied to the thinned data.

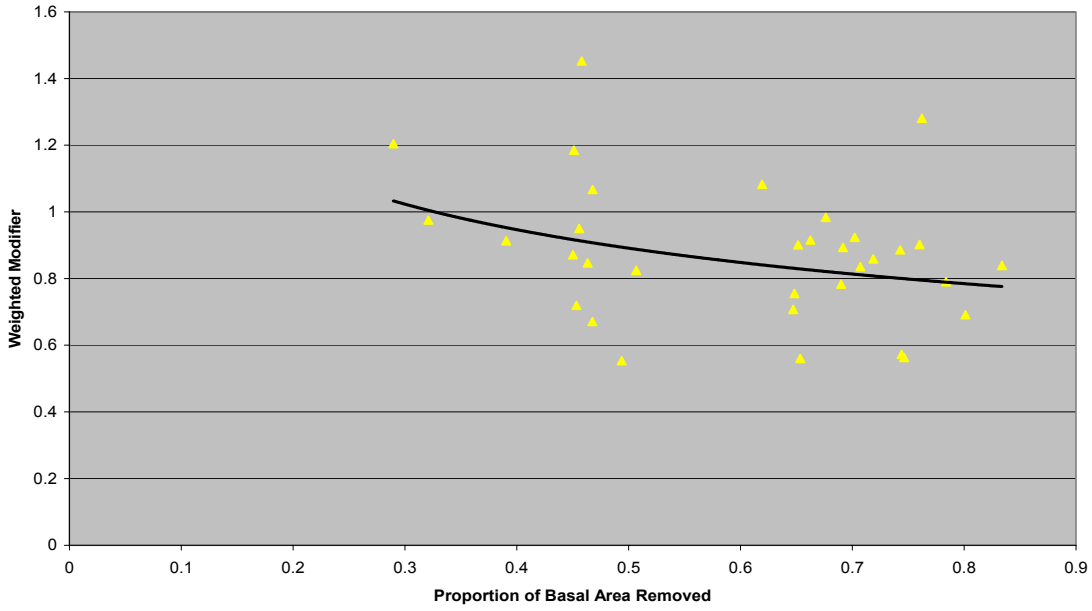

Figure 15.3 The weighted diameter increment thinning modifier data for the second year since thinning plotted across proportion of the basal area removed in thinning. The diameter increment equation was calibrated to the increment data from the last untreated growth period before being applied to the thinned data.

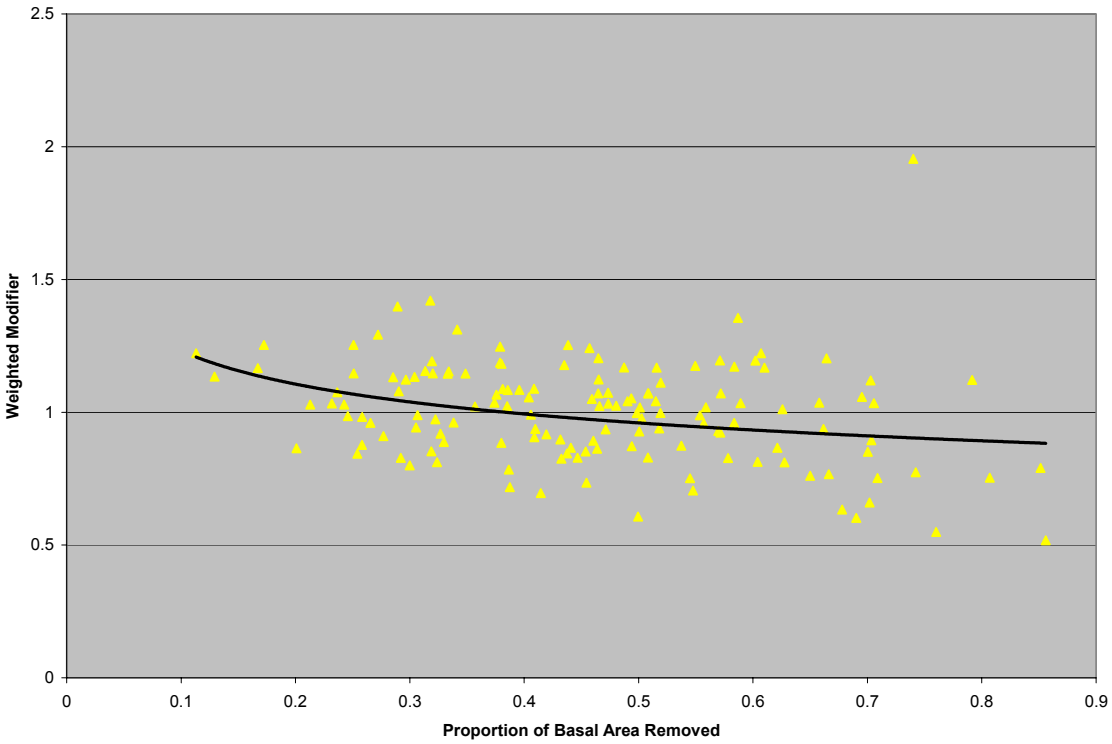

The second step of the analysis consisted of fitting the ΔD $TMOD_{j,k}$ data to Equation (15.1) using weighted nonlinear regression and a weight of $KNT_{j,k}^2$ (the number of trees used to calculate the mean values for plot "j" and measurement "k"). The resulting parameter estimates, their standard errors, t-statistics, and associated P-values are found in Table 15.6.

Examination of Figure 15.1 indicates that the 99% confidence intervals incorporate 1.0 for all $YT_{j,k}$ values with multiple observations of $TMOD_{j,k}$ except for $YT_{j,k} = 0$ (in which the upper confidence interval value was 0.97). Examination of Figure 15.2 indicates a weak trend of $TMOD_{j,k}$ declining over $PREM_{j,k}$ for $YT_{j,k} = 0$, with the trend becoming even weaker for $YT_{j,k} = 1$ (Figure 15.3). Finally, an examination of the parameter estimates, their standard errors, and associated t-statistics and P-values (Table 15.6) indicates that none of the parameters are significantly different from 0.0 at even $\alpha = 0.05$, confirming the results of the graphical analysis.

The one and two sided competition predictor variables and the crown ratio predictor variable in the untreated plot ΔD equation will automatically predict an increase in ΔD after thinning. The results of this analysis indicate that a thinning modifier to the untreated plot ΔD equation is unnecessary for red alder growing in plantations. Therefore, RAP-ORGANON will predict an unmodified increase to ΔD after thinning. This finding agrees with those of Hibbs et al. (1989) and Hibbs et al. (1995) who also reported an increase in ΔD after thinning red alder.

15.2.2 Height Increment Equation

The first step of the analysis consisted of preparing three graphs:

1. Mean TMOD for all plots and measurements and the associated 99% confidence intervals for the mean values plotted over $YT_{j,k}$ (see Figure 15.4).
2. $TMOD_{j,k}$ for $YT_{j,k} = 0$ plotted over $PREM_{j,k}$ (see Figure 15.5).
3. $TMOD_{j,k}$ for $YT_{j,k} = 1$ plotted over $PREM_{j,k}$ (see Figure 15.6).

Figure 15.4 The average, upper 99% confidence interval, and lower 99% confidence interval for the weighted height increment modifier data plotted across number of years since thinning. The height increment equation was calibrated to the increment data from the last untreated growth period before being applied to the thinned data.

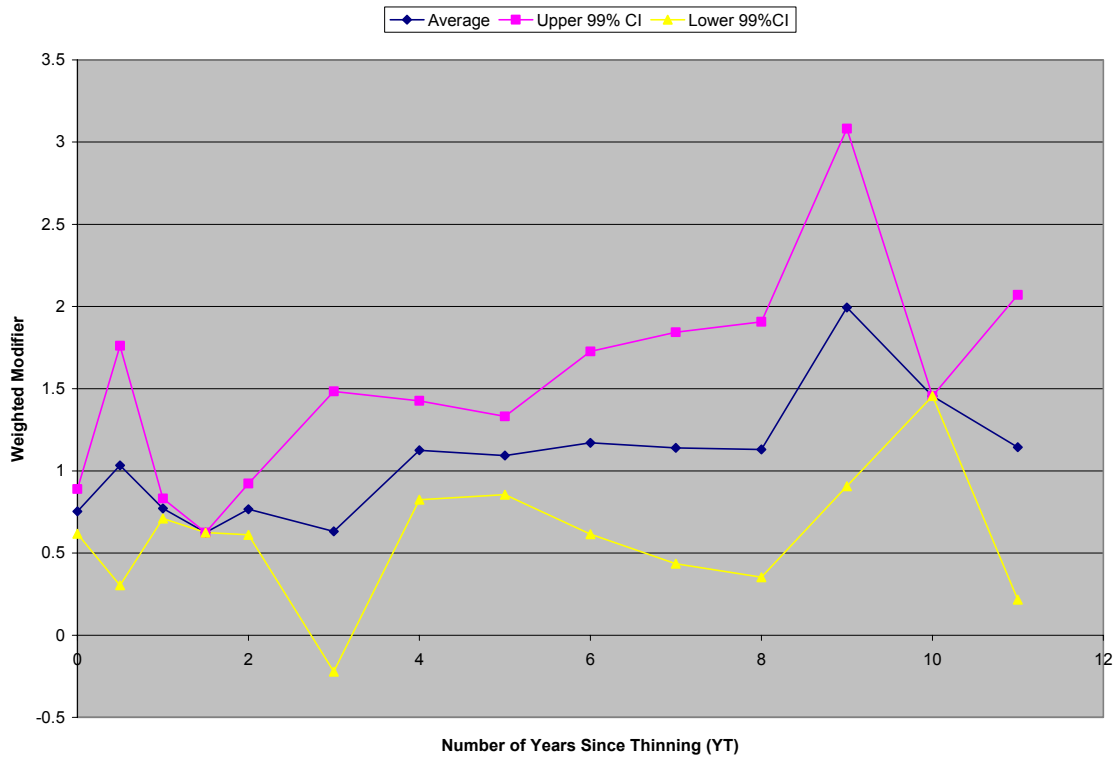

Figure 15.5 The weighted height increment thinning modifier data for the first year since thinning plotted across proportion of the basal area removed in thinning. The height increment equation was calibrated to the increment data from the last untreated growth period before being applied to the thinned data.

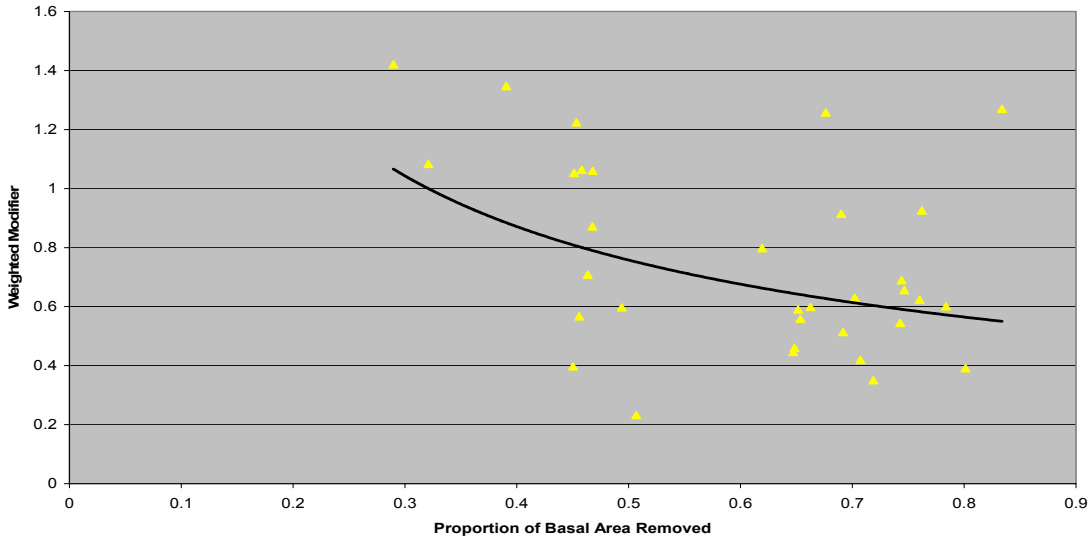

Figure 15.6 The weighted height increment thinning modifier data for the second year since thinning plotted across proportion of the basal area removed in thinning. The height increment equation was calibrated to the increment data from the last untreated growth period before being applied to the thinned data.

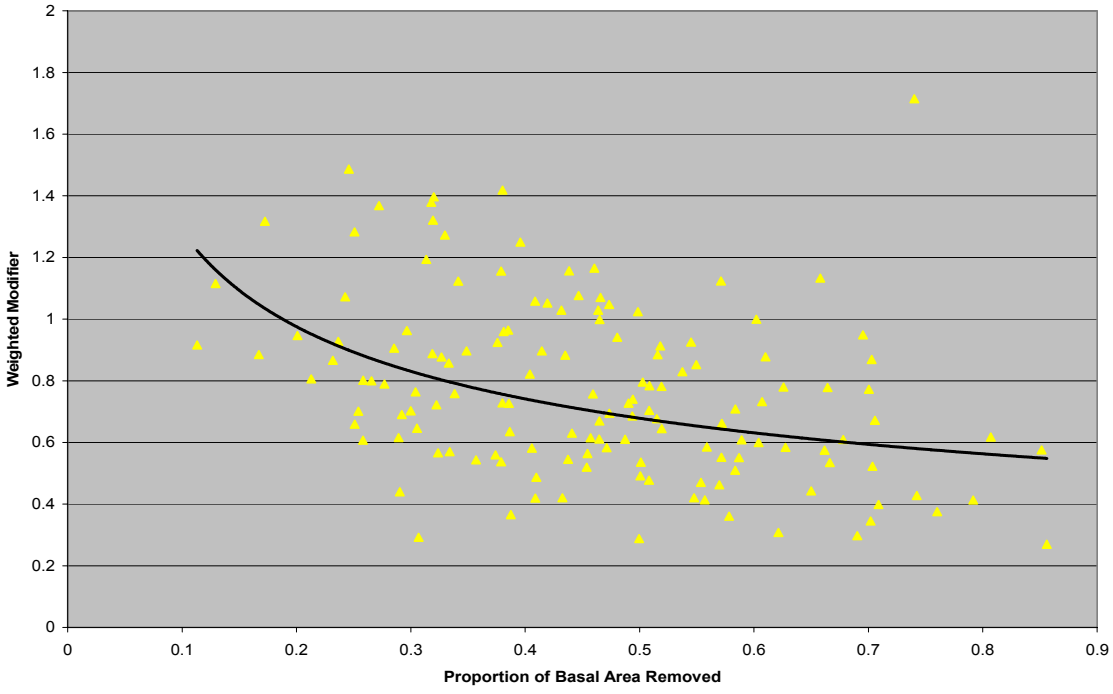

The second step of the analysis consisted of fitting the ΔH $TMOD_{j,k}$ data to Equation (15.1) using weighted nonlinear regression and a weight of $KNT_{j,k}^2$ (the number of trees used to calculate the mean values for plot "j" and measurement "k"). The resulting parameter estimates, their standard errors, t-statistics, and associated P-values are found in Table 15.7.

Table 15.7 Parameter estimates, their standard errors, their t-statistics, and the probability that the parameter estimates are zero (P-Value) for the plantation grown red alder annual ΔH thinning modifier equation.

Parameter	Estimate	Standard Error	t-statistic	P-Value
b_1	-0.757261183	0.235354	-3.22	0.00143
b_2	1.46517901	0.6045547	2.42	0.01595
b_3	-0.416582579	0.1706844	-2.44	0.01523

Examination of Figure 15.4 indicated that the 99% confidence intervals did not incorporate 1.0 for four of the five smallest values of $YT_{j,k}$ (the one value that did enclose 1.0 had only seven observations). Examination of Figure 5 indicated a trend of $TMOD_{j,k}$ declining over $PREM_{j,k}$ for values of $YT_{j,k} = 0$, with the trend becoming stronger for values of $YT_{j,k} = 1$ (Figure 15.6). Finally, an examination of the parameter estimates, their standard errors, and associated t-statistics and P-values (Table 15.7) indicated that all of the parameters are significantly different from 0.0 at $\alpha = 0.05$, confirming the results of the graphical analysis.

A perusal of the confidence interval about b_2 indicated that the parameter was not significantly different from 1.0 so the model was simplified by setting b_2 to 1.0 and re-estimating the other two parameters. The parameter estimates, their standard errors, and associated t-statistics and P-values for the reduced model are found in Table 15.8.

Table 15.8 Parameter estimates, their standard errors, their t-statistics, and the probability that the parameter estimates are zero (P-Value) for the plantation grown red alder reduced annual ΔH thinning modifier equation.

Parameter	Estimate	Standard Error	t-statistic	P-Value
b_1	-0.613313694	0.1049267	-5.85	0.00001
b_2	1.0	NA	NA	NA
b_3	-0.443824038	0.1817644	-2.44	0.01518

The one sided competition predictor variable and the crown ratio predictor variable in the untreated plot ΔH equation will automatically predict an increase in ΔH after thinning. The results of this analysis indicate that a thinning modifier to the untreated plot ΔH equation is necessary for red alder growing in plantations.

A graph of the ΔH modifier (Figure 15.7) showed that there was a substantial reduction in predicted ΔH immediately after thinning, with the size of the reduction being related to the proportion of the basal area removed in thinning. Figure 15.7 also indicated that the reduction was basically gone after ten years.

Figure 15.7 Height increment thinning modifier with b2 set to 1.0 for red alder plantations plotted across the number of years since thinning for three levels of the proportion of the basal area removed (PREM) in thinning.

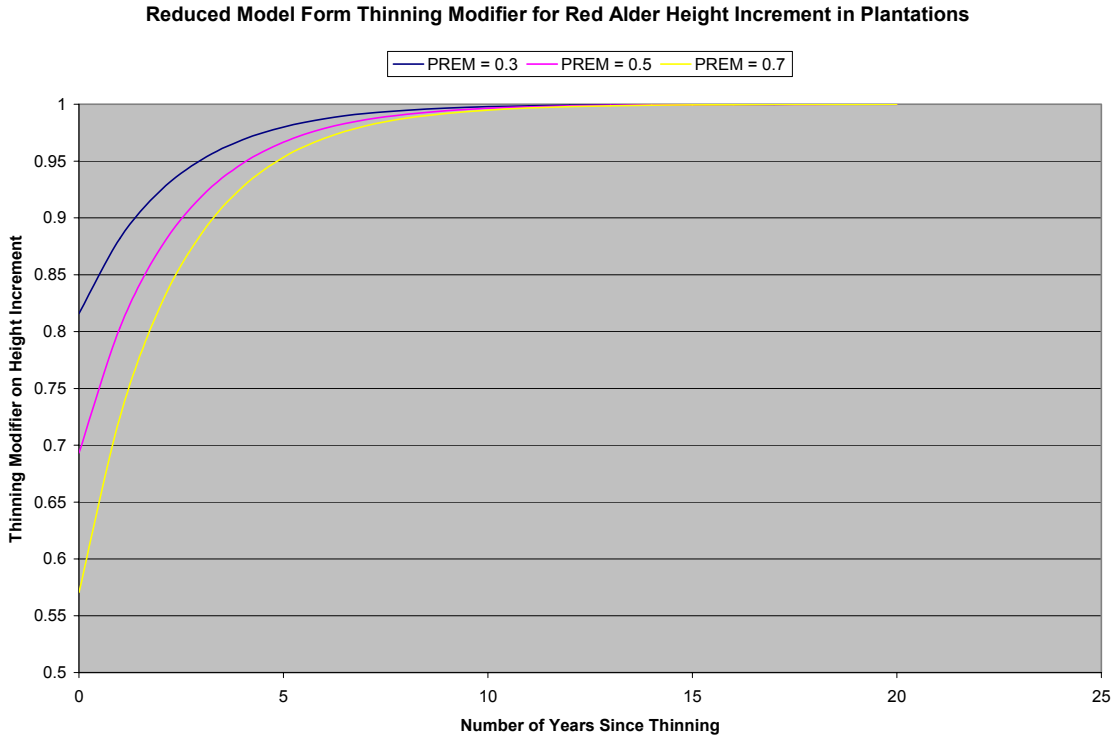

A survey of the basic data indicated that there was an increase in height damage after thinning that may have contributed to the decrease in ΔH. As Table 15.9 indicates, the frequency of both broken tops and forking above breast height was reduced at the time of thinning over the average found on the untreated plots but then increased to values equal to or greater than found on untreated plots as time from thinning increased. However, it is unlikely that these damage rates would explain the full amount of decreased ΔH found in this study. Weiskittel et al. (2009) reported that the dominant height increment of red alder was significantly slower on low density plots. Perhaps a similar effect upon ΔH also occurs after thinning.

Table 15.9 Frequency of tree damage that might affect ΔH.

Source of Data	Percentage of Trees with Damage	
	Broken Top	Forked Above BH
Untreated Trees at All Measurements	0.42	2.62
Residual Trees at Removal Measurement	0.09	1.23
Residual Trees at 1 to 3 Years after Removals	1.93	1.91
Residual Trees at 4 to 9 Years after Removals	0.89	4.06

Regardless of the cause, the reduction in ΔH immediately after thinning in red alder has also been reported by Hibbs et al. (1989). They found that five year ΔH rates immediately after thinning had been reduced by 47% for the crop trees on the mechanical thinned treatment, and Hibbs et al. (1995) reported that the reduction was gone 10 years after the thinning. Hann et al. (2003) also found that thinning resulted in decreased ΔH after treatment for both Douglas-fir and western hemlock, but top damage was not identified as a possible cause. They also reported that the effect of thinning was basically gone after ten years.

15.2.3 Crown Recession Equation

The first step of the analysis consisted of preparing six graphs:

1. Mean TMOD values for the ΔHCB equation that uses TAGE using all plots and measurements and the associated 99% confidence intervals for the mean values plotted over $YT_{j,k}$ (see Figure 15.8).
2. The TAGE ΔHCB equation $TMOD_{j,k}$ values restricted to $YT_{j,k} = 0$ plotted over $PREM_{j,k}$ (see Figure 15.9).
3. The TAGE ΔHCB equation $TMOD_{j,k}$ values restricted to $YT_{j,k} = 1$ plotted over $PREM_{j,k}$ (see Figure 15.10).
4. Mean TMOD values for the ΔHCB equation that uses GEA using all plots and measurements and the associated 99% confidence intervals for the mean values plotted over $YT_{j,k}$ (see Figure 15.11).
5. The GEA ΔHCB equation $TMOD_{j,k}$ values restricted to $YT_{j,k} = 0$ plotted over $PREM_{j,k}$ (see Figure 15.12).
6. The GEA ΔHCB equation $TMOD_{j,k}$ values restricted to $YT_{j,k} = 1$ plotted over $PREM_{j,k}$ (see Figure 15.13).

Figure 15.8 The average, upper 99% confidence interval, and lower 99% confidence interval for the weighted crown recession with total stand age modifier data plotted across number of years since thinning. The crown recession equation with total stand age was calibrated to the increment data from the last untreated growth period before being applied to the thinned data.

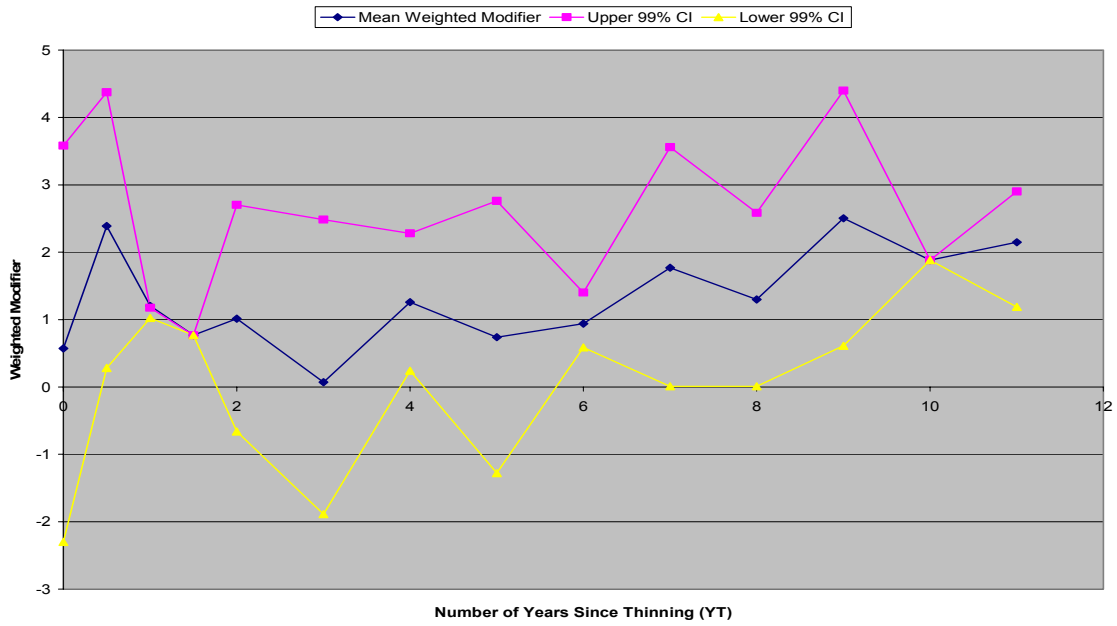

Figure 15.9 The weighted crown recession with total stand age thinning modifier data for the first year since thinning plotted across proportion of the basal area removed in thinning. The crown recession with total age equation was calibrated to the increment data from the last untreated growth period before being applied to the thinned data.

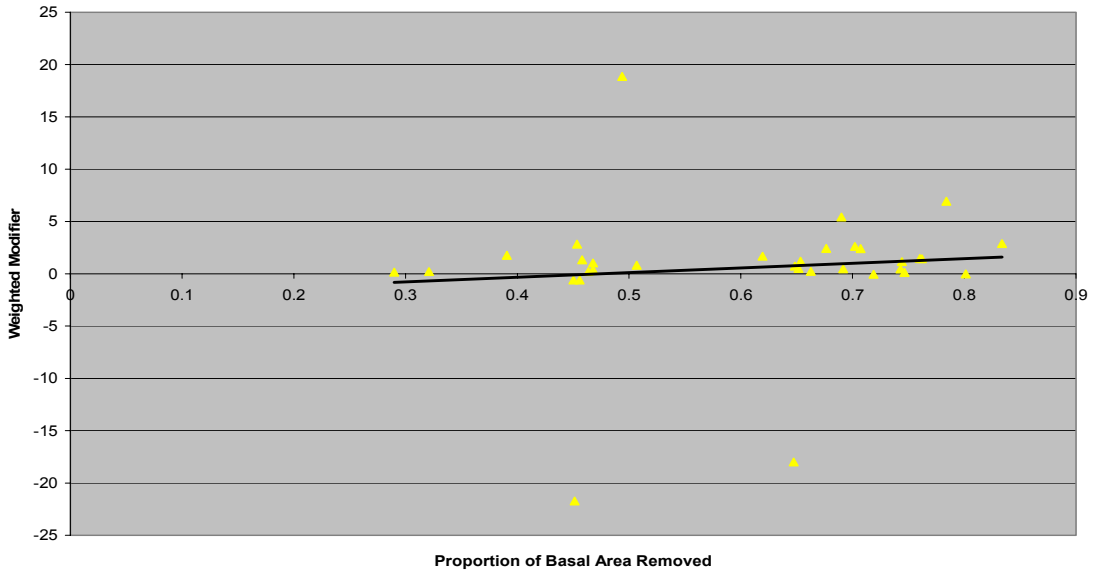

Figure 15.10 The weighted crown recession with total stand age thinning modifier data for the second year since thinning plotted across proportion of the basal area removed in thinning. The crown recession with total age equation was calibrated to the increment data from the last untreated growth period before being applied to the thinned data.

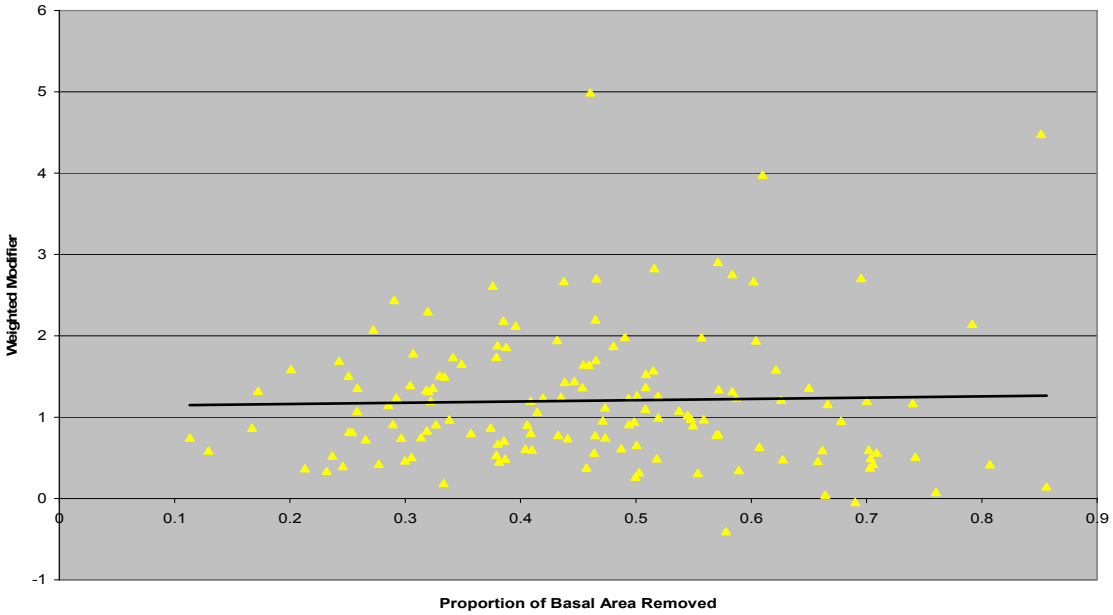

Figure 15.11 The average, upper 99% confidence interval, and lower 99% confidence interval for the weighted crown recession with growth effective age modifier data plotted across number of years since thinning. The crown recession equation with growth effective age was calibrated to the increment data from the last untreated growth period before being applied to the thinned data.

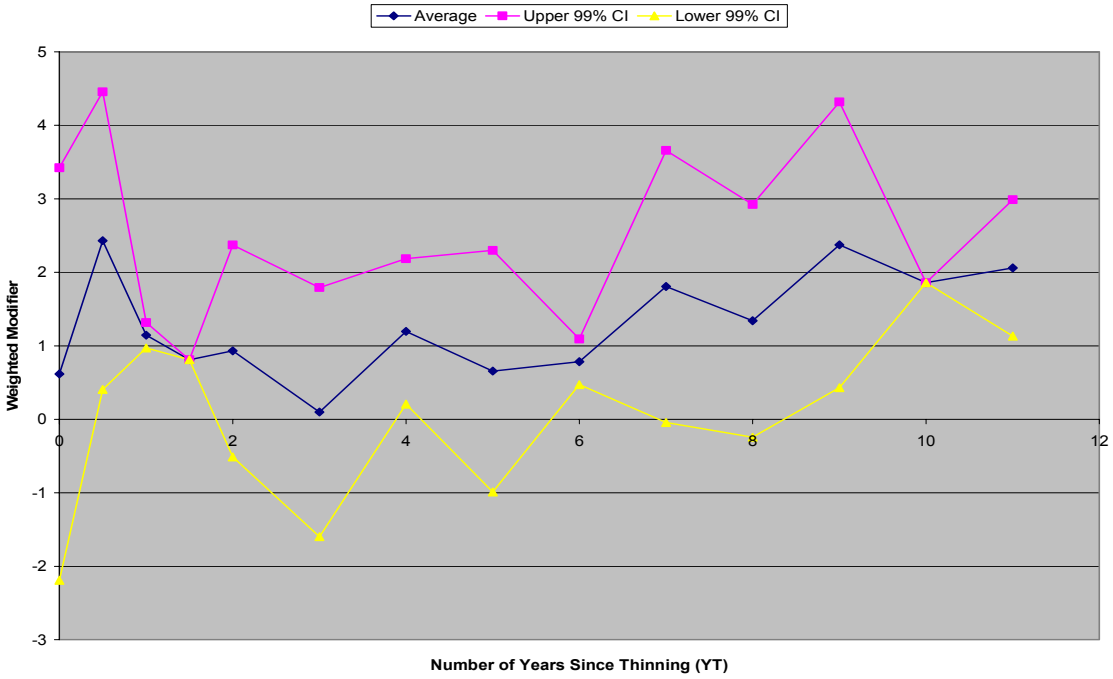

Figure 15.12 The weighted crown recession with growth effective age thinning modifier data for the first year since thinning plotted across proportion of the basal area removed in thinning. The crown recession with growth effective age equation was calibrated to the increment data from the last untreated growth period before being applied to the thinned data.

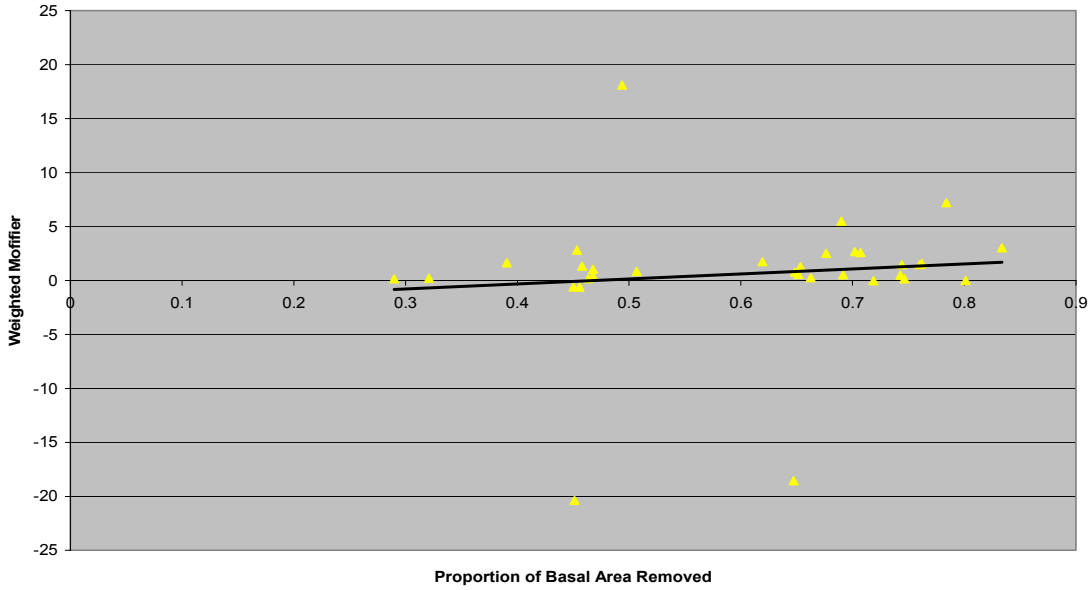

Figure 15.13 The weighted crown recession with growth effective age thinning modifier data for the second year since thinning plotted across proportion of the basal area removed in thinning. The crown recession with growth effective age equation was calibrated to the increment data from the last untreated growth period before being applied to the thinned data.

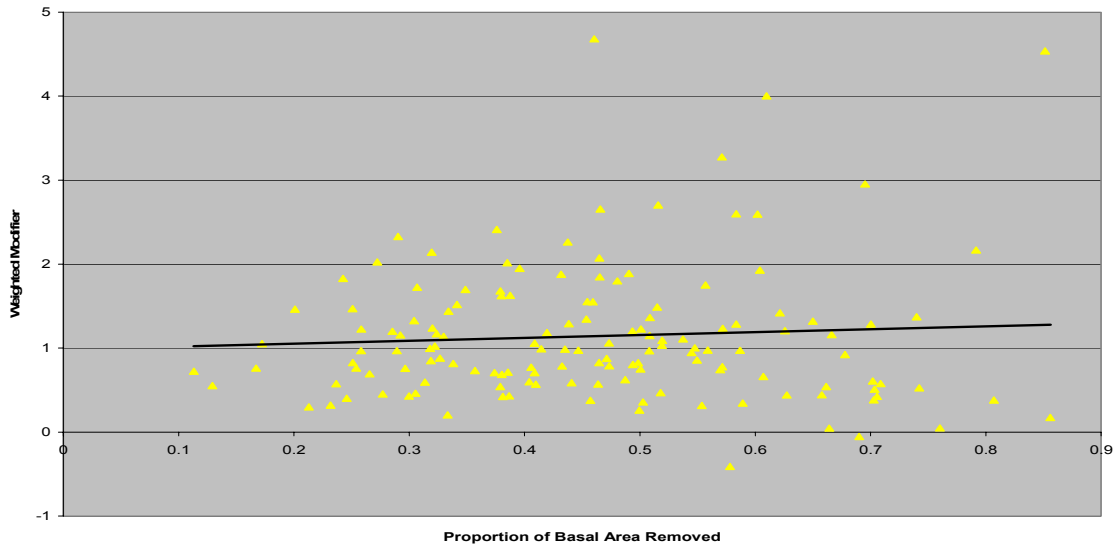

The second step of the analysis consisted of fitting the TAGE ΔHCB equation $TMOD_{j,k}$ data and the GEA ΔHCB equation $TMOD_{j,k}$ data to Equation (15.1) using weighted nonlinear regression and a weight of $KNT_{j,k}^2$ (the number of trees used to calculate the mean values for plot "j" and measurement "k"). The resulting parameter estimates, their standard errors, t-statistics, and associated P-values for the TAGE ΔHCB equation are found in Table 15.10 and the values for the GEA ΔHCB equation are found in Table 15.11.

Table 15.10 Parameter estimates, their standard errors, their t-statistics, and the probability that the parameter estimates are zero (P-Value) for the plantation grown red alder annual ΔHCB thinning modifier equation that adjusts the ΔHCB equation with TAGE.

Parameter	Estimate	Standard Error	t-statistic	P-Value
b_1	0.00608610882	0.03394093	0.18	0.85781
b_2	-0.513562892	0.8216631	-0.63	0.53242
b_3	0.478763228	0.5105082	0.94	0.34908

Table 15.11 Parameter estimates, their standard errors, their t-statistics, and the probability that the parameter estimates are zero (P-Value) for the plantation grown red alder annual ΔHCB thinning modifier equation that adjusts the ΔHCB equation with GEA.

Parameter	Estimate	Standard Error	t-statistic	P-Value
b_1	0.00335789586	0.02254608	0.15	0.88170
b_2	-0.56810717	0.9234714	-0.62	0.53889
b_3	0.52191494	0.6079908	0.86	0.39133

Examination of Figure 15.8 indicates that the 99% confidence intervals for the TAGE ΔHCB equation $TMOD_{j,k}$ values incorporate 1.0 for all but two of the $YT_{j,k}$ values with multiple observations of $TMOD_{j,k}$. Examination of Figure 15.11 indicates that the 99% confidence intervals for the GEA ΔHCB equation $TMOD_{j,k}$ values incorporate 1.0 for all but one of the $YT_{j,k}$ values with multiple observations of $TMOD_{j,k}$. Examination of Figures 15.9 and 15.12 indicates very weak trends of $TMOD_{j,k}$ increasing over $PREM_{j,k}$ for $YT_{j,k} = 0$. These very weak trends across $PREM_{j,k}$ are also evident for $YT_{j,k} = 1$ (Figures 15.10 and 15.13). Finally, an examination of the parameter estimates, their standard errors, and associated t-statistics and P-values for the TAGE ΔHCB modifier equation (Table 15.10) and the GEA ΔHCB modifier equation (Table 15.11) indicates that none of the parameters are significantly different from 0.0 at even $\alpha = 0.05$, confirming the results of the graphical analysis.

The indirect method of predicting ΔHCB utilizes an untreated plot HCB equation that includes one and two competition predictor variables. Therefore, the indirect method will automatically predict a reduction in ΔHCB after thinning. Similarly, the direct ΔHCB equation for untreated plots contains a two sided competition predictor variable and a crown ratio predictor variable which will automatically predict a decrease in ΔHCB after thinning. The results of this analysis indicate that a thinning modifier to the direct untreated plot ΔHCB equation is unnecessary for red alder growing in plantations. Therefore, RAP-ORGANON will predict an unmodified reduction to ΔHCB after thinning. This finding agrees with that of Hibbs et al. (1995) who also reported a reduction to ΔHCB after thinning red alder.

15.2.4 Probability of Mortality Equation

The analysis consisted of fitting the $PMT_{\bullet,j,k}$ data to Equation (15.2) for both model forms (with CR predictor variables but no BA predictor variable and with a BA predictor variable but no CR predictor variables) using iteratively reweighted nonlinear regression and a weight (WT) of:

$$WT = KNT_{i,j}^{\ 2} / [(\hat{PMT}_{\bullet,i,j})(1.0 - \hat{PMT}_{\bullet,i,j})]$$

The resulting parameter estimates, their standard errors, t-statistics, and associated P-values for the PM equation with the CR predictor variables (but no BA predictor variable) are found in Table 15.12, and the PM equation with the BA predictor variable (but no CR predictor variables) are found in Table 15.13.

Table 15.12 Parameter estimates, their standard errors, their t-statistics, and the probability that the parameter estimates are zero (P-Value) for the plantation grown red alder PM thinning modifier equation that adjusts the PM equation with crown ratio but no basal area predictor variables.

Parameter	Estimate	Standard Error	t-statistic	P-Value
b_0	0.702248308	0.1939828	3.62	0.00034
b_1	-1.36883595	0.6451703	-2.12	0.03467
b_2	-1.56200751	2.862894	-0.55	0.58573

Table 15.13 Parameter estimates, their standard errors, their t-statistics, and the probability that the parameter estimates are zero (P-Value) for the plantation grown red alder PM thinning modifier equation that adjusts the PM equation with basal area but no crown ratio predictor variables.

Parameter	Estimate	Standard Error	t-statistic	P-Value
b_0	0.707443303	0.2080343	3.40	0.00076
b_1	-0.872669889	0.7001822	-1.25	0.21359
b_2	-1.90376820	7.317224	-0.26	0.79490

The maximum likelihood ratio test, commonly called the G-statistic for this application, was then used to test whether the inclusion of the thinning transformation explained a significant amount of additional variation. The G-statistic uses the difference in deviance between Equation (2) with just the intercept term and the full Equation (15.2) and is calculated by:

$$G = -2.0[DIFF1 + DIFF2]$$

Where,

$$DIFF1 = \sum_{j=1}^{n_j}\sum_{k=1}^{n_k} PMT_{\bullet,j,k} \ln(\hat{PMTR}_{j,k}) - \sum_{j=1}^{n_j}\sum_{k=1}^{n_k} PMT_{\bullet,j,k} \ln(\hat{PMTF}_{j,k})$$

$$DIFF2 = \sum_{j=1}^{n_j}\sum_{k=1}^{n_k} PST_{\bullet,j,k} \ln(\hat{PSTR}_{j,k}) - \sum_{j=1}^{n_j}\sum_{k=1}^{n_k} PST_{\bullet,j,k} \ln(\hat{PSTF}_{j,k})$$

$PMTR_{i,j}$ = Predicted probability of mortality using the reduced model

$PMTF_{i,j}$ = Predicted probability of mortality using the full model

$PSTR_{i,j}$ = Predicted probability of survival using the reduced model

$PSTF_{i,j}$ = Predicted probability of survival using the full model

The G-statistic is chi-squared distributed with two degrees of freedom. A G-statistic value above the critical chi-square value indicates the full model is significantly improved over the reduced model with just an intercept. Table 15.14 contains the resulting G-statistics and associated critical chi-square values for both PM models.

Table 15.14 The G-statistics and associated critical chi-square values at $\alpha = 0.05$ for the PM equation with crown ratio but no basal area predictor variables and the PM equation with basal area but no crown ratio predictor variables.

PM Model	G-Statistic	Critical Chi-Square
With CR	0.032772	5.99
With BA	-0.002238	5.99

Examination of the parameter estimates, their standard errors, and associated t-statistics and P-values for the PM equation with the CR predictor variables (but no BA predictor variable) in

Table 15.12 shows that b_2 parameter was not significantly different from 0.0 at even $\alpha = 0.05$ and the b_1 parameter was not significantly from 0.0 at $\alpha = 0.01$. Examination of the parameter estimates, their standard errors, and associated t-statistics and P-values for the PM equation with the BA predictor variable (but no CR predictor variables) in Table 15.13 shows that both the b_1 and b_2 parameter were not significantly different from 0.0 at even $\alpha = 0.05$. These results indicate that the thinning transformation does not improve the prediction of mortality after thinning. These findings were supported by the G-statistics reported in Table 15.14, which did not exceed the critical chi-square values for either model. It appears that the mortality rates after thinning were larger than predicted by the untreated PM equations (as indicated by the significant b_0 parameter for both models) but the increase could not be attributed to the thinnings themselves.

The one sided competition predictor variable and the crown ratio or two sided predictor variable(s) in the untreated plot PM equation will predict a reduction in predicted PM after thinning. The results of this analysis indicate that a thinning modifier to the untreated plot PM equation is unnecessary for red alder growing in plantations. Therefore, RAP-ORGANON will predict an unmodified reduction to PM after thinning. This finding agrees with those of Hibbs et al. (1989) and Hibbs et al. (1995) who also reported a reduction to PM after thinning red alder.

15.3 Literature Cited

Hann, D.W. and M.L. Hanus. 2002a. Enhanced diameter-growth-rate equations for undamaged and damaged trees in southwest Oregon. Forest Research Lab., Oregon State University, Corvallis, Oregon. Research Contribution 39. 54p.

Hann, D.W., Hanus, M.L., 2002b. Enhanced height growth rate for undamaged and damaged trees in southwest Oregon. Forest Research Lab., Oregon State University, Corvallis, Oregon. Research Contribution 41. 41p.

Hann, D.W. D.D. Marshall and M.L. Hanus. 2003. Equations for predicting height-to-crown-base, 5-year diameter growth rate, 5-year height growth rate, 5-year mortality rate and maximum size-density trajectory for Douglas-fir and western hemlock in the coastal region of the Pacific Northwest. Forest Research Lab., Oregon State University, Corvallis, Oregon. Research Contribution 40. 83p.

Hibbs, D.E., W.H. Emmingham, and M.C. Bondi. 1989. Thinning red alder: effects of method and spacing. Forest Science 35: 16-26.

Hibbs, D.E., W.H. Emmingham, and M.C. Bondi. 1995. Responses of red alder to thinning. Western Journal of Applied Forestry 10: 17-23.

Oliver, C.W., Larson, B.C., 1996. Forest stand dynamics: Update edition. Wiley, New York, NY.

Tappeiner, J.C., Maguire, D.A., Harrington, T.B., 2007. Silviculture and ecology of western U.S. forests. Oregon State University, Corvallis, OR.

Weiskittel, A.R., D.W. Hann, D.E. Hibbs, T.Y. Lam, and A.A. Bluhm. 2009. Modeling top height growth of red alder plantations. Forest Ecology and Management 258: 323-331.

16.0 Evaluation of RAP-ORGANON for Making Stand-Level Predictions

Because of the architecture of RAP-ORGANON, all of the equations and their evaluations have been made at the tree-level. However, the model will be used to make stand-level predictions. Therefore, the objective of this evaluation was to determine how well the resulting system of tree-level equations that constitute RAP-ORGANON do at predicting stand-level development of red alder plantations.

16.1 Data

The data used to make the stand-level evaluations came from the control plots used to develop the untreated equations. However, a number of plots and measurement were removed from the modeling data set before conducting the stand-level evaluations:

1. Twenty five plots with species other than red alder were removed in order to not confound the results of the evaluations with these other species.
2. Fifty five measurements in the pure alder data set were removed because they contained trees under breast height. These removals were always in the first measurement period of the plots affected.

Missing heights and heights to crown base were imputed using the equations described in chapters 2 and 8, respectively. For each plot and measurement, the regional equation was first calibrated to the measured values (if any) and then calibrated equation was applied to the unmeasured trees.

The stand-level evaluations were made both on single period growth projections and on the longest projections possible for each plot. There were 569 observations of stand change in the single growth period data set and 139 observations in the longest projections possible data set.

16.2 Analysis Methods and Results

16.2.1 Single Growth Period Evaluation

For the single growth period evaluation, projections were made with the following equations and ORGANON defaults: (1) crown recession was calculated indirectly, (2) the mortality equation that incorporated crown ratio was used, (3) the optional “limit on maximum size-density” was turned off (i.e., not selected), and (4) the tripling option was turned off (i.e., not selected). These selections correspond to the standard equation forms used in other versions of ORGANON and settings that are traditional defaults in ORGANON. Residuals consisting of predicted minus actual values were calculated for net increment in basal area per acre, mortality rate, survival rate, net increment in total stem cubic foot volume per acre, gross increment in basal area per acre, and gross increment in total stem cubic foot volume per acre. Because there were a range of growth periods in the data set, the residuals were standardized to periodic annual residuals by dividing the original residuals by the length of their growth periods.

Many stand-level models predict values at the end of the growth period instead of increment values. As a result, the fit statistics in those studies are reported on ending values. Differences between predicted minus actual end of growth period values were, therefore, also calculated for

ending surviving number of trees per acre, ending net basal area per acre, and ending net total stem cubic foot volume per acre.

Statistics calculated for the short projection residuals or differences were the average residual/difference, the average residual/difference expressed as a percentage of the average actual value, the adjusted coefficient of determination (R_a^2) without bias (i.e., the average residual/difference removed before calculation), and R_a^2 with bias (i.e., the average residual/difference not removed before calculation). Results for the annualized residuals are found in Table 16.1 and results for the end of growth period differences are found in Table 16.2. In addition, graphs of the periodic annual residuals of gross total stem cubic foot volume per acre increment and of gross basal area per acre increment were plotted over the predicted increment (Figures 16.1 and 16.5), the length of the growth period (Figures 16.2 and 16.6), the initial planting density (Figures 16.3 and 16.7), and red alder site index (Figures 16.4 and 16.8). Figures 16.1 and 16.5 were displayed by vertical lines, with the yellow lines representing the full range in residuals for each length of growth period and the black lines representing one standard deviation in residuals about the mean.

Table 16.1 Periodic annual residual analysis for single growth periods with residuals calculated as predicted minus actual. Projections were made with: (1) indirect estimation of crown recession, (2) mortality equation with crown ratio, (3) the limit on maximum size density turned off, and (4) tripling turned off.

	Periodic Annual Residuals (Predicted Minus Actual)			
Attribute	Average	Average as Percent of Actual	R_a^2 Without Bias	R_a^2 With Bias
Net Basal Area Increment	-0.21	-2.9	0.813	0.809
Mortality	+1.54	+21.7	0.464	0.450
Survival	-1.54	-0.8	0.998	0.998
Net Total Stem Cubic Foot Volume Increment	-3.45	-1.9	0.810	0.809
Gross Basal Area Increment	-0.14	-1.8	0.828	0.826
Gross Total Stem Cubic Foot Volume Increment	-1.90	-1.0	0.829	0.829

Table 16.2 End of Growth Period Differences for single growth periods with differences calculated as predicted minus actual. Projections were made with: (1) indirect estimation of crown recession, (2) mortality equation with crown ratio, (3) the limit on maximum size density turned off, and (4) tripling turned off.

Attribute	End of Growth Period Differences (Predicted Minus Actual)			
	Average	Average as Percent of Actual	R_a^2 Without Bias	R_a^2 With Bias
Surviving Number of Trees per Acre	-5.26	-1.01	0.994	0.994
Net Basal Area per Acre	-0.40	-0.71	0.981	0.981
Net Total Stem Cubic Foot Volume per Acre	-5.25	-0.44	0.983	0.983

Figure 16.1 Periodic annual residuals for gross total stem cubic foot volume increment per acre (TSCFVG) plotted over predicted annual gross total stem cubic foot volume increment per acre. Residuals were calculated as predicted minus actual basal area increment. Single growth period projections were made with: (1) indirect estimation of crown recession, (2) mortality equation with crown ratio, (3) the limit on maximum size density turned off, and (4) tripling turned off.

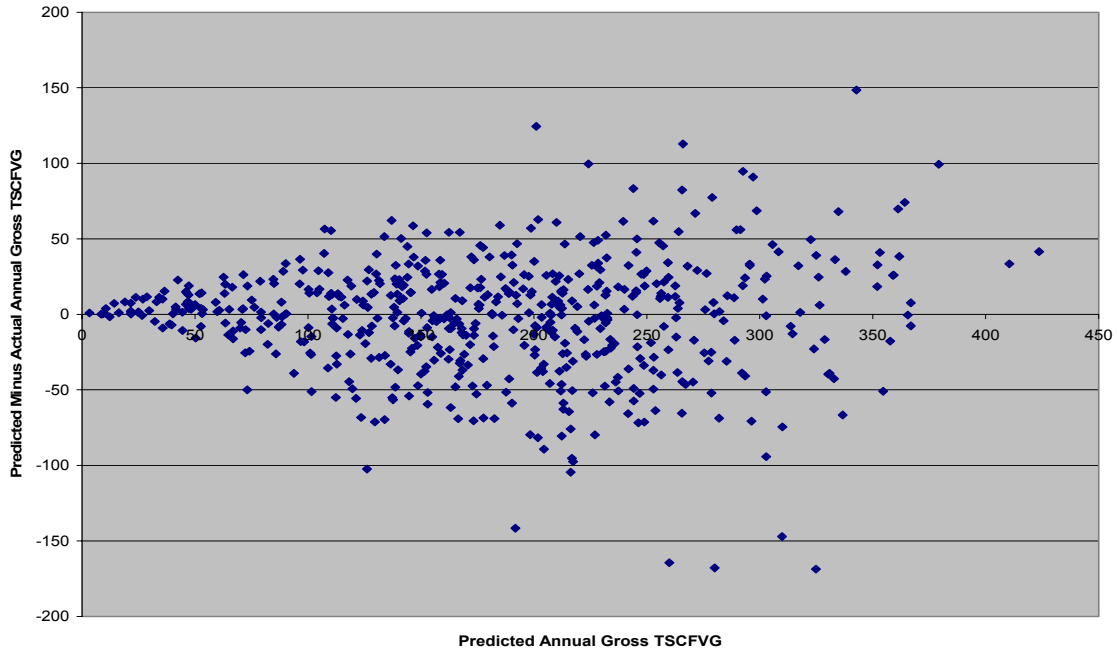

Figure 16.2 Periodic annual residuals for gross total stem cubic foot volume increment per acre (TSCFVG) plotted over length of growth period. The yellow lines indicate the full range of the residuals and the black lines with hash marks indicate one standard deviation about the mean residuals. Residuals were calculated as predicted minus actual basal area increment. Single growth period projections were made with: (1) indirect estimation of crown recession, (2) mortality equation with crown ratio, (3) the limit on maximum size density turned off, and (4) tripling turned off.

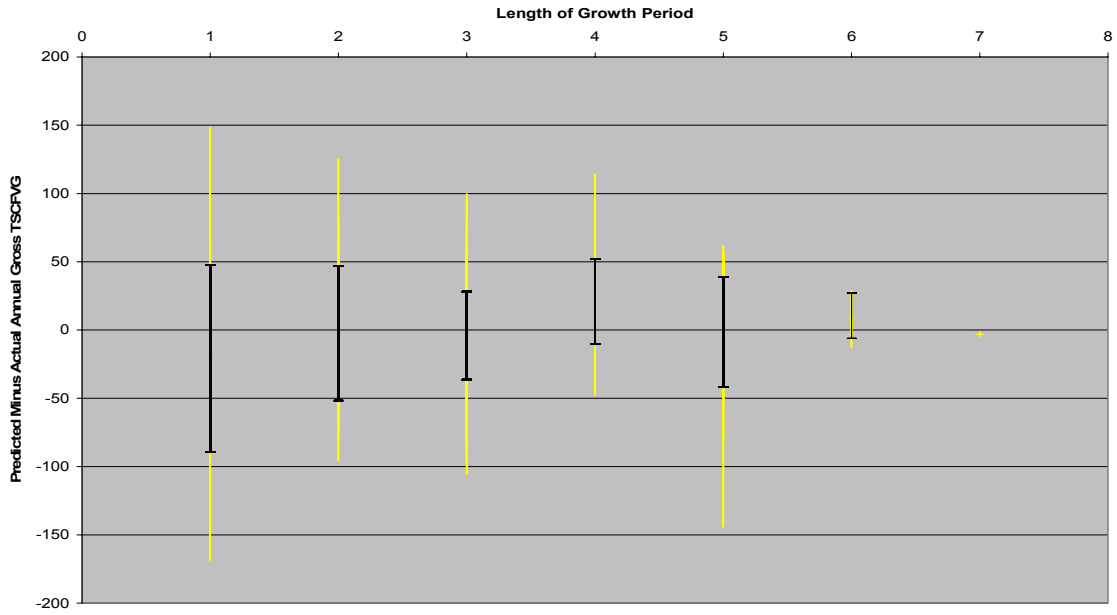

Figure 16.3 Periodic annual residuals for gross total stem cubic foot volume increment per acre (TSCFVG) plotted over planting density. Residuals were calculated as predicted minus actual basal area increment. Single growth period projections were made with: (1) indirect estimation of crown recession, (2) mortality equation with crown ratio, (3) the limit on maximum size density turned off, and (4) tripling turned off.

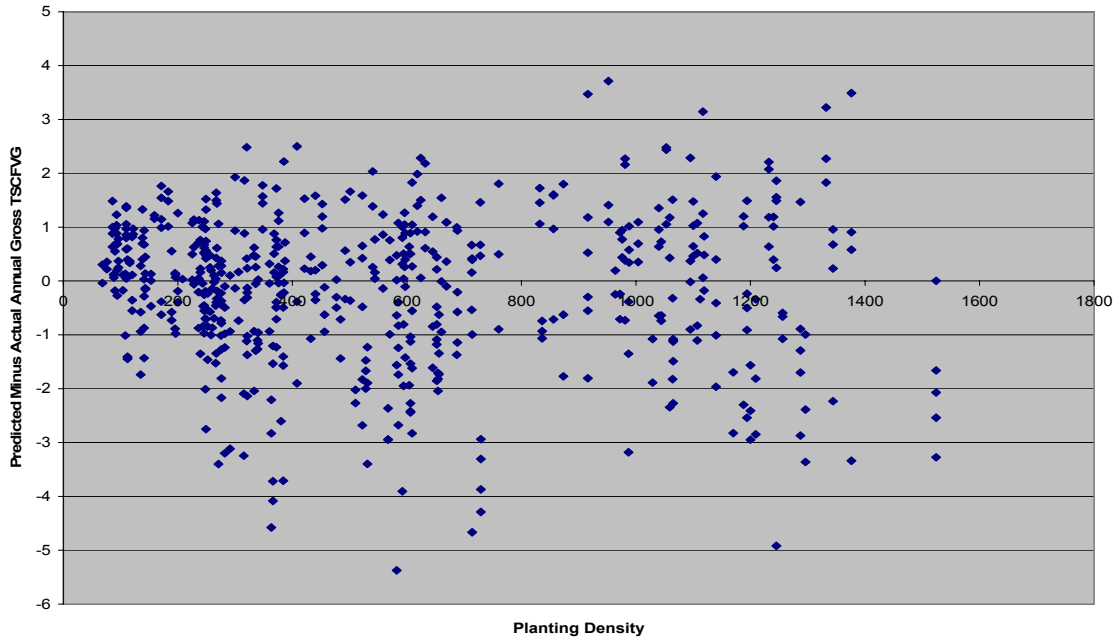

Figure 16.4 Periodic annual residuals for gross total stem cubic foot volume increment per acre (TSCFVG) plotted red alder site index. Residuals were calculated as predicted minus actual basal area increment. Single growth period projections were made with: (1) indirect estimation of crown recession, (2) mortality equation with crown ratio, (3) the limit on maximum size density turned off, and (4) tripling turned off.

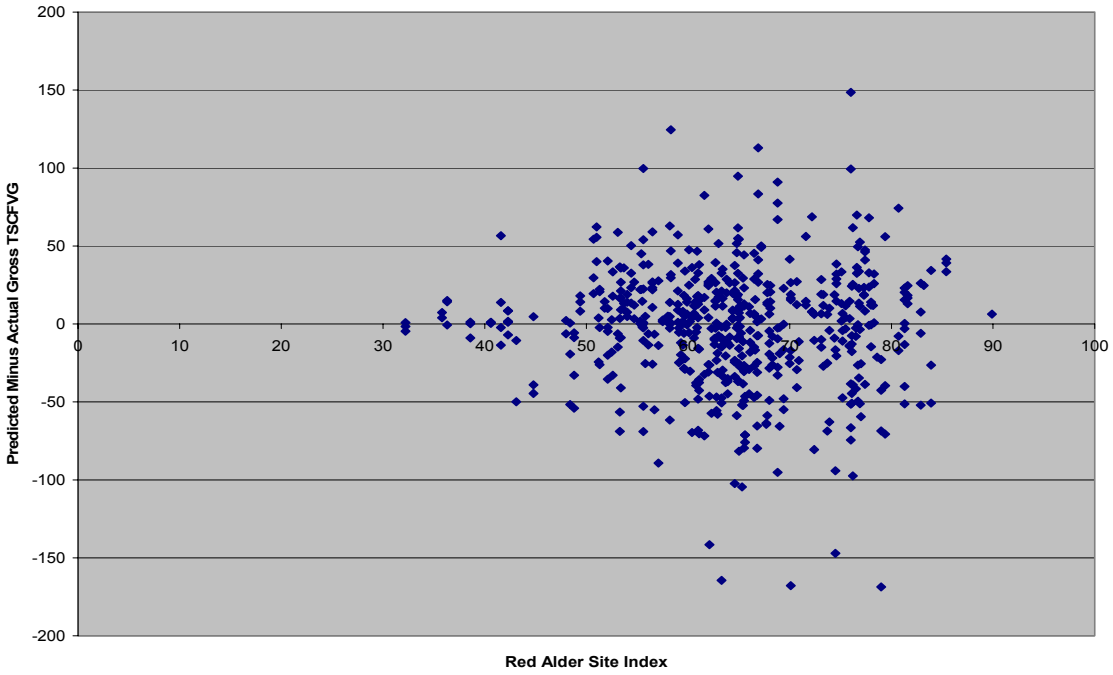

Figure 16.5 Periodic annual residuals for gross basal area increment per acre (BAG) plotted over predicted gross basal area increment per acre. Residuals were calculated as predicted minus actual total stem cubic foot volume increment. Single growth period projections were made with: (1) indirect estimation of crown recession, (2) mortality equation with crown ratio, (3) the limit on maximum size density turned off, and (4) tripling turned off.

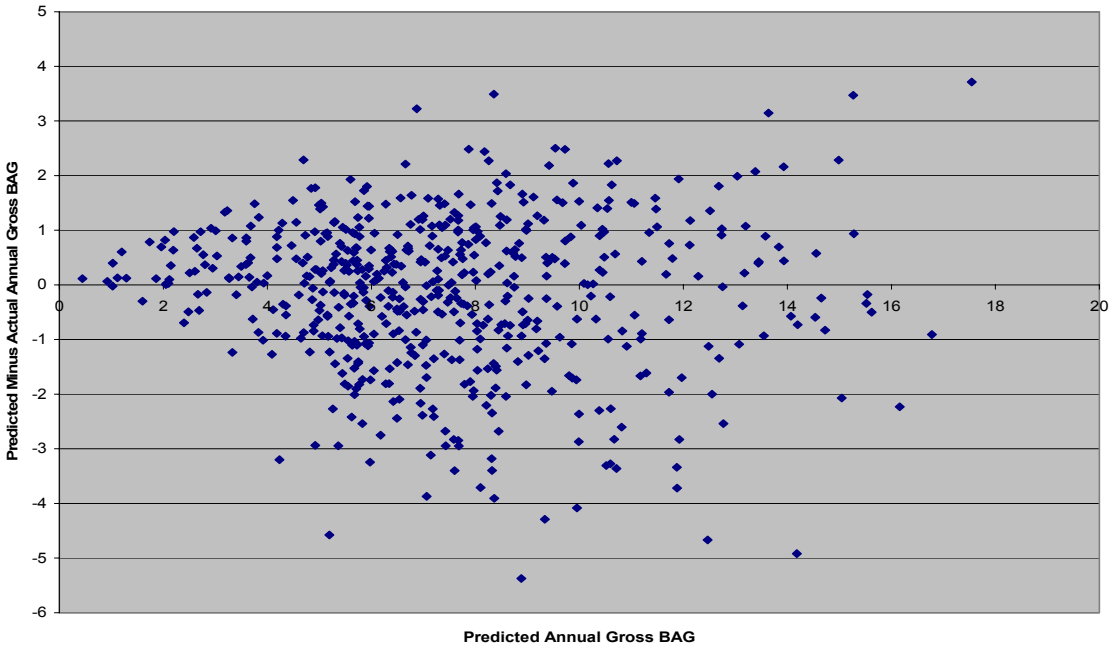

Figure 16.6 Periodic annual residuals for gross basal area increment per acre (BAG) plotted over length of growth period. The yellow lines indicate the full range of the residuals and the black lines with hash marks indicate one standard deviation about the mean residuals. Residuals were calculated as predicted minus actual total stem cubic foot volume increment. Single growth period projections were made with: (1) indirect estimation of crown recession, (2) mortality equation with crown ratio, (3) the limit on maximum size density turned off, and (4) tripling turned off.

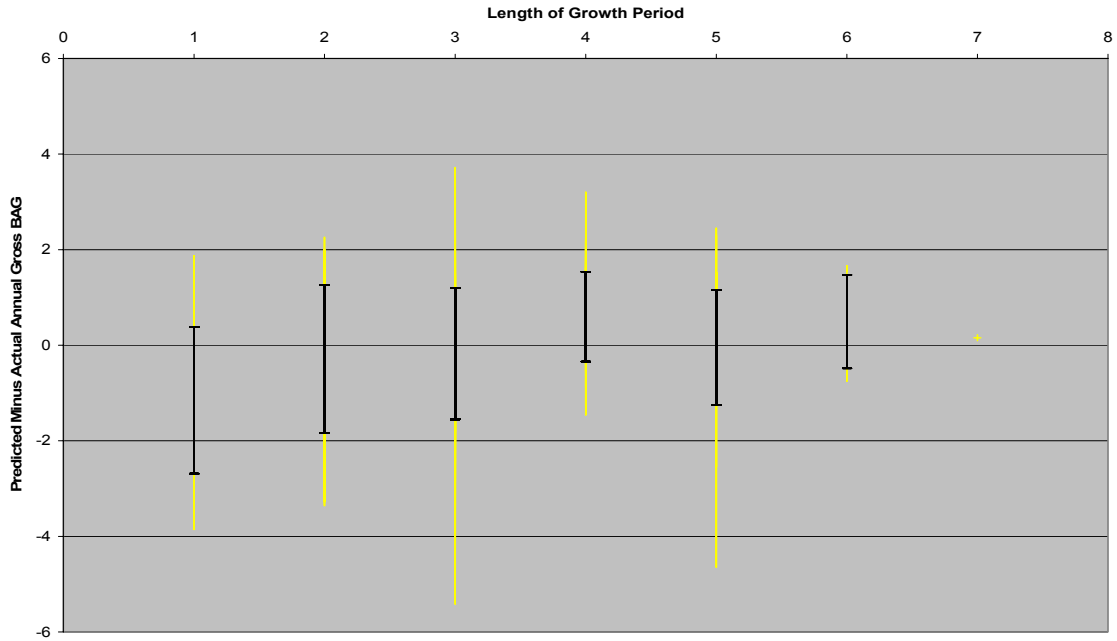

Figure 16.7 Periodic annual residuals for gross basal area increment per acre (BAG) plotted over planting density. Residuals were calculated as predicted minus actual total stem cubic foot volume increment. Single growth period projections were made with: (1) indirect estimation of crown recession, (2) mortality equation with crown ratio, (3) the limit on maximum size density turned off, and (4) tripling turned off.

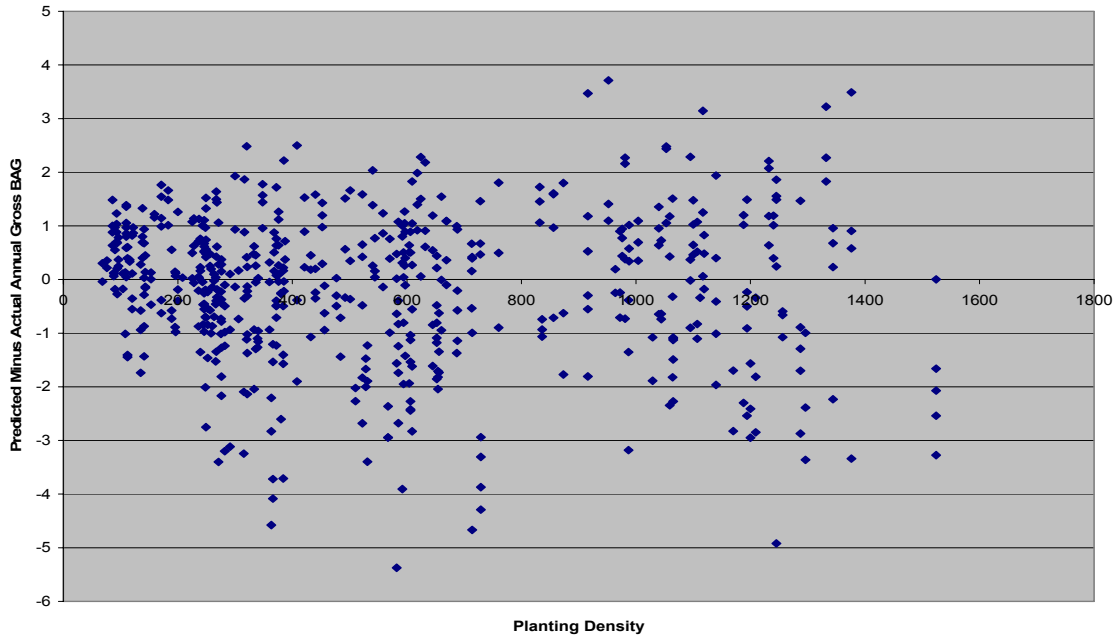

Figure 16.8 Periodic annual residuals for gross basal area increment per acre (BAG) plotted over red alder site index. Residuals were calculated as predicted minus actual total stem cubic foot volume increment. Single growth period projections were made with: (1) indirect estimation of crown recession, (2) mortality equation with crown ratio, (3) the limit on maximum size density turned off, and (4) tripling turned off.

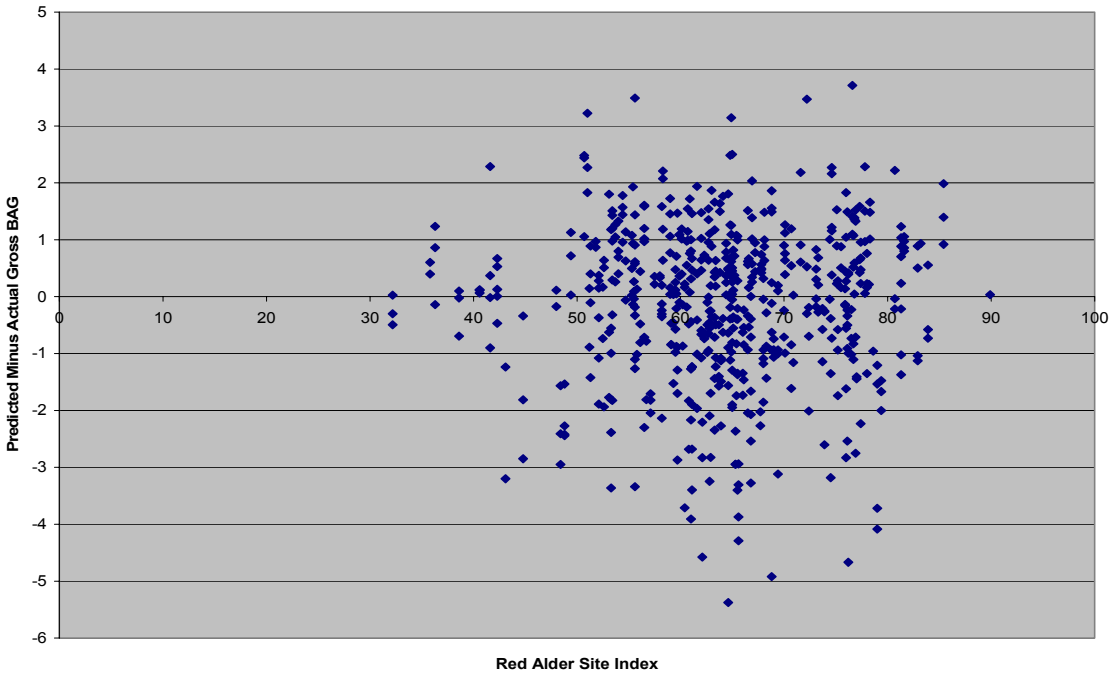

16.2.2 Longest Possible Projection Evaluation

The longest possible projection data set was used in two analyses. The first compared the predictive performance of four alternative sets of equations with the limit on maximum size-density and tripling both turned off:

1. Indirect prediction of crown recession, and predicting mortality using the equation containing crown ratio.
2. Indirect prediction of crown recession, and the use of the mortality equation containing basal area per acre instead of crown ratio.
3. Direct prediction of crown recession using the equation containing growth effective age, and predicting mortality using the equation containing crown ratio. predicting mortality using the equation containing crown ratio
4. Direct prediction of crown recession using the equation containing total age from seed, and predicting mortality using the equation containing crown ratio.

The second compared the predictive performance resulting from using four alternative sets of defaults applied to the equation combination found to be best in the first analysis:

1. The limit on maximum size-density turned off and tripling turned off.
2. The limit on maximum size-density turned off and tripling turned on.
3. The limit on maximum size-density turned on and tripling turned off.
4. The limit on maximum size-density turned on and tripling turned on.

For both analyses, residuals consisting of predicted minus actual values were calculated for mortality rate, net increment in basal area per acre, increment in top height, and net increment in

total stem cubic foot volume per acre. Because there were a range of growth periods in the data set, the residuals were standardized to periodic annual residuals by dividing the original residuals by the length of their growth periods. Statistics calculated for the longest possible projection residuals or differences were the average residual/difference, the average residual/difference expressed as a percentage of the average actual value, R_a^2 without bias, and R_a^2 with bias. The results for the first analysis are found in Table 16.3, and results for the second analysis are found in Table 16.4.

Table 16.3 Periodic annual residual analysis for longest possible projections with residuals calculated as predicted minus actual. Projections were made with the limit on maximum size density turned off and tripling turned off.

Attribute	Periodic Annual Residuals (Predicted Minus Actual)			
	Average	Average as Percent of Actual	R_a^2 Without Bias	R_a^2 With Bias
Indirect Calculation of Crown Recession and Mortality Equation with Crown Ratio				
Mortality	+1.00	+13.96	0.73	0.72
Survival	-1.00	-2.13	0.98	0.98
Net Basal Area Increment	+0.17	+2.37	0.77	0.76
Top Height Increment	+0.01	+0.32	0.93	0.93
Net Total Stem Cubic Foot Volume Increment	+4.34	+2.39	0.85	0.85
Indirect Calculation of Crown Recession and Mortality Equation with Basal Area				
Mortality	+1.34	+18.67	0.69	0.67
Net Basal Area Increment	+0.14	+1.96	0.77	0.77
Top Height Increment	+0.01	+0.33	0.94	0.93
Net Total Stem Cubic Foot Volume Increment	+3.67	+2.02	0.85	0.85
Direct Calculation of Crown Recession with GEA and Mortality Equation with Crown Ratio				
Mortality	+0.60	+8.35	0.74	0.74
Net Basal Area Increment	+1.04	+14.54	0.39	0.17
Top Height Increment	+0.03	+0.89	0.94	0.93
Net Total Stem Cubic Foot Volume Increment	+27.20	+14.97	0.59	0.45
Direct Calculation of Crown Recession with TAGE and Mortality Equation with Crown Ratio				
Mortality	+0.55	+7.61	0.74	0.74
Net Basal Area Increment	+1.00	+13.98	0.38	0.18
Top Height Increment	+0.02	+0.76	0.93	0.93
Net Total Stem Cubic Foot Volume Increment	+26.17	+14.40	0.59	0.46

Table 16.4 Periodic annual residual analysis for longest possible projections with residuals calculated as predicted minus actual. Projections were made with the indirect calculation of crown recession and mortality equation with crown ratio.

Attribute	Periodic Annual Residuals (Predicted Minus Actual)			
	Average	Average as Percent of Actual	R_a^2 Without Bias	R_a^2 With Bias
Limit on Maximum Size Density Turned Off and Tripling Turned Off				
Mortality	+1.00	+13.96	0.73	0.72
Survival	-1.00	-2.13	0.98	0.98
Net Basal Area Increment	+0.17	+2.37	0.77	0.76
Top Height Increment	+0.01	+0.32	0.93	0.93
Net Total Stem Cubic Foot Volume Increment	+4.34	+2.39	0.85	0.85
Limit on Maximum Size Density Turned Off and Tripling Turned On				
Mortality	+1.14	+15.82	0.73	0.71
Net Basal Area Increment	+0.13	+1.77	0.77	0.77
Top Height Increment	-0.02	-0.66	0.94	0.94
Net Total Stem Cubic Foot Volume Increment	+2.86	+1.58	0.85	0.85
Limit on Maximum Size Density Turned On and Tripling Turned Off				
Mortality	+4.58	+63.70	0.44	0.23
Net Basal Area Increment	-0.09	-1.21	0.77	0.77
Top Height Increment	+0.01	+0.35	0.93	0.93
Net Total Stem Cubic Foot Volume Increment	-1.00	-0.55	0.85	0.85
Limit on Maximum Size Density Turned On and Tripling Turned On				
Mortality	+4.53	+62.94	0.45	0.25
Net Basal Area Increment	-0.11	-1.59	0.77	0.77
Top Height Increment	-0.02	-0.61	0.94	0.94
Net Total Stem Cubic Foot Volume Increment	-2.15	-1.18	0.85	0.85

The best combination of model and defaults was then used to explore the effect of length of growth period, for the longest possible growth periods, on predictive performance. Again, residuals consisting of predicted minus actual values were calculated for mortality rate, net increment in basal area per acre, increment in top height, and net increment in total stem cubic foot volume per acre. The residuals were standardized to periodic annual residuals by dividing the original residuals by the length of their growth periods. Statistics calculated for each length of projection were the average residual and the standard deviation of the residuals. In addition, graphs of the actual periodic annual values plotted over the predicted periodic annual values were done for:

1. Mortality rate (Figure 16.9)
2. Survival rate (Figure 16.10)
3. Increment in net basal area per acre (Figure 16.11)
4. Increment in top height (Figure 16.12)
5. Increment in net total stem cubic foot volume per acre (16.13).

A one to one line was also added to the graphs as a reference for evaluations.

Figure 16.9 Actual annual mortality rate plotted across predicted annual mortality rate for the longest projections possible. Projections were made with: (1) indirect estimation of crown recession, (2) mortality equation with crown ratio, (3) the limit on maximum size density turned off, and (4) tripling turned off.

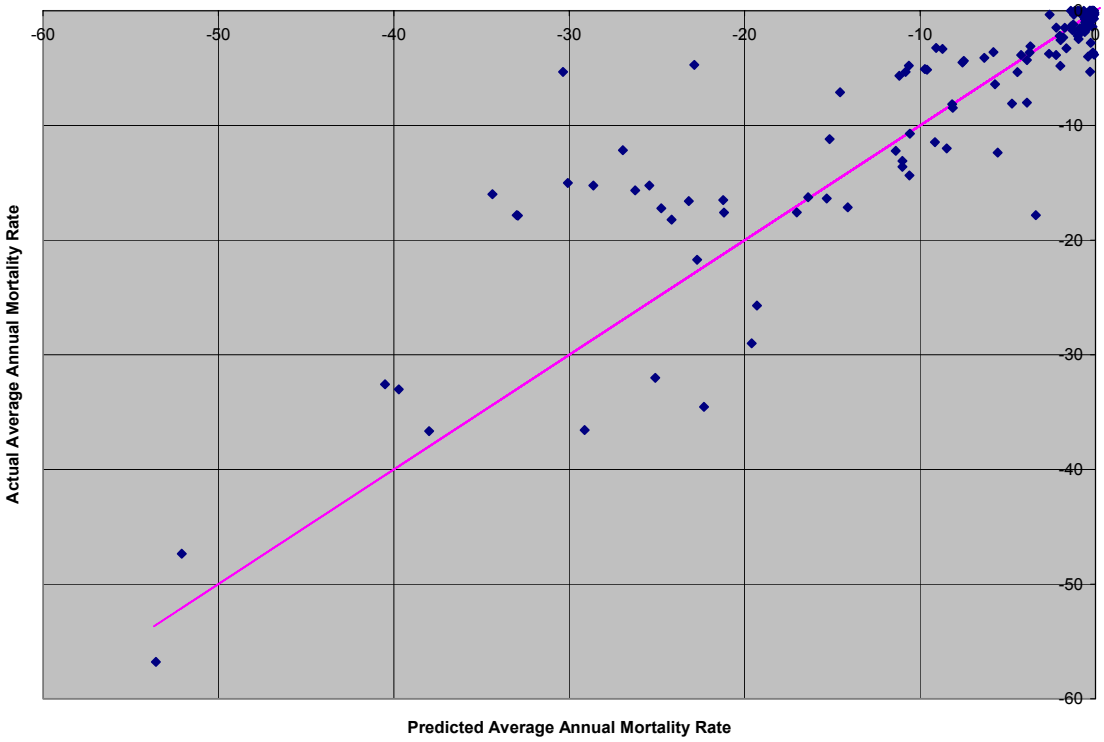

Figure 16.10 Actual annual survival rate plotted across predicted annual survival rate for the longest projections possible. Projections were made with: (1) indirect estimation of crown recession, (2) mortality equation with crown ratio, (3) the limit on maximum size density turned off, and (4) tripling turned off.

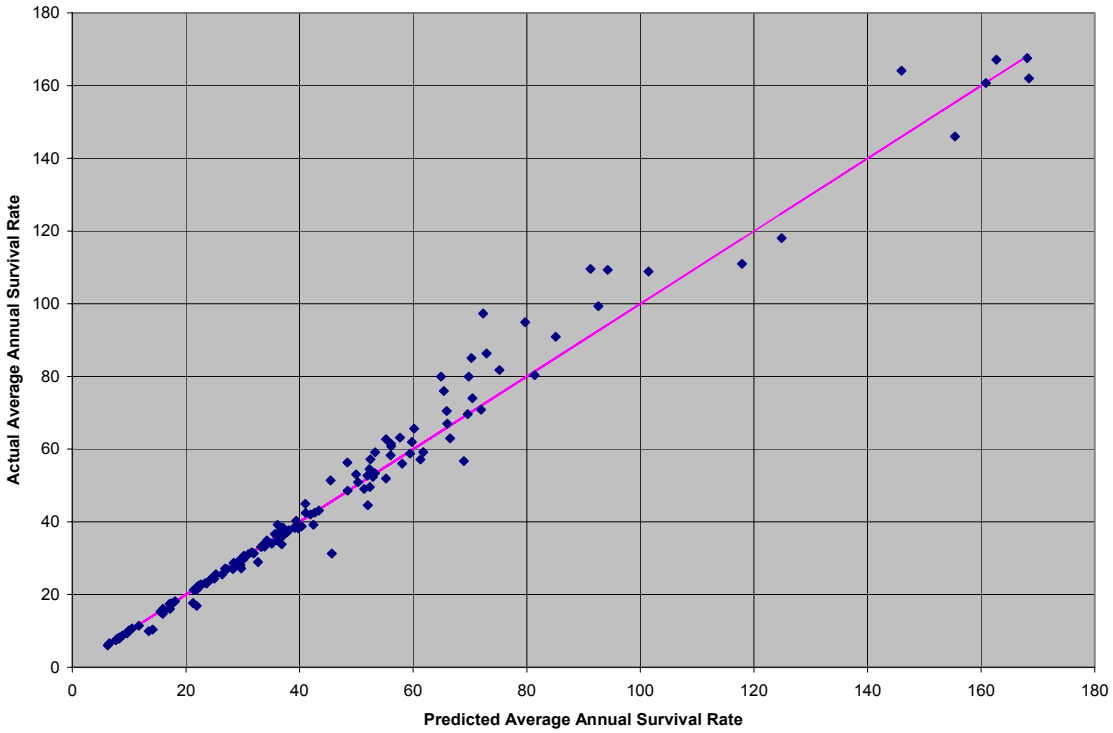

Figure 16.11 Actual annual basal area increment plotted across predicted annual basal area increment for the longest projections possible. Projections were made with: (1) indirect estimation of crown recession, (2) mortality equation with crown ratio, (3) the limit on maximum size density turned off, and (4) tripling turned off.

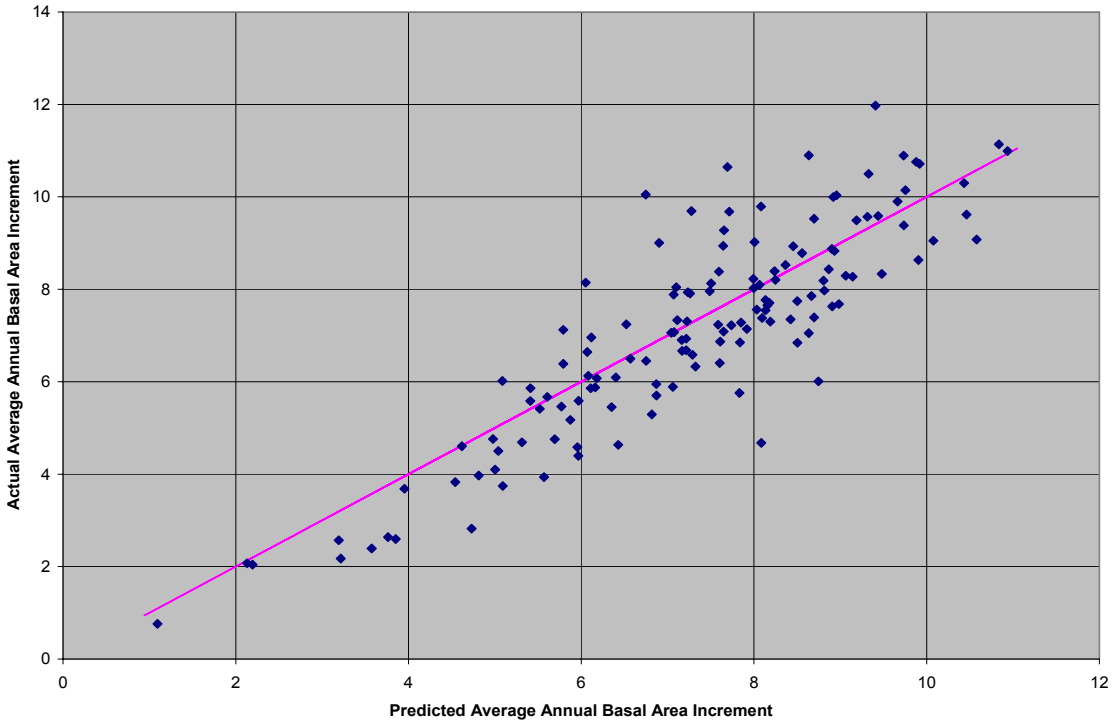

Figure 16.12 Actual annual top height increment plotted across predicted annual top height increment for the longest projections possible. Projections were made with: (1) indirect estimation of crown recession, (2) mortality equation with crown ratio, (3) the limit on maximum size density turned off, and (4) tripling turned off.

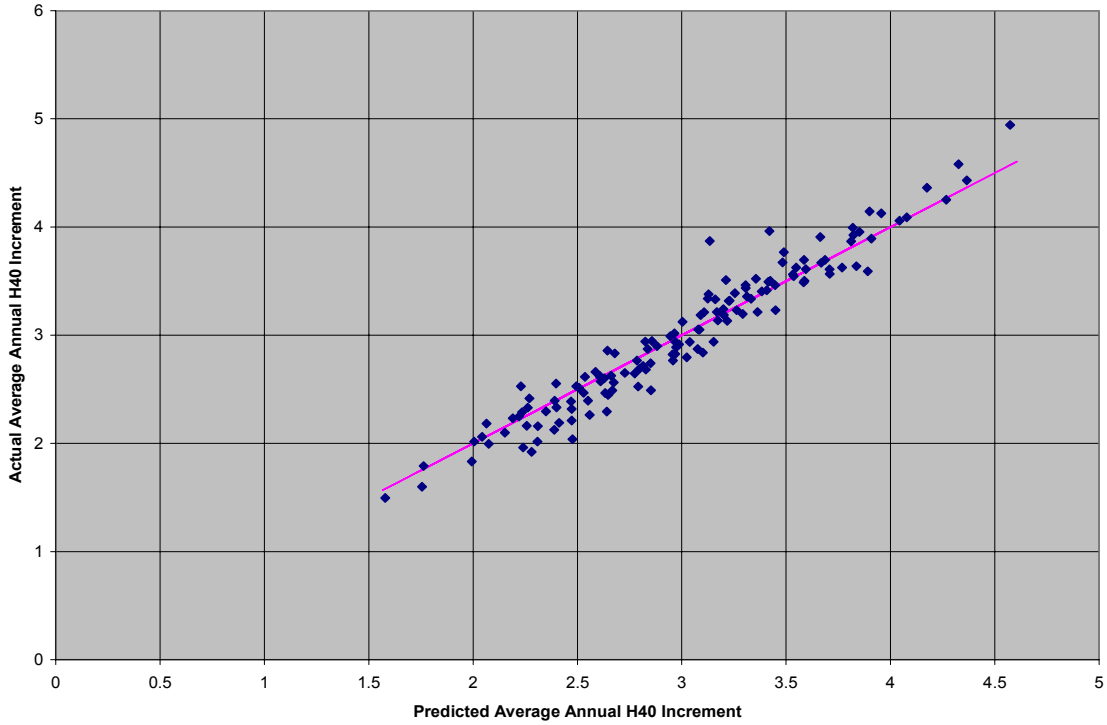

Figure 16.13 Actual annual total stem cubic foot volume increment plotted across predicted annual total stem cubic foot volume increment for the longest projections possible. Projections were made with: (1) indirect estimation of crown recession, (2) mortality equation with crown ratio, (3) the limit on maximum size density turned off, and (4) tripling turned off.

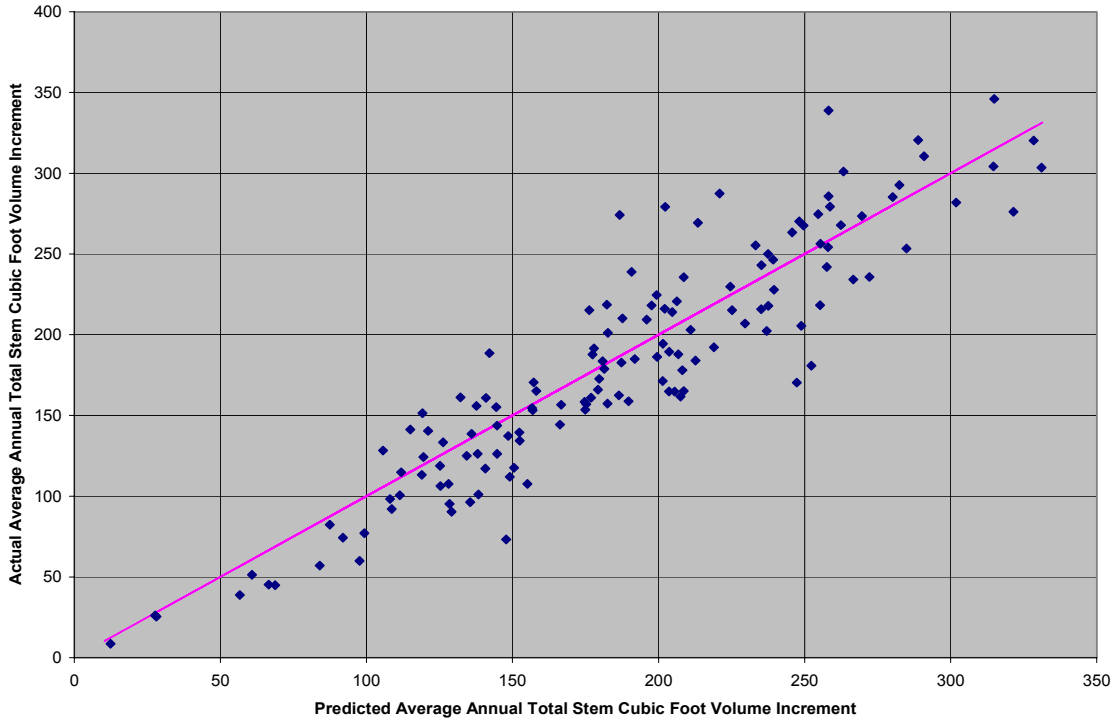

To parallel the short growth period analyses, differences between predicted minus actual end of growth period values were also calculated for surviving number of trees per acre at the end of the projection, ending net basal area per acre, ending top height, and ending net total stem cubic foot volume per acre. Statistics calculated for these differences were the average difference, the average difference expressed as a percentage of the average actual value, R_a^2 without bias, and R_a^2 with bias. In addition, graphs of the actual end of projection values plotted over the predicted end of projection values were done for:

1. Surviving number of trees (Figure 16.14)
2. Net basal area per acre (Figure 16.15)
3. Top height (Figure 16.16)
4. Net total stem cubic foot volume per acre (Figure16.17).

Again, a one to one line was also added to the graphs as a reference for evaluations.

Figure 16.14 Actual number of trees per acre at the end of the longest possible projections plotted across predicted number of trees per acre at the end of the longest possible projections. Projections were made with: (1) indirect estimation of crown recession, (2) mortality equation with crown ratio, (3) the limit on maximum size density turned off, and (4) tripling turned off.

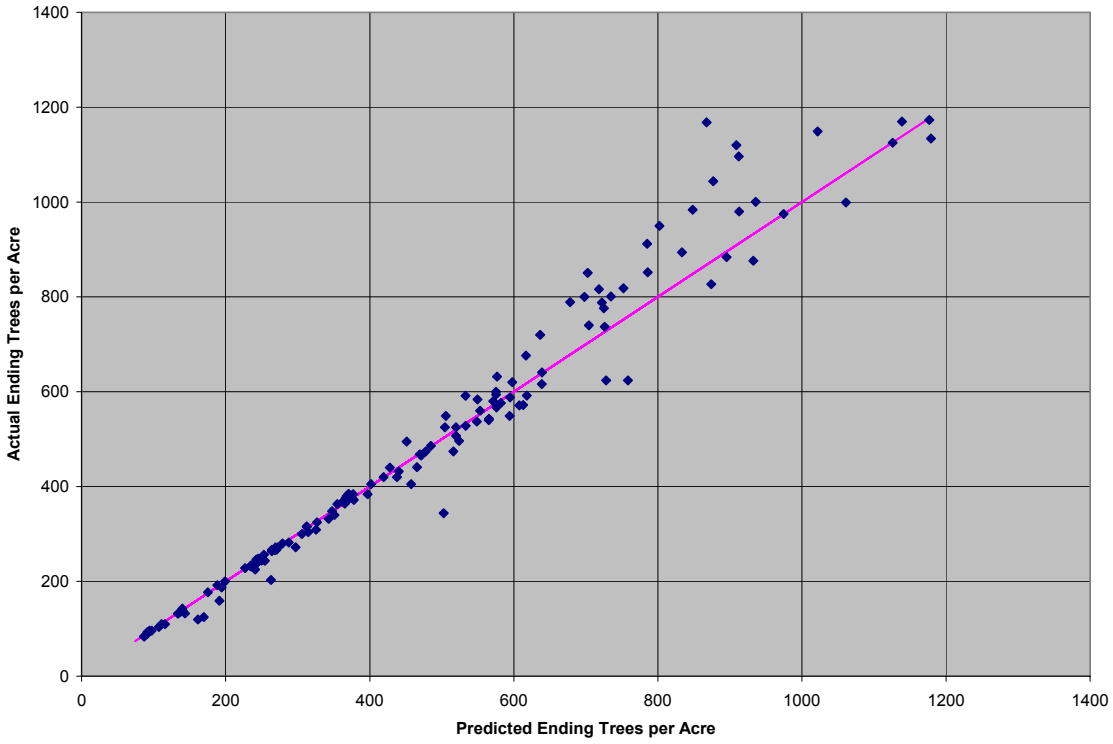

Figure 16.15 Actual basal area per acre at the end of the longest possible projections plotted across predicted basal area per acre at the end of the longest possible projections. Projections were made with: (1) indirect estimation of crown recession, (2) mortality equation with crown ratio, (3) the limit on maximum size density turned off, and (4) tripling turned off.

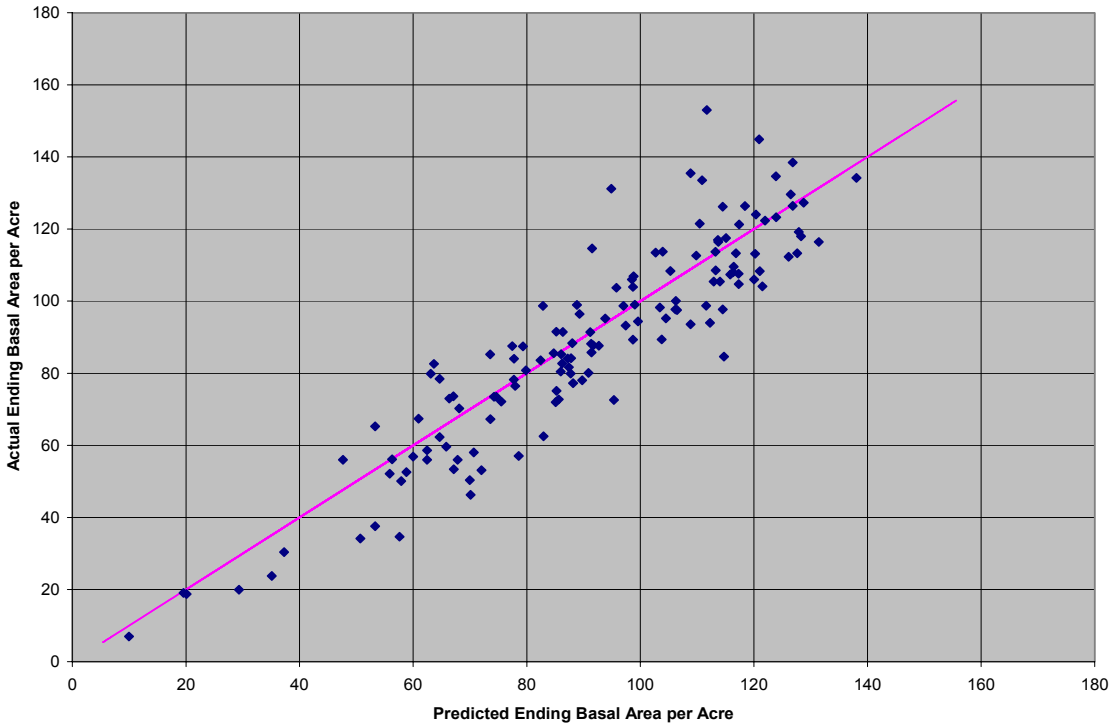

Figure 16.16 Actual top height at the end of the longest possible projections plotted across predicted top height at the end of the longest possible projections. Projections were made with: (1) indirect estimation of crown recession, (2) mortality equation with crown ratio, (3) the limit on maximum size density turned off, and (4) tripling turned off.

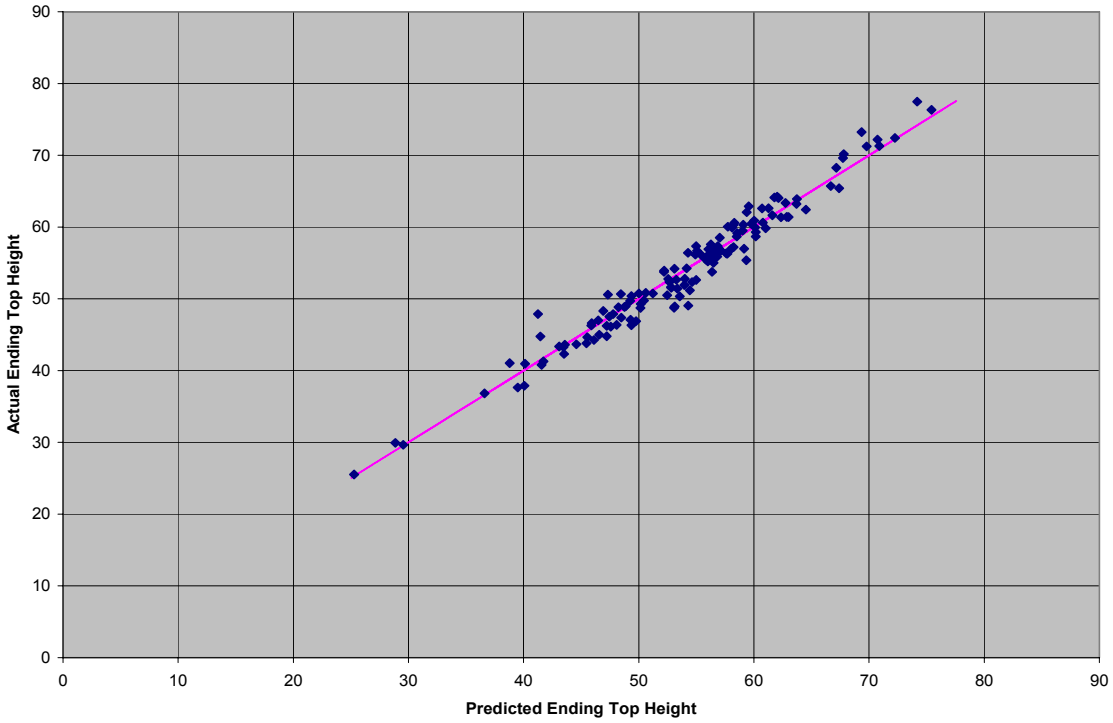

Figure 16.17 Actual total stem cubic foot volume per acre at the end of the longest possible projections plotted across predicted total stem cubic foot volume per acre at the end of the longest possible projections. Projections were made with: (1) indirect estimation of crown recession, (2) mortality equation with crown ratio, (3) the limit on maximum size density turned off, and (4) tripling turned off.

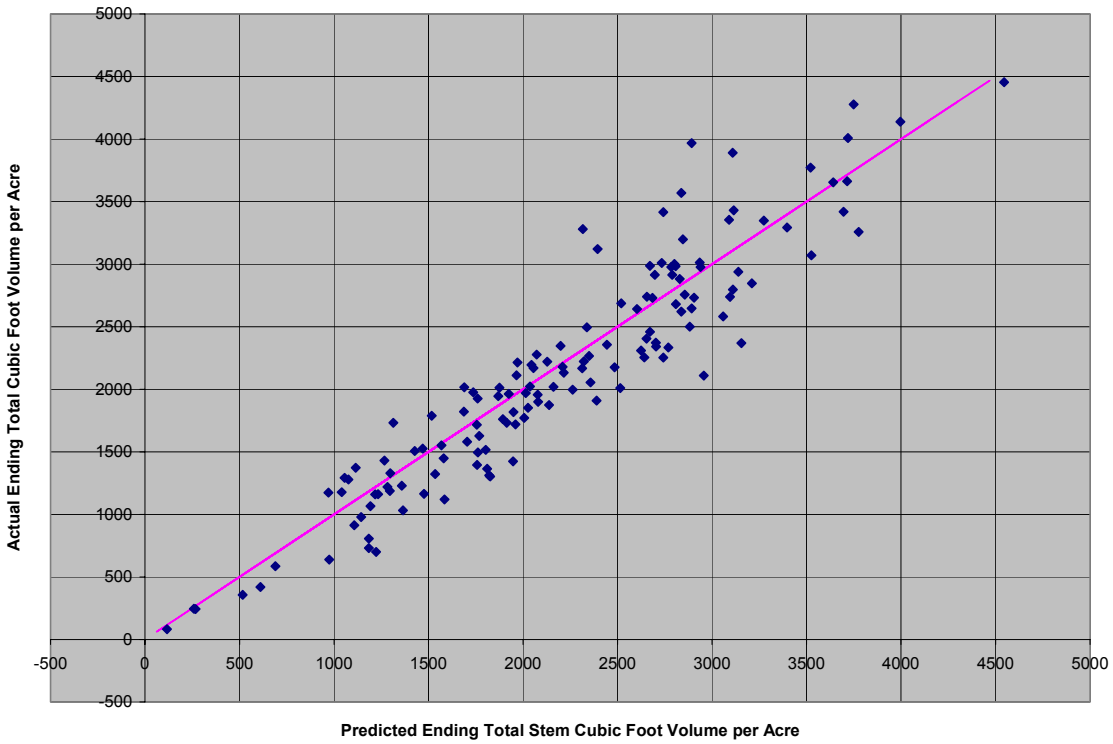

16.3 Discussion

In reviewing the results of this evaluation, one must remember that:

1. The evaluation data was a subset of the modeling data.
2. A significant proportion of the heights and height to crown bases on each plot/measurement had to be imputed (i.e., predicted) before being projected because these attributes were subsampled. This fact is important because ORGANON is a tree-level model that predicts stand attributes into the future by first predicting future diameters, heights, heights to crown base, and expansion factors for all trees on the plot and then transforming/summarizing the tree attributes to get estimates of future stand attributes. Therefore, anything that affects the accuracy and precision of the tree-level predictions will also affect the accuracy of the stand-level predictions. Measurement error theory states loss of accuracy in prediction can occur when an equation is developed with measured independent variables and then applied to predicted independent variables.

Both of these data restrictions can lessen the apparent accuracy of the stand-level predictions from a model that accurately depicts the full population when all members are measured for height and height to crown base. In this report, accuracy combines both bias and precision.

The results in Table 16.1 show that, when applied to single growth periods, RAP-ORGANON over predicted the mortality rate by about 22% and under predicted survival by somewhat less than one percent. This apparent contradiction is explained by the fact that the actual mortality

rate was low in the data set. As a result, small differences in residuals can express themselves as large percent differences. For example, a plot with 1,000 trees per acre that experiences one tree dying during the growth period but 1.2 trees were predicted to die would have a 20% over prediction in mortality rate and a 0.02% under prediction in survival rate.

Net increments in basal area per acre and total stem cubic foot volume per acre were also under predicted by approximately 2 to 3%. An over prediction of mortality should cause an under prediction of net increments in basal area per acre and total stem cubic foot volume per acre. How much of the under prediction is due to the over prediction of mortality can be evaluated by comparing the relative sizes of the under predictions in the net and gross increments in basal area per acre and total stem cubic foot volume per acre. Because the gross values were under predicted by 1 to 2% (approximately 1% less than the net values) indicates that the over prediction in mortality is only part of the reason that the net and gross increments in basal area per acre and total stem cubic foot volume per acre were under predicted. The fact that the impact of the over prediction in mortality was relatively small indicates that the additional mortality is occurring in the small diameter trees. The R_a^2 (with bias incorporated) value was 0.450 for predicted mortality rate, 0.998 for predicted survival rate, and 0.809 for both net basal area per acre increment and net total stem cubic foot volume per acre increment. As a comparison, Matney and Sullivan (1982) reported fits of their stand level loblolly pine equations resulted in R^2 values of 0.58 for mortality, 0.80 for net basal area per acre increment, and 0.85 for net total stem cubic foot volume increment (R^2 values are always higher than R_a^2 values). Finally, examination of the residuals shown in Figures 16.1 to 16.8 indicates no severe problems with trends over the attributes plotted on the x-axis.

Matney and Sullivan (1982) was the only whole stand growth modeling study in plantations that could be found which reported fit statistics for increment predictions. Most of the whole stand studies for plantations that could be found in the US literature predicted either yield values or end of growth period values instead of increments. Table 16.2 shows fit statistics for end of growth period differences. Use of ending attributes instead of increments reduces the percent bias and increases the R_a^2 values. The R_a^2 (with bias incorporated) was 0.994 for predicted surviving number of trees per acre, 0.981 for predicted net basal area per acre, and 0.983 for predicted net total stem cubic foot volume per acre. Reported R^2 values for predicting net basal area per acre at the end of the growth period were 0.913 (Bailey et al. 1989), 0.93 (Pienaar et al. 1990), 0.95 (Pienaar and Rheney 1990), and 0.97 (Hasenauer et al. 1997). Reported R^2 values for predicting surviving number of trees per acre at the end of the growth period were 0.966 (Bailey et al. 1989), 0.94 (Pienaar et al. 1990), and 0.95 (Pienaar and Rheney 1990). Finally, Pienaar et al. (1990) reported a R^2 value 0f 0.94 for predicting net total stem cubic foot volume per acre at the end of the growth period. The outcome of the increment evaluation and the end of growth period evaluation is that the single growth period results are as good as has been reported for fits of stand-level equations that predict the values directly.

Table 16.3 contains the periodic annual analysis results for the longest possible projections when different component equations are used in RAP-ORGANON. All runs were made with the limit on maximum size-density option and tripling option turned off. The first combination used the indirect approach for calculating crown recession and it used the mortality equation that incorporated crown ratio, which is the traditional ORGANON method for calculating crown recession and the traditional ORGANON model form for determining mortality. The first combination is also the one used in the single growth period analyses. In this combination, RAP-ORGANON over predicted the periodic annual mortality rate by nearly 14%, under predicted the periodic annual survival by about 2%, over predicted net periodic annual increments in basal

area per acre and total stem cubic foot volume per acre by approximately 2%, and over predicted periodic annual top height by just a little. Even with the biases, the RAP-ORGANON was able to explain 72% of the variation in the periodic annual mortality rate, 98% of the variation in periodic annual survival rate, 78% of the variation in the periodic annual net basal area increment, 93% of the variation in the top height increment, and 85% of the variation in the periodic annual net total stem cubic foot volume increment.

The second combination also used the indirect approach for calculating crown recession but it used the mortality equation that incorporated basal area instead of crown ratio. In this combination, the over prediction bias for mortality rate was increased to nearly 19%, while the over prediction biases in net increments in basal area per acre and total stem cubic foot volume per acre were reduced slightly (Table 16.3). The slight over prediction bias for top height increment remained about the same. As a result, the mortality model that incorporated basal area instead of crown ratio was not used in the remaining analyses.

The third and forth combinations used a direct predictor of crown recession and the mortality equation with crown ratio. The third combination used the direct crown recession equation that incorporated growth effective age (GEA), while the fourth combination used the direct crown recession equation that incorporated total age from seed. A comparison of the results for these two combinations indicates that they performed very similarly (Table 16.3). While both reduced the over prediction bias in mortality rate, they also greatly increased the over prediction biases for net increments in basal area per acre and total stem cubic foot volume per acre. Furthermore, there was a great reduction in the amount of variation (including bias) explained in the net increments of basal area per acre and total stem cubic foot volume per acre explained by RAP-ORGANON. These results are consistent with the suspicion that the direct crown recession equations were under estimating crown recession resulting in longer crown lengths than predicted by the indirect method of predicting crown recession. Longer crowns would cause reduced mortality rates and increased diameter and height increments. As a result of these findings, only the indirect method of predicting crown recession was used in the remaining analyses.

Table 16.4 contains the periodic annual analysis results for the longest possible projections when different defaults are used in the final RAP-ORGANON version containing the indirect method of estimating crown recession and the mortality model with crown ratio. The first combination of defaults uses the limit on maximum size-density turned off and tripling turned off. This combination has been used in all previous analyses and is the basis of comparison for the remaining combinations. The second combination of defaults uses the limit on maximum size-density turned off and tripling turned on. The main effect of this combination is to increase the over prediction of mortality by approximately 2%, slightly reduce the over prediction biases for the net increments in basal area per acre and total stem cubic foot volume per acre, and change the slight over prediction bias in top height to a slight under prediction bias.

The third and fourth combinations of defaults turn the limit on maximum size-density on. The third option keeps the tripling option off, and the fourth option turns tripling on. The major impact of these two combinations is to increase the over prediction bias in mortality by four fold. As a result, the over prediction biases for the net increments in basal area per acre and total stem cubic foot volume per acre turn into under prediction biases of 1 to 2% (Table 16.4). Furthermore, the amount of variation (including bias) in the periodic annual mortality rate explained by RAP-ORGANON was reduced to one third of the value with the limit on maximum size-density turned off, but the amount of variation (including bias) explained for the other stand

components examined remained basically unchanged. Using tripling provided a slight further reduction in the under prediction biases for the net increments in basal area per acre and total stem cubic foot volume per acre and the increment in top height.

When the option of limiting the maximum size-density is selected, a species specific maximum size-density trajectory is used to restrict stand development in a manner that keeps the stand on or below the maximum size-density trajectory as it develops over time. These results may indicate that the maximum size-density trajectory developed by Puettmann et al. (1993) may be too constraining. Unfortunately, examination of the data sets used to develop RAP-ORGANON indicated that most stands had not reached the maximum size-density line and, as a result, a new maximum size-density trajectory could not be developed.

Table 16.5 contains the periodic annual analysis results for the longest possible projections calculated for the different lengths of projections. Two statistics are presented in Table 16.5: average residuals and the standard deviations of the residuals. Examination of these results shows no pronounced trends of increasing average residuals or standard deviations of the residuals as length of projections increased for any of the stand attributes examined.

Table 16.5 Periodic annual residual analysis for longest possible projections with residuals calculated as predicted minus actual. Projections were made with: (1) indirect estimation of crown recession, (2) mortality equation with crown ratio, (3) the limit on maximum size density turned off, and (4) tripling turned off.

Length of Projection	Number of Observations	Periodic Annual Residuals (Predicted Minus Actual)			
		Mortality	Net Basal Area Increment	Top Height Increment	Net Total Stem Cubic Foot Volume Increment
Averages					
6	1	+9.40	+0.13	-0.54	-22.17
7	7	-0.75	-0.32	+0.15	-3.29
8	1	+1.10	-2.09	+0.09	-32.27
9	16	-1.15	-0.43	-0.14	-14.38
10	26	-2.15	+0.25	+0.09	+8.25
11	42	-0.37	+0.42	+0.03	+12.03
12	14	-2.08	+0.48	+0.07	+13.12
13	3	-2.02	+1.07	+0.07	+25.54
14	29	-0.69	+0.02	-0.07	-2.39
Standard Deviations					
6	1	0.00	0.00	0.00	0.00
7	7	8.62	1.96	0.13	39.85
8	1	0.00	0.00	0.00	0.00
9	16	5.01	1.07	0.21	27.15
10	26	5.33	0.85	0.11	21.38
11	42	4.71	1.04	0.17	29.60
12	14	7.65	0.86	0.18	22.37
13	3	4.77	0.44	0.02	11.82
14	29	4.07	0.97	0.08	27.85

Figures 16.9 through 16.13 show graphs of actual periodic annual values plotted over predicted periodic annual values for mortality, survival, net basal area per acre increment, top height increment, and net total stem cubic foot volume per acre increment. Also shown is the one to one line (i.e., a 45-degree line on a square graph). Ideally, one would like to see all data points fall on the one to one line. The mortality and survival graphs are of particular interest. All previous analyses have examined predicted minus actual mortality rates. However, rate of mortality in these stands is low and conversely the rate of survival is very high. As a result, models developed to predict survival will always have higher indices of fit than those developed to predict mortality. The reason for this can be seen in Figures 16.9 and 16.10. A model that predicts low occurring mortality rates relatively poorly can still be an excellent predictor of survival.

Table 16.6 shows fit statistics for end of growth period differences on the longest possible projections. As with the single growth period projections, use of ending attributes instead of increments reduces the percent bias and increases the R_a^2 values. The R_a^2 (with bias incorporated) was 0.96 for predicted surviving number of trees per acre, 0.83 for predicted net basal area per acre, 0.96 for predicted top height, and 0.88 for predicted net total stem cubic foot volume per acre. Finally, Figures 16.14 through 16.17 show graphs of actual ending values plotted over predicted ending values for number of trees per acre, net basal area per acre, top height, and net total stem cubic foot volume per acre. Also shown is the one to one line (i.e., a 45-degree line on a square graph). Again, one would ideally like to see all data points fall on the one to one line.

Table 16.6 End of Growth Period Differences for longest possible projections with differences calculated as predicted minus actual. Projections were made with: (1) indirect estimation of crown recession, (2) mortality equation with crown ratio, (3) the limit on maximum size density turned off, and (4) tripling turned off.

	End of Growth Period Differences (Predicted Minus Actual)			
Attribute	Average	Average as Percent of Actual	R_a^2 Without Bias	R_a^2 With Bias
Surviving Number of Trees per Acre	-11.33	-1.29	0.96	0.96
Net Basal Area per Acre	+2.13	+2.5	0.84	0.83
Top Height	+0.08	+0.15	0.96	0.96
Net Total Stem Cubic Foot Volume per Acre	+52.59	+2.89	0.88	0.88

The conclusion from these analyses is that RAP-ORGANON performs well when projecting stand-level attributes over time.

16.4 References Cited

Bailey, R.L., T.M. Burgan, and E.J. Jokela. 1989. Fertilized midrotation-aged slash pine plantations – stand structure and yield prediction. Southern Journal of Applied Forestry 13: 76-80.

Hasenauer, H., H.E. Burkhart, and R.L. Amateis. 1997. Basal area development in thinned and unthinned loblolly pine plantations. Canadian Journal of Forest Research 27: 265-271.

Pienaar, L.V. and J.W. Rheney. 1993. Yield prediction for mechanically site-prepared slash pine plantations in the southeastern coastal plain. Southern Journal of Applied Forestry 17: 163-173.

Pienaar, L.V., H.H. Page, and J.W. Rheney. 1990. Yield prediction for mechanically site-prepared slash pine plantations. Southern Journal of Applied Forestry 14: 104-109.

Puettmann, K.J., D.W. Hann, and D.E. Hibbs. 1993. Evaluation of the size-density relationships for pure red alder and Douglas-fir stands. Forest Science 39: 7-27.